



**INSTITUTO POTOSINO DE INVESTIGACIÓN
CIENTÍFICA Y TECNOLÓGICA, A.C.**

POSGRADO EN CIENCIAS AMBIENTALES

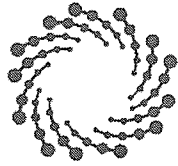
**Estrategias de control de las
comunidades microbianas durante la
fermentación oscura**

Tesis que presenta
Rodolfo Palomo Briones

Para obtener el grado de
Doctor en Ciencias Ambientales

Director de la Tesis:
Dr. Elías Razo Flores

San Luis Potosí, S.L.P., septiembre de 2018



IPICYT

Constancia de aprobación de la tesis

La tesis "***Estrategias de control de las comunidades microbianas durante la fermentación oscura***" presentada para obtener el Grado de Doctor en Ciencias Ambientales, fue elaborada por Rodolfo Palomo Briones y aprobada el diecinueve de septiembre del dos mil dieciocho por los suscritos, designados por el Colegio de Profesores de la División de Ciencias Ambientales del Instituto Potosino de Investigación Científica y Tecnológica, A.C.


Dr. Elías Razo Flores
Director de la tesis


Dra. Nguyen Esmeralda López Lozano
Miembro del Comité Tutorial


Dra. María de Lourdes Berenice Celis García
Miembro del Comité Tutorial


Hugo Oscar Méndez Acosta
Miembro del Comité Tutorial


Dr. Eric Trably
Miembro del Comité Tutorial


Dr. Nicolas Marie Charles Yves Bernet
Miembro del Comité Tutorial



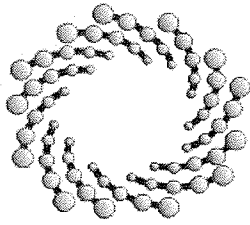
Créditos Institucionales

Esta tesis fue elaborada en los laboratorios de la División de Ciencias Ambientales del Instituto Potosino de Investigación Científica y Tecnológica, A.C., bajo la dirección del Dr. Elías Razo-Flores.

Durante la realización del trabajo, el autor recibió una beca académica del Consejo Nacional de Ciencia y Tecnología (262218).

Como parte de este trabajo se realizó una estancia de investigación internacional con el apoyo de una Beca Mixta CONACYT en el Laboratoire de Biotechnologie de l'Environnement perteneciente al Institute National de la Recherche Agronomique (INRA) en Narbonne, Francia, bajo la supervisión del Dr. Nicolas Bernet. Asimismo, se contó con el apoyo del proyecto BITA FP7-PEOPLE-2011-IRSES, proyecto 295170 "Bioprocess and Control Engineering for Wastewater Treatment".

El trabajo de investigación fue financiado por el Fondo SENER-CONACYT Sustentabilidad Energética, Clúster Biocombustibles Gaseosos, proyecto 247006.



IPICYT

Instituto Potosino de Investigación Científica y Tecnológica, A.C.

Acta de Examen de Grado

El Secretario Académico del Instituto Potosino de Investigación Científica y Tecnológica, A.C., certifica que en el Acta 013 del Libro Primero de Actas de Exámenes de Grado del Programa de Doctorado en Ciencias Ambientales está asentado lo siguiente:

En la ciudad de San Luis Potosí a los 19 días del mes de septiembre del año 2018, se reunió a las 09:25 horas en las instalaciones del Instituto Potosino de Investigación Científica y Tecnológica, A.C., el Jurado integrado por:

Dra. María de Lourdes Berenice Celis García	Presidenta	IPICYT
Dra. Nguyen Esmeralda López Lozano	Secretaria	IPICYT
Dr. Elías Razo Flores	Sinodal	IPICYT
Dr. Hugo Oscar Méndez Acosta	Sinodal externo	UdG

a fin de efectuar el examen, que para obtener el Grado de:

DOCTOR EN CIENCIAS AMBIENTALES

sustentó el C.

Rodolfo Palomo Briones

sobre la Tesis intitulada:

Estrategias de control de las comunidades microbianas durante la fermentación oscura

que se desarrolló bajo la dirección de

Dr. Elías Razo Flores

El Jurado, después de deliberar, determinó

APROBARLO

Dándose por terminado el acto a las 13:00 horas, procediendo a la firma del Acta los integrantes del Jurado. Dando fe el Secretario Académico del Instituto.

A petición del interesado y para los fines que al mismo convengan, se extiende el presente documento en la ciudad de San Luis Potosí, S.L.P., México, a los 19 días del mes de septiembre de 2018.

Mtra. Ivonne Lizette Cuevas Vélez
Jefa del Departamento del Posgrado

Dr. Horacio Flores Zúñiga
Secretario Académico



Dedicatorias

A mi amada familia:

Quisiera que esta tesis sea muestra de que la dedicación, perseverancia y trabajo duro fructifican tarde o temprano. Y que importa poco de dónde vengas, pero importa muchísimo saber a dónde ir.

Familia, por supuesto que este logro es también de ustedes. De corazón, mamá, papá, hermanos, espero que lo consideren como suyo, créanlo. Porque, aunque el sendero que me tocó caminar fue duro, sinuoso, y a veces oscuro, contaba con un súper poder que no aprendí de nadie más sino de ustedes. No lo comprendía hasta hace poco, pero ustedes me enseñaron desde muy pequeño a tener fe.

Y no digo solamente tener fe en Dios, que quizás algo hubo de eso, sino tener fe en que estamos en el camino correcto, tener fe en que el esfuerzo fructifica, tener fe en que los malos momentos serán temporales, tener fe en uno mismo.

Mamá, papá, Erik, Abisay, Edson, no saben la felicidad que siento de compartir la vida con ustedes.

A mi artista preferida:

Babe, lo logramos. Espero sepas que esta tesis es producto del esfuerzo de ambos, de nuestra insistencia por alcanzar esos sueños que a veces nos pueden parecer inalcanzables. Gracias amor por todo tu apoyo durante tanto tiempo, por estar a mi lado en todo momento, por soportar mis frustraciones y mis lágrimas, por iluminar cada mañana, por compartirme tu pasión por el arte (llegué a pensar en dejarlo todo y unirme a tu clan de artistas 😊), por confiar en mí, por darme la paz y la tranquilidad para continuar. Soy el hombre más afortunado por vivir a tu lado.

Agradecimientos

Al Dr. Elías Razo Flores, por su invaluable guía en la conceptualización, desarrollo, discusión y presentación de todas las secciones que comprenden el presente trabajo de tesis. Gracias por su confianza.

A la Dra. Ma. Lourdes Berenice Celis García, por su excelente apoyo en el desarrollo y discusión de este trabajo. Gracias por su paciencia y por su atención exhaustiva de la calidad de la investigación.

Al Dr. Eric Trably y al Dr. Nicolas Bernet, por su dirección, apoyo y confianza brindados durante mi estancia en sus laboratorios (LBE-INRA). Gracias también por su disposición para contribuir en la discusión de los resultados.

Al Dr. Hugo Oscar Méndez Acosta y la Dra. Nguyen Esmeralda López Lozano, por su apoyo experto y de gran calidad para discutir las distintas secciones de este trabajo, especialmente en temas de control, transferencia de masa y comunidades microbianas.

A M. en C. Guillermo Vidriales Escobar, M. en C. Juan Pablo Rodas Ortiz, M. en C. Duce Isela de Fátima Partida Gutiérrez, Ing. Clémence Pages, M. en C. Elizabeth Cortés Cedillo, por su apoyo técnico y administrativo durante la realización de este proyecto.

A Miguel Ángel Cortés Carmona, Karen Lizeth Galindo Hernández, Viviana Ruiz Díaz, José de Jesús Montoya Rosales, Angelo Mari, por su apoyo en la realización de distintos experimentos durante mi estancia en el grupo de investigación.

Table of contents

Constancia de aprobación de la tesis	ii
Créditos institucionales	iii
Acta de examen	iv
Dedicatorias	v
Agradecimientos	vi
Table of contents	vii
List of tables	x
List of figures	xi
Resumen	xiv
Abstract	xv

Chapter I. Dark fermentative hydrogen production

1.1 Introduction	2
1.2 Dark fermentative hydrogen production	2
1.3 What do we know about dark fermentation in continuous systems?	4
1.3.1 Systematic review of dark fermentation in continuous stirred-tank reactors	6
1.4 Challenges of dark fermentation biotechnology	14
1.4.1 Homoacetogenesis	15
1.4.2 Lactic acid bacteria	17
1.4.3 Mass transfer limitations	19
1.5 Scope and structure of the research	21
1.6 References	22

Chapter II. The hydraulic retention time as a control tool of productivity, efficiency and microbial communities

2.1 Summary	27
2.2 Introduction	28
2.3 Materials and methods	30
2.3.1 Inoculum source and substrate	30

2.3.2	Experimental conditions	31
2.3.3	Analytical methods	31
2.3.4	Microbial community analysis	31
2.3.5	Multivariate analysis and Pearson's correlation	32
2.3.6	Microbial community networks	33
2.4	Results and discussion	33
2.4.1	HRT determines dark fermentation performances and metabolites distribution	33
2.4.2	HRT shapes the microbial community and modifies the metabolic pathways	39
2.4.3	A microbial interaction network displays an ecosystem dominated by mutual exclusive interactions	44
2.5	Conclusions	45
2.6	References	46
Chapter III. Hydrogen metabolic patterns driven by <i>Clostridium-Streptococcus</i> community shifts in a CSTR at different organic loading rates		
3.1	Summary	51
3.2	Introduction	52
3.3	Materials and methods	53
3.3.1	Inoculum and substrate	53
3.3.2	Experimental setup	53
3.3.3	Analytical methods	54
3.3.4	Capillary electrophoresis-single strand conformation polymorphism	54
3.3.5	Illumina sequencing and microbial community analysis	55
3.4	Results	56
3.4.1	Dark fermentation performance	56
3.4.2	Microbial community analysis	59
3.5	Discussion	60
3.5.1	Highly efficient H ₂ -producing phase	61
3.5.2	Lactate and formate are favored at high OLR	63
3.6	Conclusions	67
3.7	References	67
Chapter IV. Enhancement of mass transfer conditions to increase the productivity and efficiency of dark fermentation		

4.1 Summary	72
4.2 Introduction	73
4.3 Materials and methods	74
4.3.1 Inoculum and fermentation medium	74
4.3.2 Bioreactor set-up and operational conditions	74
4.3.3 Analytical methods	75
4.3.4 Determination of k_{LA} and dissolved H_2 concentration	76
4.3.5 Microbial community analysis	77
4.3.6 Hydrogen consumption	78
4.4 Results and discussion	79
4.4.1 k_{LA} determination in dark fermentative system	79
4.4.2 The k_{LA} as key mechanism controlling the productivity and efficiency of dark fermentation	79
4.4.3 The enhancement of k_{LA} intensifies the metabolic routes leading to H_2 production.	82
4.4.4 Microbial community	84
4.4.4 The dual capacity of hydrogenogenic biomass	85
4.5 Conclusions	87
4.6 References	88
Chapter V. Strategies of control of microbial communities during dark fermentation: Conclusions and perspectives	
5.1 General discussion and conclusions	92
5.2 Perspectives	94
5.2.1 The way forward in H_2 research	94
5.2.2 Going back to homoacetogens	99
5.4 References	100
Appendix	105
About the author	109

List of tables

Table 1.1. Summary of hydrogen production performance in several reactor configurations studied by our research group.	5
Table 1.2. Multifactorial ANOVA of the volumetric H ₂ production rate in CSTR reactors.	8
Table 1.3. Multifactorial ANOVA of the H ₂ molar yield in CSTR reactors.	8
Table 1.4. Classification of lactic acid bacteria metabolism. Modified from De Angelis and Gobbetti (2011).	18
Table 2.1. Selection of studies of biohydrogen production in continuous stirred-tank reactors.	35
Table 2.2. Summary of the performance of four continuous stirred-tank reactors reactors operated at different values of hydraulic retention time.	36
Table 3.1. Summary of the steady state performance of dark fermentative continuous stirred-tank reactors operated under different organic loading rates.	61
Table 3.2. Growth kinetic parameters of representative species of H ₂ producing bacteria and lactic acid bacteria..	65
Table 3.3. Gibbs' energy of acetate and formate autotrophic reactions.	66
Table 4.1. Volumetric mass transfer coefficients at different stirring velocities in stirred-tank reactors.	80
Table 4.2. Selection of literature works aiming the improvement of H ₂ transfer conditions of dark fermentation systems.	82
Table 4.3. Affiliation of DGGE bands from samples taken under different H ₂ mass transfer conditions.	85
Table 4.4. Theoretical determinations of H ₂ consumption by homoacetogenesis.	86
Table 4.5. Summary of H ₂ consumption experiments. For both experimental conditions two additional serum bottles were set-up to account for the inoculum activity (without addition of H ₂ gas) and the contribution of physicochemical phenomena (<i>e.g.</i> mass transfer).	87
Table A1. List of variables reviewed and considered for the statistical analysis.	105
Table A2. Variables transformed to fit a normal distribution.	107

List of figures

- Figure 1.1.** Main dark fermentative metabolic routes from glucose as model substrate. Left side: acetate pathway. Right side: butyrate pathway. 3
- Figure 1.2.** Number of articles on dark fermentation with continuous stirred-tank reactors and suspended biomass from 2007 to 2017. 6
- Figure 1.3.** Percentage of articles classified by type of substrate in dark fermentation literature. 7
- Figure 1.4.** Percentage of articles classified by A) pH, B) hydraulic retention time (h), C) temperature (°C) and D) stirring velocity (rpm) in dark fermentation literature. 7
- Figure 1.5.** Overview of the effects of A) type of substrate, B) inoculum source and C) pretreatment type on the volumetric hydrogen production rate (VHPR). S-1: Beverage wastewater; S-2: Cheese whey; S-3: Fructose; S-4: Glucose; S-5: Lignocellulosic hydrolysate; S-6: Molasses; S-7: Other wastewater; S-8: Starch; S-9: Sucrose; S10: Xylose; I-1: Acclimated culture; I-2: Acidogenic and methanogenic sludge; I-3: Aerobic sludge; I-4: Anaerobic sludge; I-5: Compost; I-6: Cracked cereals; I-7: Hot spring culture; I-8: Hydrogen producing sludge; I-9: Indigenous; I-10: Marine sediment; I-11: Pure culture. P-1: Acclimation; P-2: Acid and acclimation; P-3: Aeration; P-4: Heat; P-5: Heat and acid. 9
- Figure 1.6.** Overview of the effects of A) hydraulic retention time (HRT), B) pH, C) Stirring velocity and D) substrate concentration on the volumetric hydrogen production rate. 10
- Figure 1.7.** Overview of the effects of A) inoculum source, B) pretreatment type, C) hydraulic retention time (HRT), D) substrate concentration, and E) stirring velocity on hydrogen molar yield. I-1: Acclimated culture; I-2: Acidogenic and methanogenic sludge; I-3: Aerobic sludge; I-4: Anaerobic sludge; I-5: Compost; I-6: Cracked cereals; I-7: Hot spring culture; I-8: Hydrogen producing sludge; I-9: Indigenous; I-10: Marine sediment; I-11: Pure culture. P-1: Acclimation; P-2: Acid and acclimation; P-3: Aeration; P-4: Heat; P-5: Heat and acid. 11
- Figure 1.8.** Matrix of Pearson's correlations between the multiple variables involved in hydrogen production in continuous stirred-tank reactors. 14
- Figure 1.9.** Metabolic pathways of lactic acid bacteria. A) Homolactic fermentation. B) Heterolactic fermentation. Adapted from Reddy et al., 2008. 17
- Figure 1.10.** The H₂ mass transfer mechanism during the continuous operation of dark fermentative systems. 19
- Figure 1.11.** Effects of the H₂ partial pressure on the Gibbs free energy ($\Delta G'$) of H₂ production from A) ferredoxin, B) NADH, and C) ferredoxin+NADH at different ratios of oxidized/reduced electron carriers. Gibbs free energy is reported at standard physiological conditions (pH 7 and 25°C). 20

Figure 2.1. Schematic representation of the experimental set-up.	30
Figure 2.2. Summary of the influence of the hydraulic retention time on the performance of continuous stirred-tank reactors during dark fermentation. For each case, the three last samples were considered. Bars with the same lower case letter were not significantly different at a level 0.05 according with Tukey's tests.	34
Figure 2.3. Matrix of Pearson's correlations obtained with the corrplot package in R environment. Only correlations with $p < 0.05$ are displayed. HY: H ₂ yield (mol H ₂ /mol lactose); VHPR: Volumetric hydrogen production rate (L H ₂ /L-d); Formate, Acetate, Propionate, Lactate, Butyrate, Ethanol, Succinate and Propionate were considered as production yields (mmol VFA/mol lactose); HRT: hydraulic retention time (h). Microorganisms were analyzed in terms of their relative abundance from pyrosequencing results.	37
Figure 2.4. Summary of the influence of hydraulic retention time (HRT) on the metabolic pathways of dark fermentation based on the chemical oxygen demand. The balance was performed with the last 3 samples in the systems' operation.	38
Figure 2.5. Capillary electrophoresis-based single-strand conformation polymorphism (CE-SSCP) fingerprints of samples from four continuous stirred-tank reactors (CSTR1 - CSTR4) operated under different hydraulic retention times (HRT) (6h, 12h, 18h and 24 h). Note that 4 samples (after 2, 6, 12 and 20 HRT) were analyzed for each condition. The CE-SSCP profiles were processed to compute Bray-Curtis dissimilarities and hierarchical clustered. Shannon's diversity index and Gini's coefficients for evenness were computed for each profile as well.	40
Figure 2.6. Relative abundance of bacteria families found from continuous stirred-tank reactors (CSTR) operated under different conditions of hydraulic retention time (HRT) (6h, 12h, 18h and 24 h). For each reactor, four samples were taken in different moments of the operation (after 2, 6, 12 and 20 HRT). Families with relative abundance <1% were grouped as others.	41
Figure 2.7. Principal components analysis for relative abundance of microbial families, metabolite yields and H ₂ production performance. Samples considered were taken at times equivalent to 2, 6, 12 and 20 times the hydraulic retention time. VHPR: Volumetric H ₂ production rate.	42
Figure 2.8. Network of interactions constructed from four different similarity measurements within Cytoscape environment, using the CoNet application (Faust and Raes, 2016). Only groups presented in at least three samples with > 1% relative abundance were considered. Edges represent strong connections ($p < 0.05$) between two microbial families (nodes). Yellow edges are positive interactions while purple edges represent a strong "exclusion" interaction. The width of the edges is shown proportional to the weight of the interaction between the microbial groups, while the size of the nodes is proportional to the number of interactions of the microbial group.	44
Figure 3.1. H ₂ production performance of the continuous stirred-tank reactor operated at different values of organic loading rate. Box plots of the volumetric H ₂ production rate	57

(VHPR) and H₂ yield include all data of the corresponding periods. A) VHPR and OLR. B) H₂ yield and biomass concentration.

Figure 3.2. Linear correlations between: (A-D) H₂ yield and volatile fatty acids yields, (E-H) organic loading rate and volatile fatty acids yield. Statistical significance of the correlation is displayed according with the following legend: - Not significant, * p<0.10, ** p<0.05, *** p<0.01. 58

Figure 3.3. Balance of chemical oxygen demand (COD) of continuous stirred-tank reactor operation at different organic loading rates. The balance is based on the total COD of cheese whey powder fed into the bioreactor. 59

Figure 3.4. Microbial communities and metabolites productivities of dark fermentative systems under different values of organic loading rate (OLR). A) Ward D2 hierarchical cluster analysis based on Pearson distances; B) CE-SSCP profiles of microbial communities developed under different OLR; C) Volatile fatty acids and hydrogen yields from steady states. B, butyrate; L, lactate; A, acetate; F, formate. 62

Figure 3.5. A) Profiles of the microbial communities from the operation of the continuous stirred-tank reactor at different conditions of organic loading rate (OLR) obtained by Illumina MiSeq analysis. B) Relationship between *Clostridium* and *Streptococcus* species with the OLR. 63

Figure 3.6. Principal Components Analysis of biohydrogen production under different organic loading rates. OLR: Organic loading rate; VHPR: Volumetric H₂ production rate. 64

Figure 4.1. Schematic representation of the experimental set-up. 1, pH probe; 2, temperature sensor; 3, level sensor; 4, heat cover; 5, peristaltic pump. 75

Figure 4.2. Summary of the effects of k_{LA} on A) the volumetric H₂ production rate and B) the H₂ yield. Boxes with same letters are not significant different at p<0.05 in accordance with the Tukey test. 81

Figure 4.3. Effect of k_{LA} on A) the yield of volatile fatty acids, B) total volatile fatty acids concentration, and C) dissolved H₂ concentrations. 83

Figure 4.4. Denaturing gradient gel electrophoresis (DGGE) profiles from dark fermentation systems operated under different mass transfer conditions. The band numbers indicate samples that were sequenced (see Table 4.3). 84

Figure 4.5. H₂ consumption profiles using hydrogenogenic biomass harvested from the continuous stirred-tank reactor III. Experimental points (□), physicochemical control (-Δ-) and gompertz model (- - -). A) Experiment performed at an initial P_{H2} of 1 atm. B) Experiment performed at an initial P_{H2} of 1.4 atm. 87

Figure 5.1. Schemes for extractive dark fermentation. A) Liquid-liquid extraction, B) ion exchange, and C) electrodialysis. CA: Carboxylic acid; EA: Exchanged anion; FG: Functional group; CEM: Cation exchange membrane; AEM: Anion exchange membrane. 97

Resumen

Estrategias de control de las comunidades microbianas durante la fermentación oscura

Palabras clave: biohidrógeno, fermentación ácido-láctica, homoacetogénesis, transferencia de masa

La fermentación oscura es la alternativa más factible para la producción biológica de hidrógeno (H_2). Este bioproceso depende de la capacidad metabólica de microorganismos anaerobios que utilizan sustratos orgánicos y producen una mezcla de ácidos carboxílicos e H_2 como subproductos. En procesos continuos, la fermentación oscura ha mostrado ser estable y con altas productividades, especialmente en reactores de biomasa suspendida. Sin embargo, los rendimientos molares de H_2 reportados en la literatura se mantienen alejados de los valores teóricos (4 mol H_2 /mol hexose). Recientemente, la homoacetogénesis y la fermentación ácido láctica han sido identificadas como causas probables de los desempeños subóptimos de la producción de H_2 . En este trabajo se evaluaron diferentes parámetros de operación con el objetivo de identificar y entender las condiciones que desencadenan la homoacetogénesis y la fermentación ácido-láctica durante la producción de H_2 en reactores continuous de tanque agitado.

Se demostró que el tiempo de retención hidráulico (TRH) es un factor crítico que controla la composición de las comunidades microbianas de la fermentación oscura. Valores de TRH entre 6 y 12 h favorecen el surgimiento de una comunidad microbiana dominada por las familias *Clostridiaceae-Lachnospiraceae-Enterobacteriaceae*, las cuales llevan a cabo metabolismos asociados con la producción de H_2 . En dichas condiciones, se obtuvo una velocidad volumétrica de producción de H_2 (VVPH) de 2 L H_2 /L-d. En contraste, valores de TRH entre 18 y 24 h derivaron en el establecimiento de una comunidad microbiana de *Sporolactobacillaceae-Streptococcaceae*, que llevó a cabo la fermentación ácido láctica y desplazó a las bacterias productoras de H_2 . Asimismo, la VVPH disminuyó hasta un mínimo de 0.6 L H_2 /L-d. Posteriormente, bajo condiciones fijas de TRH (6 h), se encontró que la operación a velocidades de carga orgánica (VCO) bajas (14.7– 44.1 g lactosa/L-d) estuvo asociada con el dominio de *Clostridium spp.* Dichas condiciones favorecieron las rutas metabólicas del ácido acético y butírico, con un rendimiento molar de H_2 de 2.14 mol H_2 /mol hexosa y una VVPH entre 3.2 y 11.6 L H_2 /L-d. En contraste, VCO relativamente altas (58.8 y 88.2 g lactosa/L-d) favorecieron la aparición de *Streptococcus spp.* como bacteria co-dominante en la comunidad microbiana, cuya presencia derivó en la producción de ácido láctico. Bajo estas condiciones, la producción de ácido fórmico también se favoreció, sirviendo posiblemente como estrategia para disponer el exceso de moléculas reducidas (e.g. NADH). En este escenario, la VVPH incrementó (13.7–14.5 L H_2 /L-d), pero el rendimiento molar de H_2 disminuyó hasta 0.74 mol H_2 /mol hexosa.

Después de analizar los resultados previos, se sugirió que la diversificación de las comunidades microbianas y de las rutas metabólicas estaba posiblemente asociada con un fenómeno de inhibición causado por la acumulación de ácidos carboxílicos ó H_2 . Por lo tanto, se evaluó el impacto de las condiciones de transferencia de H_2 mediante la operación de reactores bajo distintos coeficientes de transferencia de masa (k_{La}). Se mostró que la VVPH y el rendimiento molar incrementaron 74 y 78%, respectivamente, como resultado de la mejora en las condiciones de transferencia de H_2 hacia la fase gas. Este desempeño fue impulsado por una disminución de 53% en la concentración de H_2 disuelto. Además, el análisis de 16S-DGGE reveló que la abundancia de *Clostridium sp* incrementó a valores de $k_{La} \geq 2.72$ 1/h (300 y 400 rpm) como respuesta a las menores concentraciones de H_2 disuelto. Esta respuesta fue acompañada por un incremento de los rendimientos de ácidos acético y butírico.

En general, TRH y cargas orgánicas bajas (6 h y ≤ 44.1 g lactosa/L-d), así como coeficientes de transferencia de masa mayores a 2.72 1/h fueron identificadas como las condiciones más favorables para la producción eficiente de H_2 , evitando una diversificación de las comunidades microbianas y controlando las velocidades de consumo de H_2 y de la fermentación ácido láctica.

Abstract

Strategies of control of microbial communities during dark fermentation

Keywords: biohydrogen, homoacetogenesis, lactic-acid fermentation, mass transfer

Dark fermentation is the most feasible alternative for biological hydrogen (H₂) production. Such bioprocess depends on the metabolic capacity of anaerobic microorganisms that use organic substrates and produce a mixture of short-chain carboxylic acids and H₂ as byproducts. In continuous processes, dark fermentative hydrogen production has demonstrated to be stable and highly productive, especially in suspended-growth reactors. Nevertheless, the reported H₂ yields remain far from theoretical values. In recent years, homoacetogenesis and lactic acid fermentation have been identified as possible causes of suboptimal performance of dark fermentation. In this regard, different operational parameters were evaluated with the aim to identify and understand the conditions that trigger homoacetogenesis and lactic acid fermentation during H₂ production in continuous stirred tank reactors (CSTR).

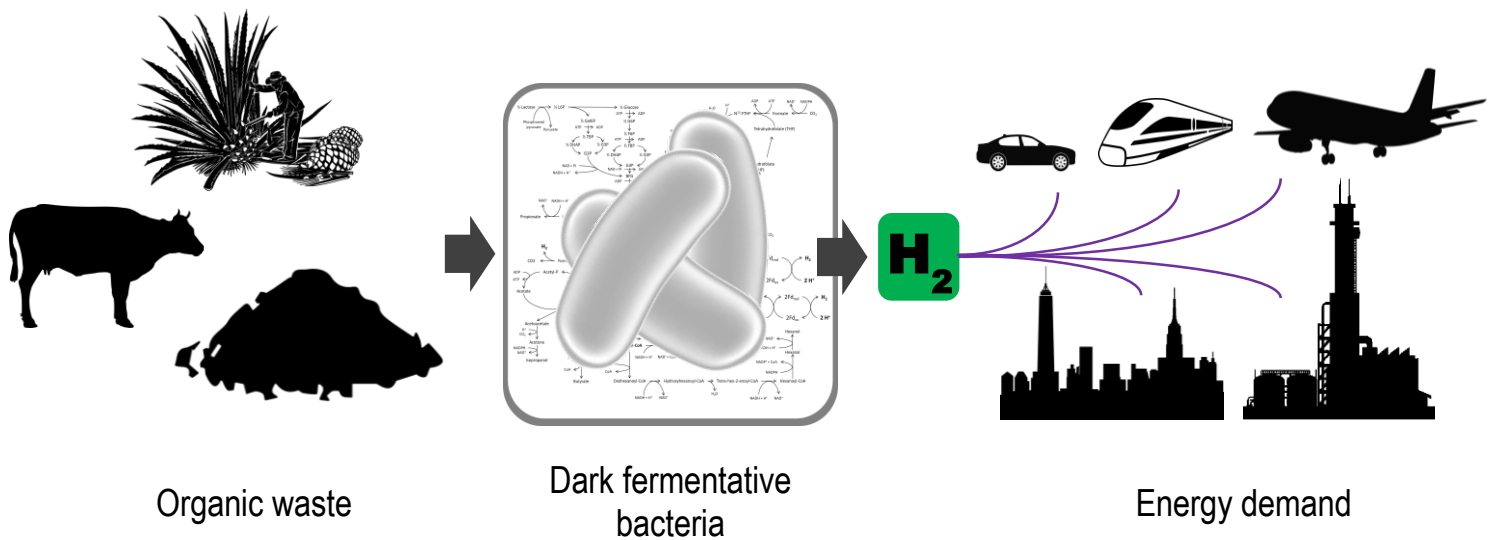
It was demonstrated that the hydraulic retention time (HRT) is a critical factor that shapes the microbial community of dark fermentation. It was shown that low values of HRT (6-12 h) favored the emergence of a microbial community dominated by *Clostridiaceae-Lachnospiraceae-Enterobacteriaceae*, which performed metabolic pathways co-producing H₂. At these conditions, a maximum volumetric H₂ production rate (VHPR) of 2 L H₂/L-d was obtained. In contrast, large values of HRT (18-24 h) led to the establishment of a microbial community composed of *Sporolactobacillaceae-Streptococcaceae* that performed lactic acid fermentation and outcompeted H₂-producing bacteria. At this stage, the VHPR dropped to a minimum of 0.6 L H₂/L-d. Afterward, at fixed HRT conditions of 6 h, it was found that the operation at low organic loading rates (OLR) (14.7– 44.1 g lactose/L-d) was associated with the dominance of *Clostridium spp.* At such conditions, the acetate and butyrate metabolic pathways were mostly favored, with an associated H₂ yield of 2.14 mol H₂/mol hexose and VHPR between 3.2 and 11.6 L H₂/L-d. In contrast, relatively high OLR (58.8 and 88.2 g lactose/L-d) favored the appearance of *Streptococcus spp.* as co-dominant bacteria leading to lactate production. The production of formate was also stimulated, possibly serving as a strategy to dispose the surplus of reduced molecules (*e.g.* NADH). In such scenario, VHPR was enhanced (13.7–14.5 L H₂/L-d) but the H₂ yield dropped to a minimum of 0.74 mol H₂/mol hexose.

In the light of these findings, it was suggested that the diversification of the microbial communities and the metabolic pathways were possibly associated with an inhibition phenomenon due to either the carboxylic acids or H₂ accumulation. In this regard, the impact of the H₂ mass transfer conditions was evaluated using a series of continuous stirred-tank reactors operated at H₂ mass transfer coefficients (k_La) ranging from 1.04 to 4.23 1/h. It was demonstrated that the VHPR and H₂ yield increased 74 and 78%, respectively, as a result of enhanced mass transfer conditions. This behavior was driven by a 53% decrease in the dissolved H₂ concentration. Moreover, the 16S-DGGE analysis and sequencing revealed that *Clostridium sp* increased its occurrence at k_La ≥ 2.72 1/h (300 and 400 rpm) as response to lower dissolved H₂ concentration. This was accompanied by an increase of acetate and butyrate yields.

Overall, short HRT (6 h), low OLR (≤ 44.1 g lactose/L-d), and mass transfer coefficient above 2.72 1/h were identified as the most suitable conditions for efficient H₂ production, avoiding excessive diversification of microbial communities and controlling the rates of H₂ consumption by homoacetogenesis and lactic-acid fermentation.

CHAPTER I

Dark fermentative hydrogen production



Highlights

- Dark fermentation is a technology under development to contribute to energy transition.
- Suspended-growth bioreactors such as CSTR seem to be the most suitable reactor configuration for H_2 production.
- H_2 production by dark fermentation is hindered by three main challenges namely homoacetogenesis, lactic acid fermentation, and mass transfer conditions.

Part of the present chapter is based on the article:
Palomo-Briones et al. 2018. Systematic review of dark fermentation in continuous stirred-tank reactors. To be submitted to *Energy and Environmental Science*.

1.1 Introduction

The worldwide transition towards sustainable energy sources is increasing its momentum since the Paris agreement signed by 195 nations in 2015. The energy transition implies, in general terms, to stimulate the diversification and development of technologies that can harvest energy from sustainable sources to replace our dependency on fossil fuels. The most developed technologies up-to-date include solar, eolic, and hydraulic. However, all of these are subjected to weather variations that can compromise the stability of the future electric-grid. Therefore, complementary technologies that can be used to equilibrate the electricity supply are also required. One of such technologies is dark fermentation, which is up-to-date the most successful biological method for the production of molecular hydrogen (H_2), the so-called fuel of the future.

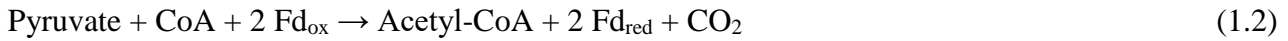
The H_2 produced in dark fermentation is considered as an excellent solution for the aforementioned issues due to 1) its large energy content (122 kJ/g), 2) its high conversion efficiencies to electricity through fuel cells, 3) the near-zero carbon emissions associated, and 4) the broad range of carbohydrate-rich substrates that can be used to produce it. Furthermore, dark fermentation technology can be integrated in multiple schemes of waste valorization and biorefinery, which highlights its potential towards the development of clean industries.

1.2 Dark fermentative hydrogen production

From a biochemical point of view, dark fermentation is the microbial process by which organic substrates are incompletely oxidized to form short-chain carboxylic acids. The process begins with the carbohydrate degradation to pyruvate by the Embden-Meyerhof-Parnas metabolic route (Eq. 1.1). The fermentation can continue through two main anaerobic pathways: the pyruvate-ferredoxin oxidoreductase (PFOR) pathway and the pyruvate-formate lyase (PFL) pathway (Cabrol et al., 2017). The PFOR pathway catalyzes the conversion of pyruvate and coenzyme A (CoA) into Acetyl-CoA and CO_2 coupled with the reduction of ferredoxin (Eq. 1.2). The reduced ferredoxin is then re-oxidized using protons as electron acceptors, which leads to the synthesis of H_2 (Eq. 1.4). The PFL catalyzes the conversion of pyruvate into formate and Acetyl-CoA (Eq. 1.3). Afterward, formate is converted to H_2 and CO_2 by the pyruvate- H_2 lyase (Eq. 1.5). Up to this extent, a maximum yield of 2 moles of H_2 per mole of glucose consumed can be obtained.

The NADH produced in the Embden-Meyerhof-Parnas route can be used by the confurcating NADH-Fd-dependent hydrogenase leading to additional H_2 production (Eq. 1.6) (Peters et al., 2015). Alternatively,

NADH can also be taken by the NADH-Fd oxidoreductase that produces reduced Fd (Eq. 1.7), which can be later used for H₂ production through Eq. 1.4 (Oh et al., 2011; Vardar-Schara et al., 2008). Through any of these pathways, 2 mol of H₂ can be produced to sum up to 4 mol per mol of hexose consumed.



The Acetyl-CoA produced either by the PFOR or PFL pathway can be later conducted to the production of acetate or butyrate (Figure 1.1). However, the synthesis of butyrate will require the consumption of two mol of NADH; therefore, the global synthesis of H₂ will be limited to a maximum yield of 2 mol H₂/mol hexose.

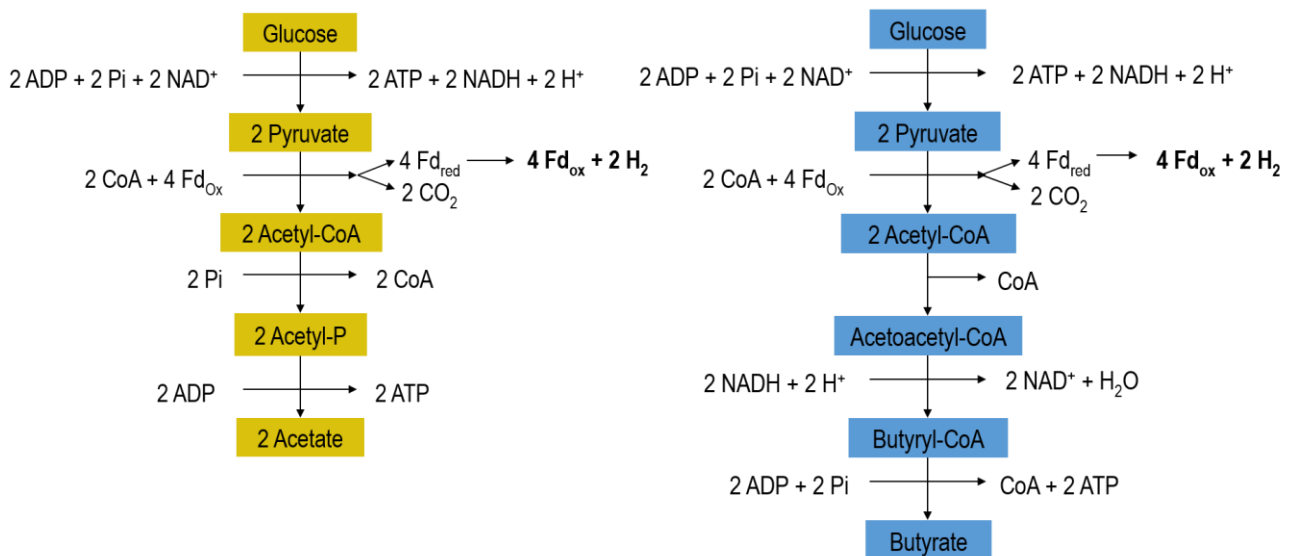


Figure 1.1. Main dark fermentative metabolic routes from glucose as model substrate. Left side: acetate pathway. Right side: butyrate pathway.

Typically, dark fermentative systems are conducted with mixed cultures, which is considered advantageous since it does not require of sterile conditions, it increases the resilience capacity against operational variations, and cultures can adapt to changes of the substrate composition (Kleerebezem and van Loosdrecht, 2007). However, the use of mixed cultures drives the fermentation to the production of a mixture of metabolites, which impacts on the H₂ molar yield. Often, the butyrate to acetate ratio (B/A) is used as indicator of the fermentation performance; for instance, a B/A ratio of 1.5 results in a theoretical molar H₂ yield of 2.5 mol H₂/mol hexose (Hawkes et al., 2007).

1.3 What do we know about dark fermentation in continuous systems?

The use of dark fermentation for the continuous H₂ production has been explored intensively worldwide. In general, the systems can be classified in accordance with the type of microbial growth, in fixed- and suspended-biomass. In the former type of bioreactors, the cellular retention time is not associated to the hydraulic retention time (HRT); therefore, such bioreactors can be operated at short HRT and high organic loading rates (OLR), and still maintain high biomass concentrations. Overall, the combinations of these features are thought to lead to high productivities in terms of volumetric H₂ production rate (VHPR). On the other hand, the operation of suspended-biomass reactors is traditionally considered to be unstable due to wash-out phenomena, especially at short HRT. For such reason, together with the relatively low biomass concentrations, they are generally referred as low-rate H₂ production systems.

However, a literature overview reveals that suspended-biomass bioreactors have actually shown higher VHPR than fixed-biomass systems (Table 1.1). In the case of continuous stirred-tank reactors (CSTR), the maximum steady-state VHPR have ranged from 2 up to 25.8 L H₂/L-d with an average of 15.5 ± 10.3 L H₂/L-d. In contrast, with fixed-biomass configurations the VHPR have been in the range of 0.4-12 L H₂/L-d with an average of 3.7 ± 3.5 L H₂/L-d. It is worth to note that, except for the TBR fed with glucose reported by Arreola-Vargas et al. (2015), none of the fixed-biomass configurations has been successfully evaluated with OLR beyond 52.9 g COD/L-d. Whereas, suspended-biomass systems have been operated with OLR values up to 190 g lactose/L-d (Cota-Navarro et al., 2011). Therefore, suspended-growth bioreactors such as the CSTR seem to be the most suitable for the production of H₂ by dark fermentation and further scaling.

Table 1.1. Summary of hydrogen production performance in several reactor configurations studied by our research group.

	Type of reactor	Substrate	OLR (g/L-d)	Steady-state VHPR (L H ₂ /L-d)	Reference
Suspende-biomass systems	CSTR	CWP	184.4 ^a	24.4	(Davila-Vazquez et al., 2009)
	CSTR	CWP	138.6 ^a	25.0	(Davila-Vazquez et al., 2009)
	CSTR	CWP	92.4 ^a	12.5	(Davila-Vazquez et al., 2009)
	CSTR	CWP	190 ^a	25.8	(Cota-Navarro et al., 2011)
	CSTR	CWP	95 ^a	16.1	(Cota-Navarro et al., 2011)
	CSTR	Lignocellulosic hydrolysates	52.2 ^b	2.5	(Contreras-Dávila et al., 2017)
Fixed-biomass systems	TBR	Glucose	160 ^b	12.0	(Arreola-Vargas et al., 2015)
	TBR	Glucose	80 ^b	12*	(Arreola-Vargas et al., 2015)
	TBR	Lignocellulosic hydrolysates	10 ^b	0.5*	(Arreola-Vargas et al., 2015)
	TBR	Lignocellulosic hydrolysates	52.9 ^b	3.5	(Contreras-Dávila et al., 2017)
	BTF	Lignocellulosic hydrolysates	5.83 ^b	1.7	(Arriaga et al., 2011)
	UASB	CWP	20 ^b	0.4	(Carrillo-Reyes et al., 2012)
	UASB	CWP	48 ^b	0.9*	(Carrillo-Reyes et al., 2014)
	EGSB	Glucose	10	2.5*	(Cisneros-Pérez et al., 2015)
	EGSB	Glucose	25.6	1.3	(Bárcenas-Ruiz et al., 2016)
	ASBBR	Glucose	120	6.2*	(Carrillo-Reyes et al., 2016)
	ASBR	Lignocellulosic hydrolysates	15 ^b	6.7	(Arreola-Vargas et al., 2013)
	AFBR	Glucose	60	5.3*	(Cisneros-Pérez et al., 2017)

CWP: cheese whey powder; CSTR: Continuous stirred-tank reactor; TBR: Trickling bed reactor; BTF: Biotrickling filter; UASB: Up-flow anaerobic sludge blank reactor; EGSB: Expanded granular sludge bed reactor; ASBBR: Anaerobic sequencing batch biofilm reactor; ASBR: Anaerobic sequencing batch reactor; AFBR: Anaerobic fluidized-bed reactor.

* approximately; ^a g lactose; ^b g chemical oxygen demand (COD)

1.3.1 Systematic review of dark fermentation

An extensive analysis of H₂ production in CSTR from the last ten years (see the methodology on Appendix I) showed that research in the field has been carried out extensively worldwide, being China (18), South Korea (10) and Greece (8) the most active countries (Figure 1.2). Moreover, the most used substrates in terms of the number of studies have been glucose (18), sucrose (13) and molasses (10). Other substrates that have been studied with lower frequency are beverage wastewater, cheese whey, fructose, lignocellulosic hydrolysates, starch, and xylose (Figure 1.3). An interesting observation was that dark fermentation research is actually well equilibrated in regard with model and complex substrates (Figure 1.3). Approximately, 45 and 55% of studies reported the use of model and complex substrates, respectively. A further analysis of the operational parameters showed that dark fermentation has been explored mainly at pH between 5 and 6 (53%), temperature of 30-40 °C (78%), HRT higher than 12 h (29%), and stirring conditions in the range of 100-200 rpm (49%) (Figure 1.4).

In addition, in deep analysis of the reported values of VHPR and H₂ yields suggested that such responses are significantly affected by a series of operational parameters, including the inoculum and pretreatment type, substrate type, pH, HRT, stirring velocity and substrate concentration (Tables 1.2 and 1.3).

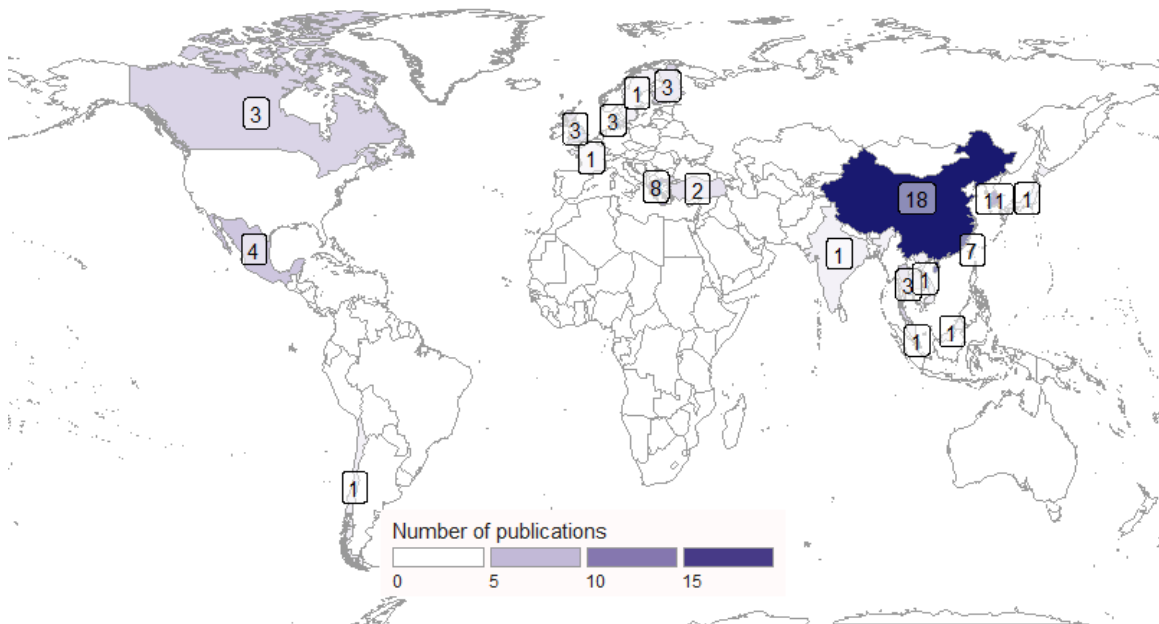


Figure 1.2. Number of articles on dark fermentation with continuous stirred-tank reactors and suspended biomass from 2007 to 2017.

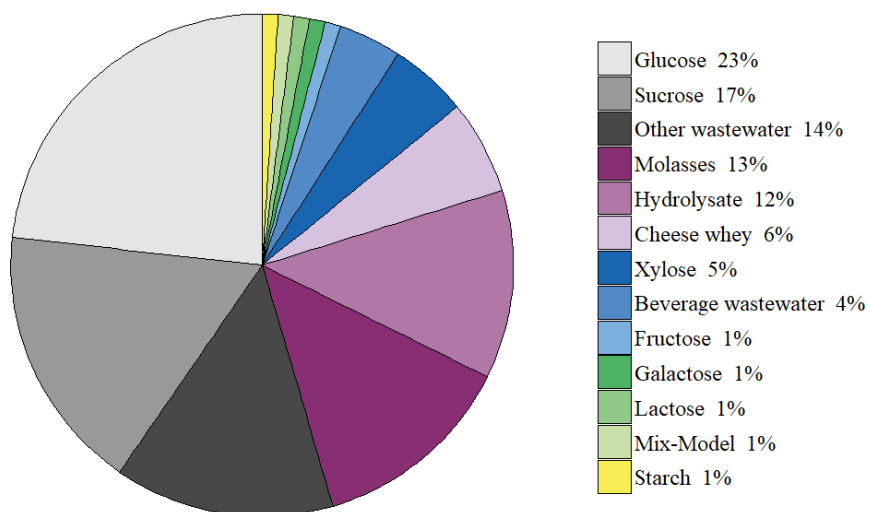


Figure 1.3. Percentage of articles classified by type of substrate in dark fermentation literature.

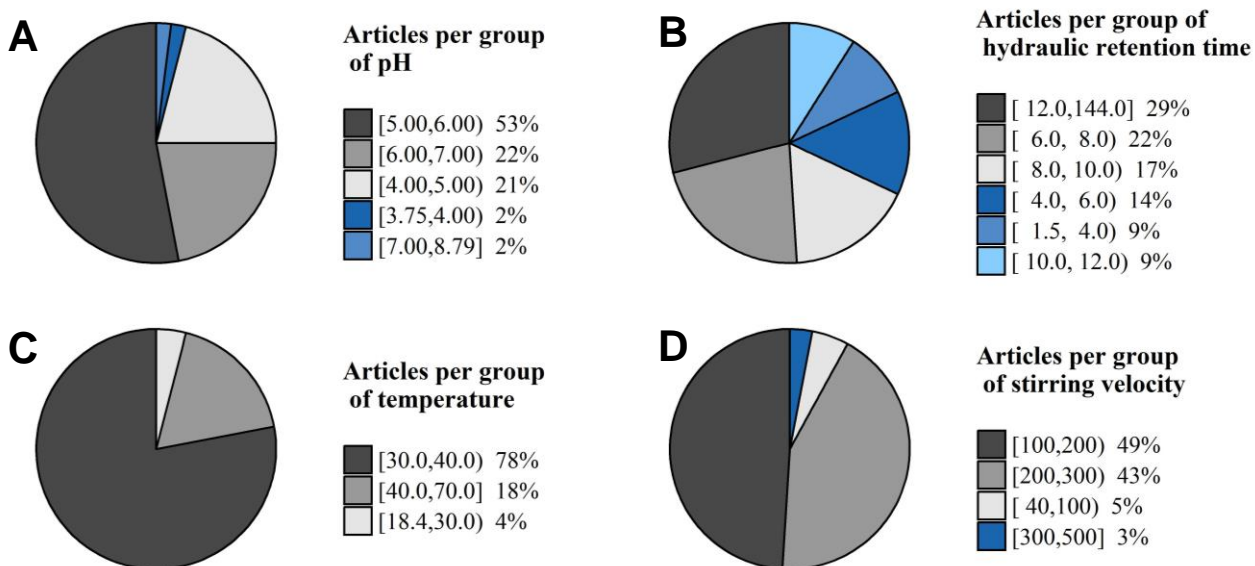


Figure 1.4. Percentage of articles classified by A) pH, B) hydraulic retention time (h), C) temperature (°C) and D) stirring velocity (rpm) in dark fermentation literature.

Table 1.2. Multifactorial ANOVA of the volumetric H₂ production rate in CSTR reactors.

Model structure:
VHPR ~ Inoculum type + Pretreatment type + Substrate type + pH + HRT + Stirring + Substrate concentration

Factor	Sum of squares	% Sum of squares	d.f.	F	p value
Inoculum	7.85	26	5	20.57	2.4 X10 ⁻¹⁴
Pretreatment type	0.47	2	2	3.09	0.049
Substrate type	7.04	23	8	11.53	1.1 X10 ⁻¹¹
pH	1.06	4	2	6.95	0.001
HRT	2.00	7	5	5.25	2.3 X10 ⁻⁴
Stirring velocity	0.66	2	1	8.70	0.004
Substrate concentration	2.98	10	5	7.80	2.7 X10 ⁻⁶
Residuals	8.17	27	107		

Table 1.3. Multifactorial ANOVA of the H₂ molar yield in CSTR reactors.

Model structure:
H₂ yield ~ Inoculum type + Pretreatment type + HRT + Stirring + Substrate concentration

Factor	Sum of squares	% Sum of squares	d.f.	F	p value
Inoculum	5.96	26	5	12.78	5.0 X10 ⁻¹⁰
Pretreatment type	1.19	5	2	6.37	0.002
HRT	1.77	8	5	3.81	0.003
Stirring velocity	0.40	2	1	4.24	0.042
Substrate concentration	1.79	8	5	3.84	0.003
Residuals	11.57	51	124		

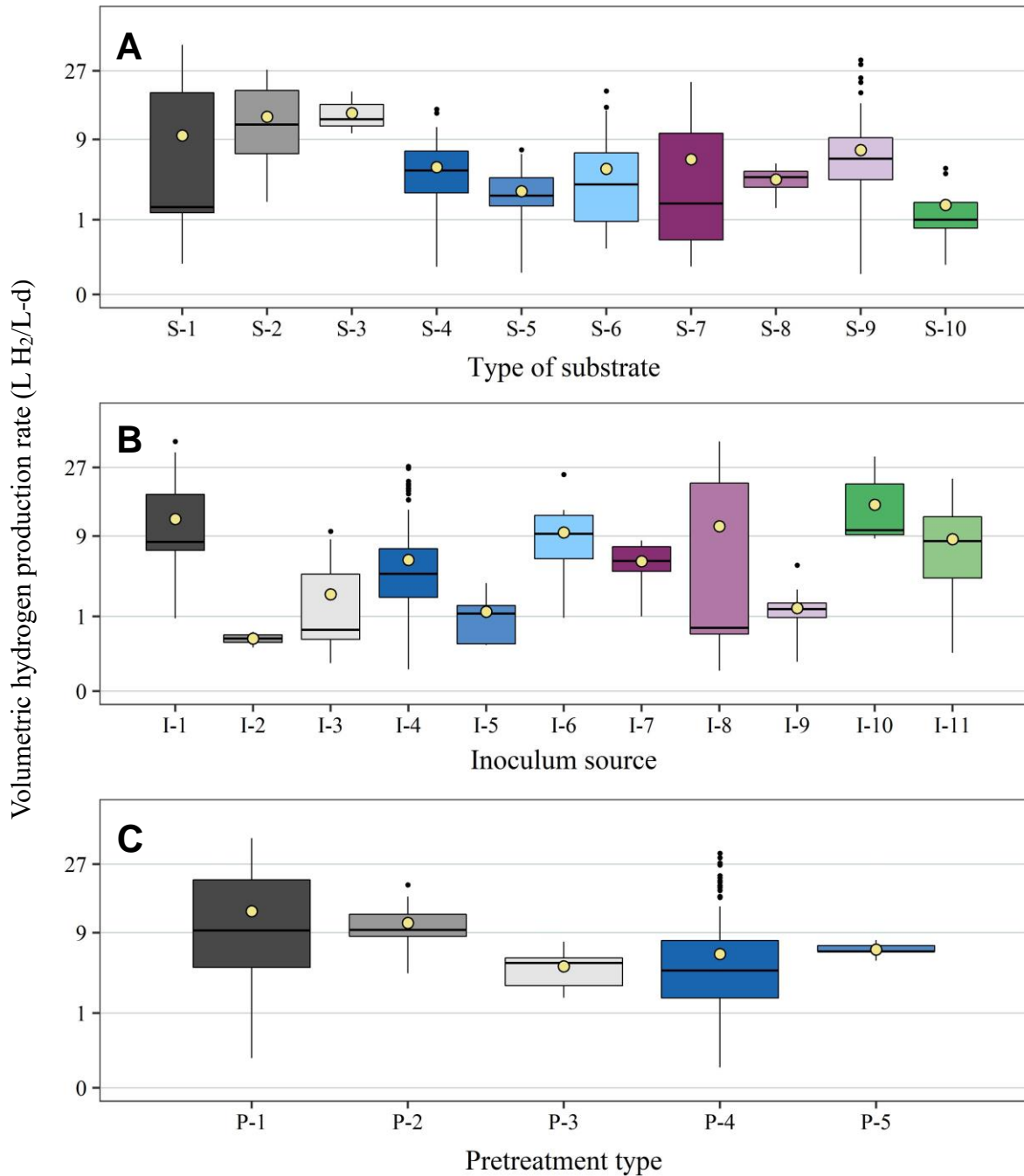


Figure 1.5. Overview of the effects of A) type of substrate, B) inoculum source and C) pretreatment type on the volumetric hydrogen production rate. S-1: Beverage wastewater; S-2: Cheese whey; S-3: Fructose; S-4: Glucose; S-5: Lignocellulosic hydrolysate; S-6: Molasses; S-7: Other wastewater; S-8: Starch; S-9: Sucrose; S10: Xylose; I-1: Acclimated culture; I-2: Acidogenic and methanogenic sludge; I-3: Aerobic sludge; I-4: Anaerobic sludge; I-5: Compost; I-6: Cracked cereals; I-7: Hot spring culture; I-8: Hydrogen producing sludge; I-9: Indigenous; I-10: Marine sediment; I-11: Pure culture. P-1: Acclimation; P-2: Acid and acclimation; P-3: Aeration; P-4: Heat; P-5: Heat and acid.

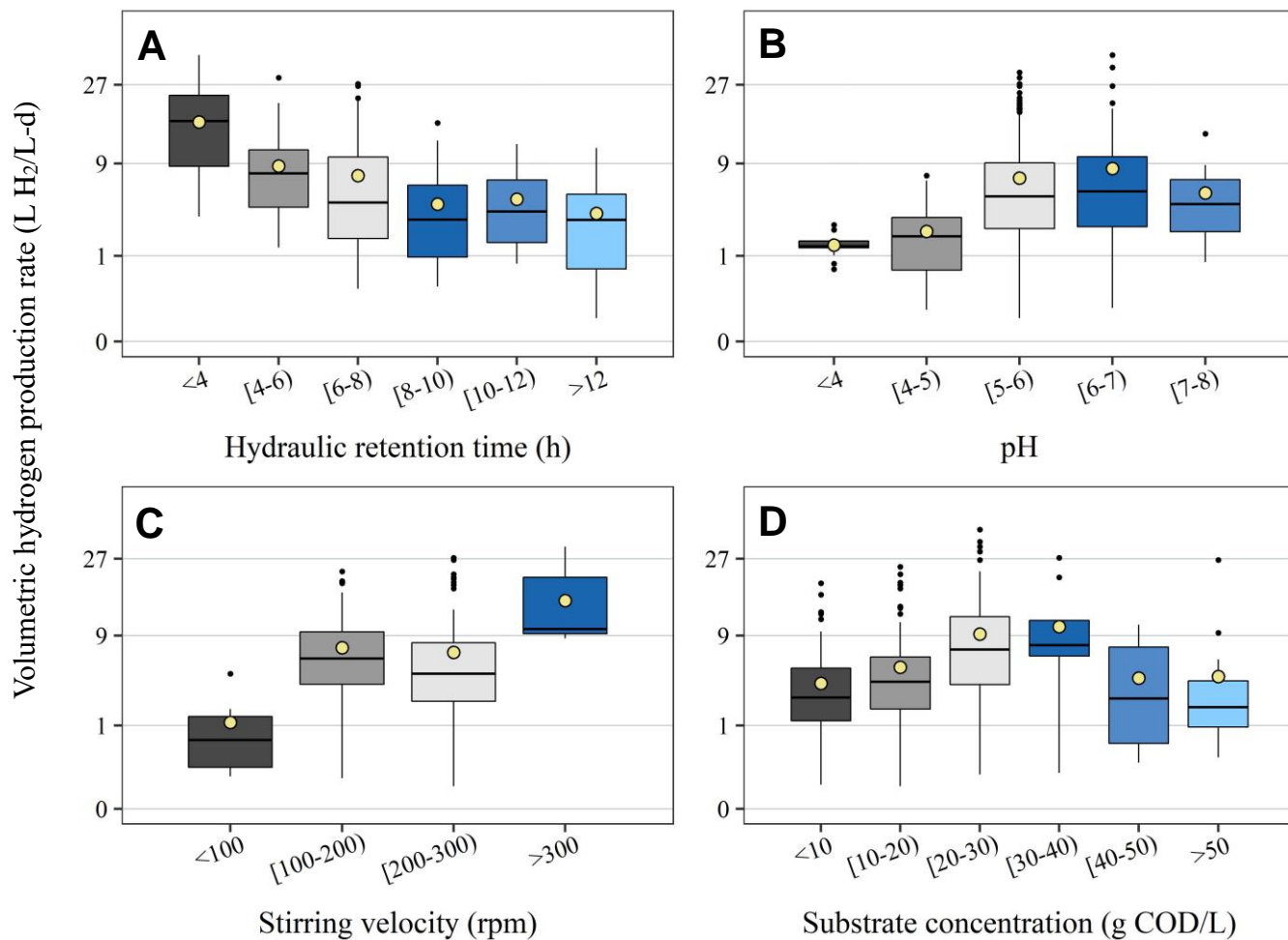


Figure 1.6. Overview of the effects of A) hydraulic retention time, B) pH, C) stirring velocity and D) substrate concentration on the volumetric hydrogen production rate.

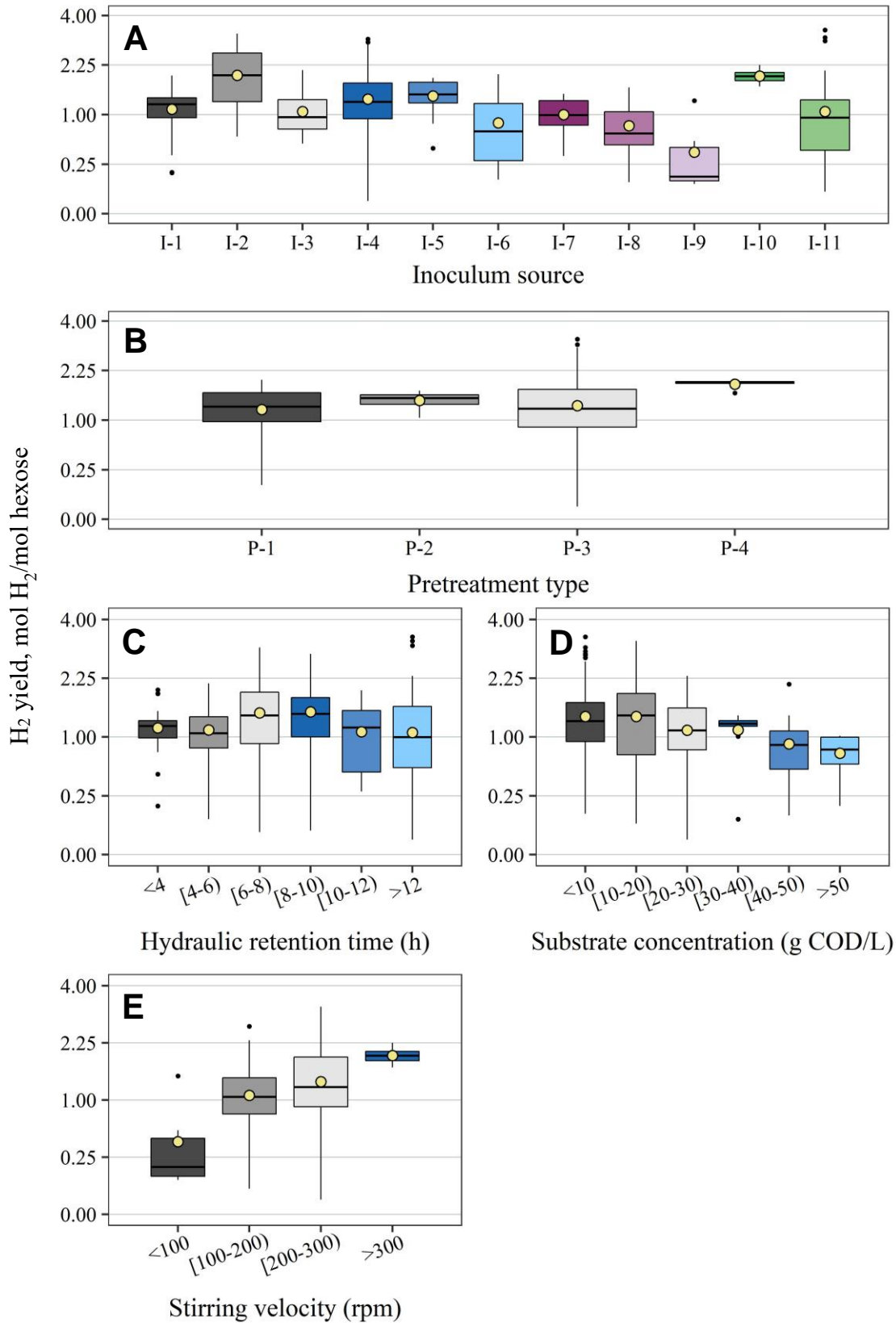


Figure 1.7. Overview of the effects of A) inoculum source, B) pretreatment type, C) hydraulic retention time, D) substrate concentration, and E) stirring velocity on the hydrogen molar yield. I-1: Acclimated culture; I-2: Acidogenic and methanogenic sludge; I-3: Aerobic sludge; I-4: Anaerobic sludge; I-5: Compost; I-6: Cracked cereals; I-7: Hot spring culture; I-8: Hydrogen producing sludge; I-9: Indigenous; I-10: Marine sediment; I-11: Pure culture. P-1: Acclimation; P-2: Acid and acclimation; P-3: Aeration; P-4: Heat and acid.

In detail, the literature analysis showed that the inoculum source has important impacts on both the productivity and efficiency of dark fermentation (Figure 1.5-B and 1.7-A). Regarding this parameter, the maximum average VHPR of 15.6 and 12.3 L H₂/L-d were reported in CSTR that used marine sediments and acclimated sludge as inoculum sources, respectively. In terms of H₂ yield, the most efficient processes were also those inoculated with marine sediment, which averaged 1.93 mol H₂/mol hexose. On the contrary, the use of indigenous microorganisms resulted in the lowest H₂ yield and one of the lowest VHPR, 0.84 mol H₂/mol hexose and 1.38 L H₂/L-d, respectively. Furthermore, anaerobic sludge, one of the most used inoculum sources in dark fermentation, averaged VHPR and H₂ yields of 2.19 L H₂/L-d and 1.35 mol H₂/mol hexose, respectively.

The substrate type is another parameter that significantly influences H₂ production. Figure 1.5A shows that fructose and cheese whey had the maximum average VHPR values of 14.4 and 13.5 L H₂/L-d, respectively. These substrates also showed two of the highest H₂ yields that were about 1.6 mol H₂/mol hexose. In contrast, reactors fed with xylose obtained an average VHPR of 1.73 L H₂/L-d and H₂ yield of 0.56 mol H₂/mol hexose, being the lowest values among the substrates reported.

Operational parameters such as substrate concentration, HRT, pH and stirring velocity also displayed significant effects on VHPR and H₂ yield. The observations in regard with the substrate feeding concentration suggest that low concentrations (< 20 g COD/L) are generally associated with relatively high H₂ yields (~1.4 mol H₂/mol hexose); meanwhile, the H₂ yield was relatively low (0.74 and 0.88 mol H₂/mol hexose) in CSTR systems operated at concentrations above 40 g COD/L. Nevertheless, by contrasting the H₂ yields and corresponding VHPR values, it becomes evident that the most suitable substrate concentrations are generally in the range of 20 to 40 g COD/L. At such conditions, the VHPR reaches the maximum average value of 10.44 L H₂/L-d (30-40 g COD/L) while the H₂ yield is still within acceptable values (1.12 mol H₂/mol hexose).

The behavior of dark fermentation in regard with HRT reveals that such parameter has slight effects on the H₂ yield but significant effects on the VHPR (Figures 1.6A and 1.7C). The highest average VHPR of 16.9 L H₂/L-d was reported for systems operated at HRT below 4 h, despite of the possibility of washout that has been broadly discussed in literature. As the HRT increases, the VHPR drops until a minimum average of 3.35 L H₂/L-d at HRT > 12 h. Thus, the use of long HRT could only be justified for substrates with high complexity, where *in situ* hydrolysis takes place before the actual dark fermentation. However, the substrates analyzed in the referred systematic review were mostly suitable for dark fermentation at

short HRT, lower or equal to 12 h. By operating at short HRT, the reaction volume required to process a certain amount of substrate will decrease, leading to important savings in reactor investment and operation. Finally, yet important, the use of short HRT cause negligible detrimental effects on the H₂ yield that are expected to be compensated by the increase of VHPR.

In regard with pH, the literature research clearly shows that values between 5 and 7 resulted in a better performance in terms of VHPR than pH values below 5 and above 7 (Figure 1.6B). The group of fermentations performed at pH 5-6 reported a VHPR of 6.95 L H₂/L-d, while those performed at pH 6-7 averaged 8.28 L H₂/L-d. According with these observations, the operation at pH between 6 and 7 seemed to be the most suitable for the productivity of dark fermentative systems. On the contrary, the operation at pH below 5 and above 7 did negatively affect the VHPR. In regard with the H₂ yield, the pH has relatively small effect on the efficiency of H₂ production, except when pH is below 4, where the H₂ yield averaged only 0.31 mol H₂/mol hexose.

Further analysis of literature also revealed an interesting relationship between the stirring velocity and the productivity and efficiency of H₂ production (Figures 1.6C and 1.7E). Under stirring velocities of 40-100 rpm, average VHPR of 1.12 L H₂/L-d and H₂ yield of 0.4 mol H₂/mol hexose were observed. In contrast, when the stirring velocity was of 300-400 rpm, the average VHPR increased up to 15.6 L H₂/L-d while the H₂ yield also escalated to 1.93 mol H₂/mol hexose. This observation clearly suggests a relevant role of the mass transfer phenomenon in dark fermentation.

Beyond the VHPR and H₂ yield, the systematic review also provided key information in regard with the production of metabolites and their relationship with the different aforementioned variables. For instance, it was clearly shown that the acetate concentration found in CSTR systems is positively linked with the substrate concentration (Figure 1.8). A similar outcome can also be observed with butyrate. Interestingly, the rate at which acetate and butyrate concentrations increase are different to each other. In such a way, acetate and butyrate are generally found at similar concentrations in systems operated at substrate concentrations below 10 g COD/L. However, as the substrate concentration increases, butyrate is produced in a higher proportion than acetate, which decreases the acetate/butyrate ratio.

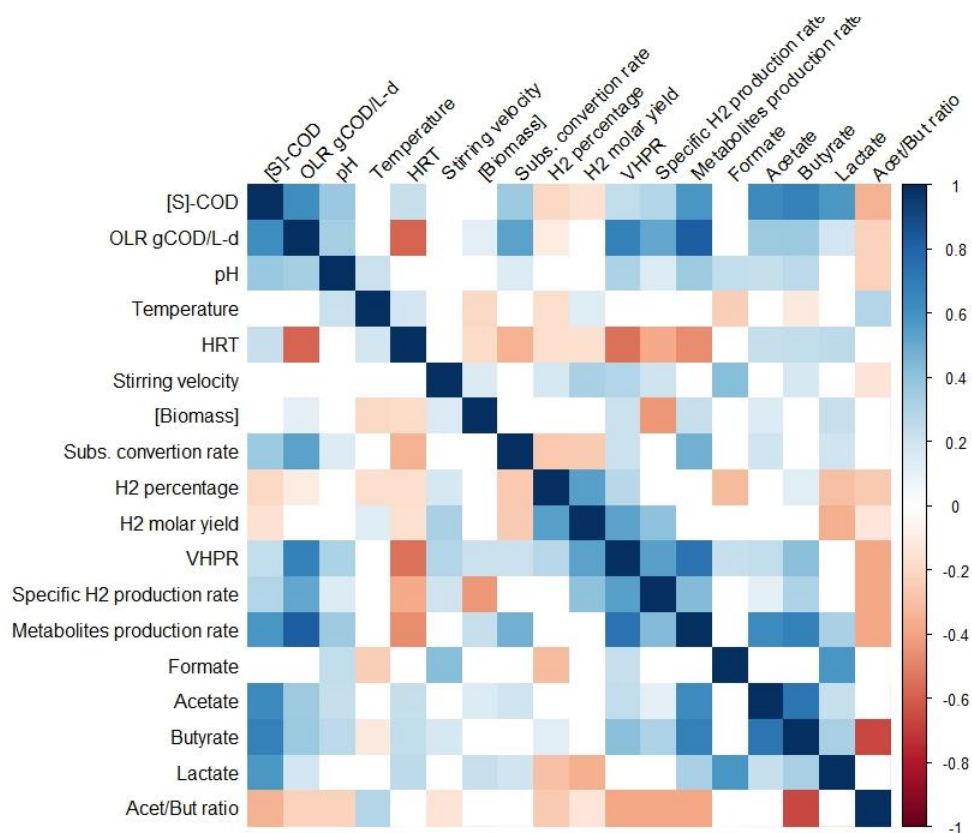


Figure 1.8. Matrix of Pearson’s correlations between the multiple variables involved in H₂ production in continuous stirred-tank reactors.

The analysis also showed that the substrate concentration is linked positively with lactate concentration. However, it is not linked to H₂ production. Indeed, it was revealed that the amount of lactate produced during dark fermentation is correlated negatively with the H₂ yield (Figure 1.8). This finding clearly suggests that the lactate production could be associated with sub-optimal conditions for H₂ production. In fact, the lactate concentration was found to be inversely related with other metabolites associated with efficient H₂ production pathways (*i.e.* butyrate and acetate) (Figure 1.8). Therefore, the increase of lactate concentrations can be annotated as a signal of metabolic shifts taking place in dark fermentation as possible response under certain environmental conditions. Besides, a strong correlation was also observed between lactate and formate concentrations; nevertheless, further research would be required to find clear explanations of this type of relationships.

1.4 Challenges of dark fermentation biotechnology

In summary, the broad analysis of literature on dark fermentation revealed a main aspect worth to highlight: The H₂ yield of dark fermentative processes is generally below the metabolic threshold of two

mol H₂/mol hexose despite of the extensive work developed worldwide for decades. Such an issue is possibly associated with the appearance of undesired metabolic routes and/or microorganisms. In this regard, two metabolic pathways have been recently identified as potential H₂ sinks: homoacetogenesis and lactic acid production. These metabolic routes can be associated in turn with different underlying causes reviewed in the previous section (1.3.1), with special emphasis on the rate at which the H₂ produced is released from the fermentation broth. In the following lines, a brief description of these three phenomena is provided.

1.4.1 Homoacetogenesis

Homoacetogens, named after their analogy to homolactic bacteria, are strict anaerobic bacteria capable to synthesize acetate from eight reducing equivalents (*e.g.* 4 mol H₂) and two mol of CO₂ through the Wood-Ljungdahl pathway (Eq. 1.8) (Diekert and Wohlfarth, 1994; Drake et al., 1997; Ljungdahl et al., 1989; Ljungdahl, 1986). Due to such capability, homoacetogens are able to produce up to three mol of acetate from one mol of glucose consumed: two from heterotrophic and one from autotrophic metabolism.



Due to their extensive metabolic capacities, homoacetogens are microorganisms widely distributed among anaerobic environments (Drake et al., 1997; Ragsdale and Pierce, 2008). However, in mesophilic conditions, their hydrogenotrophic activity is usually overlapped by hydrogenotrophic methanogenesis, which can obtain more energy from H₂ consumption. In the absence of methanogens, as it is the case of dark fermentative systems, homoacetogens are expected to play a relevant role in H₂ consumption, and therefore in the performance of H₂ production (Carrillo-Reyes et al., 2014).

Due to their negative implications in H₂ production, the prevention and control of homoacetogenesis has been focus of attention in recent years. However, given that most of homoacetogens relevant to dark fermentative systems belong to the genus *Clostridium*, the avoidance of homoacetogenesis is specially challenging. For instance, according with Oh et al. (2003), Luo et al. (2011) and Carrillo-Reyes et al. (2014), homoacetogens can survive heat treatment of the inoculum. This is because several of them are capable to sporulate, as it is the case of *Clostridium spp*, thus the heat treatment is not actually affecting homoacetogens. Particularly, Luo et al. (2011) showed that homoacetogens are only inhibited under relatively low pH (5.5) and thermophilic conditions (55°C). Similar conclusions in regard with temperature and pH were also reported by Luo et al. (2010) and Shanmugam et al. (2014). From the

thermodynamic perspective, homoacetogenesis becomes favorable at temperatures below 45°C, which can explain such observations (Kleerebezem and Van Loosdrecht, 2010).

Other factors that affect the thermodynamics of homoacetogenesis are the actual concentrations of involved species, *e.g.* H₂, CO₂, and acetate. In this concern, reducing the partial pressure of H₂ (ρ_{H_2}) and/or CO₂ (ρ_{CO_2}) could be advantageous. Kisielewska et al. (2015) used a reduced pressure reactor to evaluate the effects of such strategy on dark fermentative H₂ production. They found that a reduced pressure system produced more gas and H₂ than the atmospheric pressure reactor. Interestingly, they observed an unstable performance in the control reactor that was operated under atmospheric pressure. In the control reactor, the VHPR decreased abruptly after OLR was increased from 30 to 35 g COD/L-d. Authors attributed such behavior to the presence of homoacetogens. Contrastingly, in experiments reported by Liu and Wang (2017), homoacetogenesis was not fully controlled by reduced H₂ pressure. Their experiments showed that a reduced pressure improved the fermentation performance, however, the ratio of measured to theoretical productivity of H₂ decreased. With a different approach, Massanet-Nicolau et al. (2010) evaluated headspace flushing and bioreactor sparging with N₂ as methods to avoid H₂ consumption. Both methods were useful, but N₂ sparging was the most effective. The methods tested caused a more stable H₂ production performance and more stable acetate concentration. Similarly, Chang et al. (2012) reported that only a continuous gas releasing method combined with the CO₂ absorption into NaOH solution enhanced H₂ production and reduced its consumption by homoacetogens. More recently, Massanet-Nicolau et al. (2016) reported a system with electrochemical H₂ removal and CO₂ absorption as an effective strategy to increase H₂ yields and avoid H₂ consumption.

Operational parameters such as HRT, substrate concentration, OLR and reactor type might also influence homoacetogenesis. In a CSTR, Arooj et al. (2008) reported the effect of HRT (4-18 h) on homoacetogenesis. They found that the ratio of homoacetogenic acetate to total acetate ranged from 27 to 57% as function of HRT. Short values of HRT (4-9 h) favored the H₂ consumption and presented up to 57% of homoacetogenic acetate. On the other hand, at relatively high HRT (12-18 h), the homoacetogenesis was diminished. However, homoacetogenesis was not completely inhibited and it was present during the whole operation. Gonçalves et al. (2014) studied the influence of initial substrate concentration on H₂ consuming metabolisms in batch reactors. They reported that homoacetogenesis activity was avoided at a relatively high substrate concentration of 50 g COD/L. The mechanism behind such inhibition was not clarified, but the low pH observed (pH 5) could be possible involved. Davila-Vazquez et al. (2009) studied H₂ production with cheese whey at different OLR (92.4-184.4 g lactose/L-

d). Interestingly, they reported an unexpected decrease of the VHPR with an OLR of 184 g lactose/L-d. Such phenomenon was concomitant to the increase of acetic acid and it was suggested as an indicative of homoacetogenesis occurrence. Finally, in regard with the type of reactor, Si et al. (2015b) showed that homoacetogenesis was more favorable in packed bed reactors (PBR) than in UASB. In a PBR, homoacetogenesis accounted 11.1% of the total acetate observed while in the UASB reactor was 1.5%. The higher microbial diversity in the PBR in comparison with the UASB could be a possible explanation of such finding.

Overall, short HRT, high substrate concentrations, relatively low pH, thermophilic temperatures, continuous gas release, and CO₂ absorption showed to have important impacts to avoid homoacetogenesis. Nevertheless, studies about homoacetogenesis in H₂ production systems are still scarce and more research is needed to fully understand and control its occurrence.

1.4.2 Lactic acid bacteria

The group of lactic acid bacteria (LAB) is composed by microorganisms capable to consume a wide range of carbohydrate-rich substrates and produce lactic acid as a major metabolic product (Reddy et al., 2008). These Gram-positive organisms can grow in a wide range of temperature (5-45 °C) and pH (3.2-9.6); however, they have complex nutritional requirements because most of them are auxotrophic for amino acids, purine and pyrimidine bases, and B-group vitamins synthesis (Reddy et al., 2008; Wang et al., 2015).

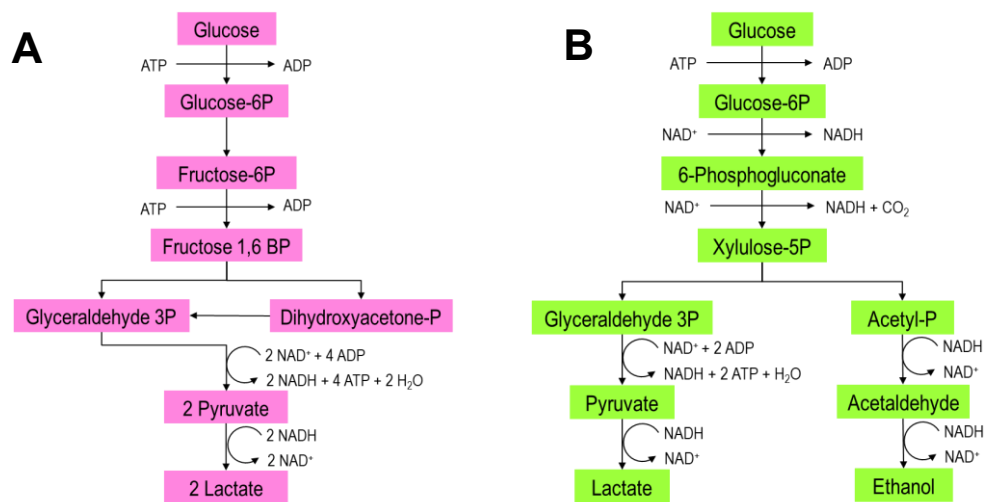


Figure 1.9. Metabolic pathways of lactic acid bacteria. A) Homolactic fermentation. B) Heterolactic fermentation. Adapted from Reddy et al. (2008).

LAB can be further classified in homolactic and heterolactic in accordance with their metabolic capacities (Figure 1.9). The former sub-group follows a metabolic route that leads to the synthesis of a maximum metabolic yield of 2 mol of lactic acid per mol of hexose. On the other hand, heterolactic bacteria conducts the carbohydrates fermentation towards the synthesis of 1 mol of lactic acid and 1 mol of ethanol per mol of hexose. Representative members of the homolactic and heterolactic sub-group are shown in Table 1.4. It is worth to note that some microorganisms have the ability to use both routes in response to environmental conditions.

Table 1.4. Classification of lactic acid bacteria metabolism. Modified from De Angelis and Gobbetti (2011).

Homolactic fermentative	Heterolactic fermentative	
	Facultative	Strict
<i>L. acidophilus</i>	<i>L. plantarum</i>	<i>L. brevis</i>
<i>L. helveticus</i>	<i>L. rhamnosus</i>	<i>L. buchneri</i>
<i>L. delbrueckii subsp. delbrueckii</i>	<i>L. coryneformis</i>	<i>L. fermentum</i>
<i>L. delbrueckii subsp. lactis</i>	<i>L. curvatus</i>	<i>L. kefi</i>
<i>L. delbrueckii subsp. bulgaricus</i>	<i>L. casei</i>	<i>L. reuteri</i>
<i>Lc. lactis</i>	<i>L. paracasei</i>	<i>Leuconostoc sp.</i>
<i>S. thermophilus</i>		
<i>S. pyogenes</i> (M1 GAS)*		
<i>S. pneumoniae</i> (ATCC 700669)*		
<i>S. agalactiae</i> (2603)*		

* KEEG pathway annotation

L.: *Lactobacillus*; *Lc.*: *Lactococcus*; *S.*: *Streptococcus*

The presence of LAB in H₂-producing systems is considered to be detrimental for the performance of dark fermentation due to substrate competition and their ability to produce bactericins (Sikora et al., 2013). For instance, Gomes et al., (2016) reported detrimental effects of LAB on H₂ production from cassava flour wastewater. They argued that the observations were ultimately caused by the presence of bacteriocins Nisin A and Nisin Z. In another study, researchers showed that the supernatant of *Lactobacillus* cultures strongly affected H₂ production by dark fermentative bacteria (Noike et al., 2002). Researchers also suggested heat pretreatment as a strategy to avoid the presence of lactic bacteria (Noike et al., 2002).

LAB have been extensively reported in H₂-producing reactors; in some cases, they were found in co-dominance with *Clostridium* species (Etchebehere et al., 2016). Thus, the inhibitory effects of LAB are possibly dependent on the fermentation conditions (pH, temperature, substrate concentration, etc.). In either case, even without bacteriocins production, LAB compete for substrate intake, leading to a decrease of the efficiency of H₂ production. In this sense, the mechanisms of appearance/disappearance of LAB and their relationship with dark fermentation are still not well understood.

1.4.3 Mass transfer limitations

H₂ transfer mechanism.

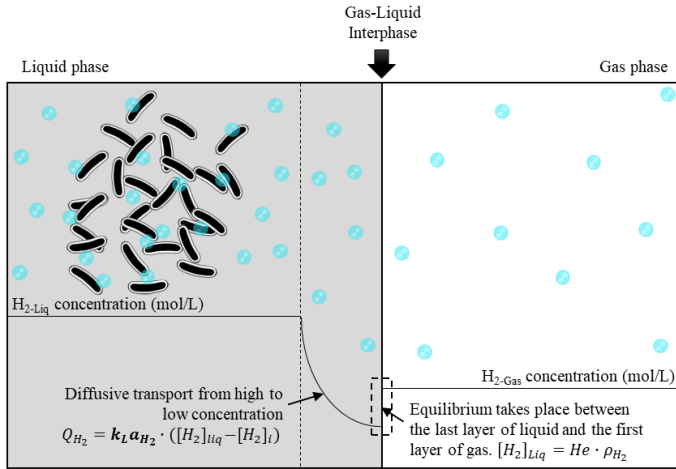


Figure 1.10. The H₂ mass transfer mechanism during the continuous operation of dark fermentative systems.

To recover H₂ in the gas phase, each H₂ molecule must overcome the resistance of the gas-liquid interphase (Figure 1.10). First, the molecules move by convective transport to the proximity of the interphase layer. Then, in accordance with the film model, diffusive transport will take place at a transfer rate proportional to the difference of concentrations between the bulk and the gas-liquid interphase (Green and Perry, 2014). The proportionality constant of such equation is the mass-transfer coefficient, $k_{L,a}$, which accounts for physical properties of the system (in particular, the diffusivity, fluid density and viscosity) and the fluid motion.

At that limit (the interphase), the liquid and gas concentrations are linked to each other by an equilibrium equation, *i.e.* the Henry's law equation. Once the molecule is transferred to the first layer of the gas phase, it will diffuse to the bulk of the gas phase also driven by a difference of concentrations. In practice, since the liquid transport is the limiting step, the gas phase transport is often neglected.

CSTR systems are often referred as efficient reactors due to the theoretical absence of gradients of substrate, nutrients, pH and temperature. Nevertheless, the interphase mass transfer efficiency cannot be given for granted. Indeed, it is possible that liquid-gas inefficient mass transfer is behind of the observations showed in Figures 1.6D and 1.7E.

What is the link between the H₂ mass transfer and dark fermentation performance?

A low H₂ partial pressure and, therefore, low dissolved H₂ concentrations are critical to reach high H₂ production rates. From a thermodynamic perspective, the feasibility of H₂ production, measured as the Gibbs free energy ($\Delta G'$), depends on the ratio of oxidized/reduced electron carriers (NAD⁺/NADH, Fd_{ox}/Fd_{red}, etc.) and the dissolved H₂ concentration within the fermentative cells. Assuming that the

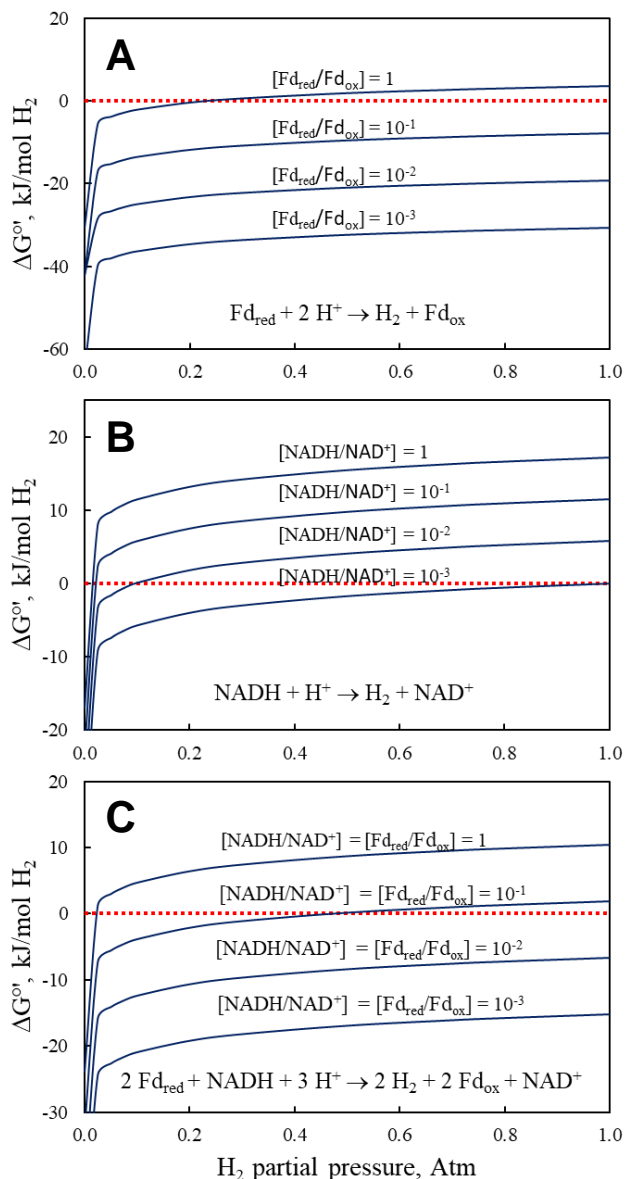


Figure 1.11. Effects of the H_2 partial pressure on the Gibbs free energy ($\Delta G'$) of H_2 production from A) ferredoxin, B) NADH, and C) ferredoxin+NADH at different ratios of oxidized/reduced electron carriers. Gibbs free energy is reported at standard physiological conditions (pH 7 and 25°C).

concomitant with the decrease of H_2 and acetone yields. Other researchers reported that the H_2 consumption activity by *Clostridium P11* increases as function of the H_2 partial pressure (Skidmore et al.,

dissolved H_2 concentration can be related with the H_2 partial pressure in the gas phase through the Henry's law, the $\Delta G'$ can also be expressed as function of the H_2 partial pressure of the fermentative system.

In general, at fixed ratios of oxidized/reduced mediators, the increase of the H_2 partial pressure leads to an increase of the $\Delta G'$ of H_2 production (Figure 1.11). Specifically, H_2 production by the ferredoxin-dependent hydrogenase (Figure 1.11A), at $[\text{Fd}_{\text{red}}]/[\text{Fd}_{\text{ox}}]=10^{-1}$, is thermodynamically feasible within the whole range of ρ_{H_2} . However, the H_2 synthesis from NADH-dependent hydrogenase is only feasible at very low ρ_{H_2} (<0.01 Atm) (Figure 1.11B). At higher ρ_{H_2} , H_2 production from NADH is thermodynamically feasible only through the electron-bifurcating mechanism that is catalyzed by the ferredoxin-NAD-dependent hydrogenase (HydABC) (Buckel and Thauer, 2013; Sieber et al., 2012; Wang et al., 2013).

Beyond the thermodynamic predictions, the detrimental effects of the increase of ρ_{H_2} has been reported experimentally. For instance, Yerushalmi et al. (1985) showed that the increase of ρ_{H_2} leads to a diversification of metabolic routes in *C. acetobutylicum* and the inhibition of H_2 production. The researchers reported that H_2 pressures above 270 kPa led to higher productivity of butanol

2013). In CSTR, Lee et al. (2012) studied the effects of reduced pressure on H₂ production; they found that H₂ production rate increased by 8% when changed from 760 to 380 mmHg.

1.5 Scope and structure of the research

Based on the challenges reviewed above, the present thesis aimed to investigate the causes behind suboptimal H₂ production. Specifically, the research focused on the environmental conditions that could trigger the appearance of homoacetogenes and LAB as well as the impacts of gas-liquid mass transfer.

As first approach, the research was orientated towards the analysis of the impacts of the HRT on dark fermentation (Chapter 2). It was hypothesized that LAB could negatively respond to the selection pressure set by HRT. In parallel, short HRT values also increase the availability of organic carbon that could force homoacetogens of the genus *Clostridium* to use it instead of the inorganic carbon (CO₂) needed for homoacetogenesis.

In the following set of experiments, the effects of the substrate concentration at fixed HRT were investigated (Chapter 3). Through this strategy, it was aimed to test if the microbial community and metabolic pathways of dark fermentation can diversify as cause of the substrate concentration. The hypothesis was that high availability of substrate can avoid the occurrence of homoacetogenesis; although, the strategy could also lead to the appearance of other undesired microorganisms.

In chapter 4, the impact of the gas-liquid mass transfer efficiency on H₂ production was investigated. In this approach, it was considered that the reduction of H₂ partial pressure could lead not only to higher productivities and efficiencies but also serve as control tool to avoid metabolic and microbial diversification.

Finally, in chapter 5, a summary of the main conclusions along with a general discussion is developed. The main objective of this chapter was to give a general perspectives of the research opportunities in the field.

1.6 References

- Arooj, M., Han, S., Kim, S., Kim, D., Shin, H., 2008. Continuous biohydrogen production in a CSTR using starch as a substrate. *Int. J. Hydrogen Energy* 33, 3289–3294. doi:10.1016/j.ijhydene.2008.04.022
- Arreola-Vargas, J., Alatríste-Mondragón, F., Celis, L.B., Razo-Flores, E., López-López, A., Méndez-Acosta, H.O., 2015. Continuous hydrogen production in a trickling bed reactor by using triticale silage as inoculum: effect of simple and complex substrates. *J. Chem. Technol. Biotechnol.* 90, 1062–1069. doi:10.1002/jctb.4410
- Arreola-Vargas, J., Celis, L.B., Buitrón, G., Razo-Flores, E., Alatríste-Mondragón, F., 2013. Hydrogen production from acid and enzymatic oat straw hydrolysates in an anaerobic sequencing batch reactor : Performance and microbial population analysis. *Int. J. Hydrogen Energy* 38, 13884–13894.
- Arriaga, S., Rosas, I., Alatríste-Mondragón, F., Razo-Flores, E., 2011. Continuous production of hydrogen from oat straw hydrolysate in a biotrickling filter. *Int. J. Hydrogen Energy* 36, 3442–3449. doi:10.1016/j.ijhydene.2010.12.019
- Bárcenas-Ruiz, C.D., Carrillo-Reyes, J., Arellano-García, L., Celis, L.B., Alatríste-Mondragón, F., Razo-Flores, E., 2016. Pretreatment and upward liquid velocity effects over granulation in hydrogen producing EGSR reactors. *Biochem. Eng. J.* 107, 75–84. doi:10.1016/j.bej.2015.12.010
- Buckel, W., Thauer, R.K., 2013. Energy conservation via electron bifurcating ferredoxin reduction and proton/Na⁺ translocating ferredoxin oxidation. *Biochim. Biophys. Acta - Bioenerg.* 1827, 94–113. doi:10.1016/j.bbabi.2012.07.002
- Cabrol, L., Marone, A., Tapia-Venegas, E., Steyer, J.-P., Ruiz-Filippi, G., Trably, E., 2017. Microbial ecology of fermentative hydrogen producing bioprocesses: useful insights for driving the ecosystem function. *FEMS Microbiol. Rev.* 41, 158–181. doi:10.1093/femsre/fuw043
- Carrillo-Reyes, J., Celis, L.B., Alatríste-Mondragón, F., Montoya, L., Razo-Flores, E., 2014. Strategies to cope with methanogens in hydrogen producing UASB reactors: Community dynamics. *Int. J. Hydrogen Energy* 39, 11423–11432. doi:10.1016/j.ijhydene.2014.05.099
- Carrillo-Reyes, J., Celis, L.B., Alatríste-Mondragón, F., Razo-Flores, E., 2014. Decreasing methane production in hydrogenogenic UASB reactors fed with cheese whey. *Biomass and Bioenergy* 63, 101–108. doi:10.1016/j.biombioe.2014.01.050
- Carrillo-Reyes, J., Celis, L.B., Alatríste-Mondragón, F., Razo-Flores, E., 2012. Different start-up strategies to enhance biohydrogen production from cheese whey in UASB reactors. *Int. J. Hydrogen Energy* 37, 5591–5601. doi:10.1016/j.ijhydene.2012.01.004
- Carrillo-Reyes, J., Trably, E., Bernet, N., Latrille, E., Razo-Flores, E., 2016. High robustness of a simplified microbial consortium producing hydrogen in long term operation of a biofilm fermentative reactor. *Int. J. Hydrogen Energy* 41, 2367–2376. doi:10.1016/j.ijhydene.2015.11.131
- Chang, S., Li, J., Liu, F., Yu, Z., 2012. Effect of different gas releasing methods on anaerobic fermentative hydrogen production in batch cultures. *Front. Environ. Sci. Eng.* 6, 901–906. doi:10.1007/s11783-012-0403-1
- Cisneros-Pérez, C., Carrillo-Reyes, J., Celis, L.B., Alatríste-Mondragón, F., Etchebehere, C., Razo-Flores, E., 2015. Inoculum pretreatment promotes differences in hydrogen production performance in EGSR reactors. *Int. J. Hydrogen Energy* 40, 6329–6339. doi:10.1016/j.ijhydene.2015.03.048
- Cisneros-Pérez, C., Etchebehere, C., Celis, L.B., Carrillo-Reyes, J., Alatríste-Mondragón, F., Razo-Flores, E., 2017. Effect of inoculum pretreatment on the microbial community structure and its performance during dark fermentation using anaerobic fluidized-bed reactors. *Int. J. Hydrogen Energy* 42, 9589–9599. doi:10.1016/j.ijhydene.2017.03.157
- Contreras-Dávila, C.A., Méndez-Acosta, H.O., Arellano-García, L., Alatríste-Mondragón, F., Razo-Flores, E., 2017. Continuous hydrogen production from enzymatic hydrolysate of Agave tequilana bagasse: Effect of

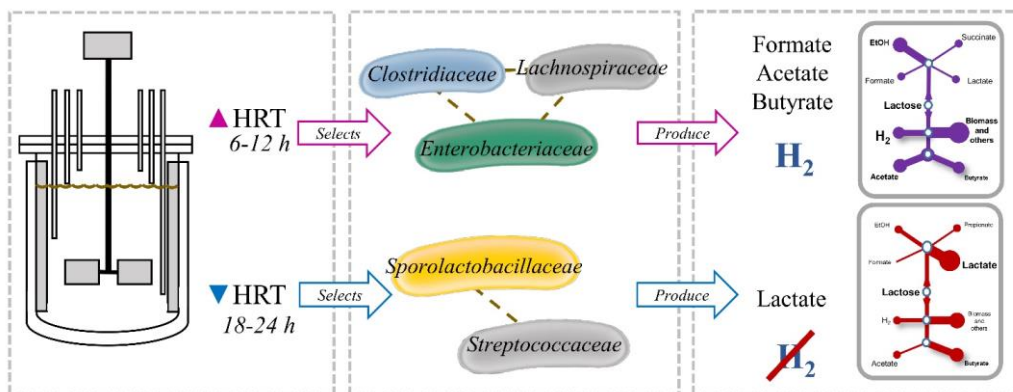
- the organic loading rate and reactor configuration. *Chem. Eng. J.* 313, 671–679. doi:10.1016/j.cej.2016.12.084
- Cota-Navarro, C.B., Carrillo-Reyes, J., Davila-Vazquez, G., Alatraste-Mondragón, F., Razo-Flores, E., 2011. Continuous hydrogen and methane production in a two-stage cheese whey fermentation system. *Water Sci. Technol.* 64, 367–374. doi:10.2166/wst.2011.631
- Davila-Vazquez, G., Cota-Navarro, C.B., Rosales-Colunga, L.M., de León-Rodríguez, A., Razo-Flores, E., 2009. Continuous biohydrogen production using cheese whey: Improving the hydrogen production rate. *Int. J. Hydrogen Energy* 34, 4296–4304. doi:10.1016/j.ijhydene.2009.02.063
- De Angelis, M., Gobbetti, M., 2011. *Lactobacillus* SPP.: General Characteristics, in: Fuquay, J.W., Fox, P.F., McSweeney, P.L.H. (Eds.), *Encyclopedia of Dairy Science*. Elsevier.
- Diekert, G., Wohlfarth, G., 1994. Metabolism of homocetogens. *Antonie Van Leeuwenhoek* 66, 209–21.
- Drake, H.L., Daniel, S.L., Küsel, K., Matthies, C., Kuhner, C., Braus-Stromeyer, S., 1997. Acetogenic bacteria: what are the in situ consequences of their diverse metabolic versatilities? *BioFactors* 6, 13–24. doi:10.1002/biof.5520060103
- Etchebere, C., Castelló, E., Wenzel, J., del Pilar Anzola-Rojas, M., Borzacconi, L., Buitrón, G., Cabrol, L., Carminato, V.M., Carrillo-Reyes, J., Cisneros-Pérez, C., Fuentes, L., Moreno-Andrade, I., Razo-Flores, E., Filippi, G.R., Tapia-Venegas, E., Toledo-Alarcón, J., Zaiat, M., 2016. Microbial communities from 20 different hydrogen-producing reactors studied by 454 pyrosequencing. *Appl. Microbiol. Biotechnol.* 100, 3371–3384. doi:10.1007/s00253-016-7325-y
- Gomes, S.D., Fuess, L.T., Mañunga, T., Feitosa de Lima Gomes, P.C., Zaiat, M., 2016. Bacteriocins of lactic acid bacteria as a hindering factor for biohydrogen production from cassava flour wastewater in a continuous multiple tube reactor. *Int. J. Hydrogen Energy* 41, 8120–8131. doi:10.1016/j.ijhydene.2015.11.186
- Gonçalves, M.R., Costa, J.C., Pereira, M. a., Abreu, A. a., Alves, M.M., 2014. On the independence of hydrogen production from methanogenic suppressor in olive mill wastewater. *Int. J. Hydrogen Energy* 39, 6402–6406. doi:10.1016/j.ijhydene.2014.02.056
- Green, D., Perry, R., 2014. *Perry's Chemical Engineer Handbook*, Igarss 2014. doi:10.1007/s13398-014-0173-7.2
- Hawkes, F., Hussy, I., Kyazze, G., Dinsdale, R., Hawkes, D., 2007. Continuous dark fermentative hydrogen production by mesophilic microflora: Principles and progress. *Int. J. Hydrogen Energy* 32, 172–184. doi:10.1016/j.ijhydene.2006.08.014
- Kisielewska, M., Dębowski, M., Zieliński, M., 2015. Improvement of biohydrogen production using a reduced pressure fermentation. *Bioprocess Biosyst. Eng.* 38, 1925–1933. doi:10.1007/s00449-015-1434-3
- Kleerebezem, R., van Loosdrecht, M.C., 2007. Mixed culture biotechnology for bioenergy production. *Curr. Opin. Biotechnol.* 18, 207–212. doi:10.1016/j.copbio.2007.05.001
- Kleerebezem, R., Van Loosdrecht, M.C.M., 2010. A Generalized Method for Thermodynamic State Analysis of Environmental Systems. *Crit. Rev. Environ. Sci. Technol.* 40, 1–54. doi:10.1080/10643380802000974
- Lee, K.-S., Tseng, T.-S., Liu, Y.-W., Hsiao, Y.-D., 2012. Enhancing the performance of dark fermentative hydrogen production using a reduced pressure fermentation strategy. *Int. J. Hydrogen Energy* 37, 15556–15562. doi:10.1016/j.ijhydene.2012.04.039
- Liu, Y., Wang, Y., 2017. Directional enhancement of fermentative coproduction of hydrogen and acetic acid from glucose via control of headspace pressure. *Int. J. Hydrogen Energy* 42, 4095–4101. doi:10.1016/j.ijhydene.2016.09.083
- Ljungdahl, L.G., Hugenholtz, J., Wiegel, J., 1989. Acetogenic and Acid-Producing Clostridia, in: *Clostridia*. Springer US, Boston, MA, pp. 145–191. doi:10.1007/978-1-4757-9718-3_5

- Ljungdhal, L.G., 1986. The Autotrophic Pathway of Acetate Synthesis in Acetogenic Bacteria. *Annu. Rev. Microbiol.* 40, 415–450. doi:10.1146/annurev.mi.40.100186.002215
- Luo, G., Karakashev, D., Xie, L., Zhou, Q., Angelidaki, I., 2011. Long-term effect of inoculum pretreatment on fermentative hydrogen production by repeated batch cultivations: Homoacetogenesis and methanogenesis as competitors to hydrogen production. *Biotechnol. Bioeng.* 108, 1816–1827. doi:10.1002/bit.23122
- Luo, G., Xie, L., Zou, Z., Zhou, Q., Wang, J.-Y., 2010. Fermentative hydrogen production from cassava stillage by mixed anaerobic microflora: Effects of temperature and pH. *Appl. Energy* 87, 3710–3717. doi:10.1016/j.apenergy.2010.07.004
- Massanet-Nicolau, J., Guwy, A., Dinsdale, R., Premier, G., Esteves, S., 2010. Production of hydrogen from sewage biosolids in a continuously fed bioreactor: Effect of hydraulic retention time and sparging. *Int. J. Hydrogen Energy* 35, 469–478. doi:10.1016/j.ijhydene.2009.10.076
- Massanet-Nicolau, J., Jones, R.J., Guwy, A., Dinsdale, R., Premier, G., Mulder, M.J.J., 2016. Maximising biohydrogen yields via continuous electrochemical hydrogen removal and carbon dioxide scrubbing. *Bioresour. Technol.* 218, 512–517. doi:10.1016/j.biortech.2016.06.115
- Noike, T., Takabatake, H., Mizunoc, O., Ohbab, M., 2002. Inhibition of hydrogen fermentation of organic wastes by lactic acid bacteria. *Int. J. Hydrogen Energy* 27, 1367–1371. doi:10.1016/S0360-3199(02)00120-9
- Oh, S.-E., Van Ginkel, S., Logan, B.E., 2003. The Relative Effectiveness of pH Control and Heat Treatment for Enhancing Biohydrogen Gas Production. *Environ. Sci. Technol.* 37, 5186–5190. doi:10.1021/es034291y
- Oh, Y.K., Raj, S.M., Jung, G.Y., Park, S., 2011. Current status of the metabolic engineering of microorganisms for biohydrogen production. *Bioresour. Technol.* 102, 8357–8367. doi:10.1016/j.biortech.2011.04.054
- Peters, J.W., Schut, G.J., Boyd, E.S., Mulder, D.W., Shepard, E.M., Broderick, J.B., King, P.W., Adams, M.W.W., 2015. [FeFe]- and [NiFe]-hydrogenase diversity, mechanism, and maturation. *Biochim. Biophys. Acta - Mol. Cell Res.* 1853, 1350–1369. doi:10.1016/j.bbamcr.2014.11.021
- Ragsdale, S.W., Pierce, E., 2008. Acetogenesis and the Wood-Ljungdahl pathway of CO₂ fixation. *Biochim. Biophys. Acta - Proteins Proteomics* 1784, 1873–1898. doi:10.1016/j.bbapap.2008.08.012
- Reddy, G., Altaf, M., Naveena, B.J., Venkateshwar, M., Kumar, E.V., 2008. Amylolytic bacterial lactic acid fermentation - A review. *Biotechnol. Adv.* 26, 22–34. doi:10.1016/j.biotechadv.2007.07.004
- Shanmugam, S.R., Chaganti, S.R., Lalman, J.A., Heath, D.D., 2014. Statistical optimization of conditions for minimum H₂ consumption in mixed anaerobic cultures: Effect on homoacetogenesis and methanogenesis. *Int. J. Hydrogen Energy* 39, 15433–15445. doi:10.1016/j.ijhydene.2014.07.143
- Si, B., Liu, Z., Zhang, Y., Li, J., Xing, X.-H., Li, B., Duan, N., Lu, H., 2015. Effect of reaction mode on biohydrogen production and its microbial diversity. *Int. J. Hydrogen Energy* 40, 3191–3200. doi:10.1016/j.ijhydene.2015.01.030
- Sieber, J.R., McInerney, M.J., Gunsalus, R.P., 2012. Genomic insights into syntrophy: the paradigm for anaerobic metabolic cooperation. *Annu. Rev. Microbiol.* 66, 429–52. doi:10.1146/annurev-micro-090110-102844
- Sikora, A., Baszczyk, M., Jurkowski, M., Zielenkiewicz, U., 2013. Lactic Acid Bacteria in Hydrogen-Producing Consortia: On Purpose or by Coincidence?, in: *Lactic Acid Bacteria - R & D for Food, Health and Livestock Purposes*. InTech. doi:10.5772/50364
- Skidmore, B.E., Baker, R.A., Banjade, D.R., Bray, J.M., Tree, D.R., Lewis, R.S., 2013. Syngas fermentation to biofuels: Effects of hydrogen partial pressure on hydrogenase efficiency. *Biomass and Bioenergy* 55, 156–162. doi:10.1016/j.biombioe.2013.01.034
- Vardar-Schara, G., Maeda, T., Wood, T.K., 2008. Metabolically engineered bacteria for producing hydrogen via fermentation. *Microb. Biotechnol.* 1, 107–125. doi:10.1111/j.1751-7915.2007.00009.x

- Wang, S., Huang, H., Kahnt, J., Thauer, R.K., 2013. A reversible electron-bifurcating ferredoxin- and NAD-Dependent [FeFe]-Hydrogenase (HydABC) in *Moorella thermoacetica*. *J. Bacteriol.* 195, 1267–1275. doi:10.1128/JB.02158-12
- Wang, Y., Tashiro, Y., Sonomoto, K., 2015. Fermentative production of lactic acid from renewable materials: Recent achievements, prospects, and limits. *J. Biosci. Bioeng.* 119, 10–18. doi:10.1016/j.jbiosc.2014.06.003
- Yerushalmi, L., Volesky, B., Szczesny, T., 1985. Effect of increased hydrogen partial pressure on the acetone-butanol fermentation by *Clostridium acetobutylicum*. *Appl. Microbiol. Biotechnol.* 22, 103–107. doi:10.1007/BF00250028

CHAPTER II

The hydraulic retention time as a control tool of productivity, efficiency and microbial communities.



Highlights

- Dark fermentation microbial community was strongly shaped by HRT
- A maximum volumetric hydrogen production rate of 2000 mL/L-d was found at 6h of HRT
- Two different microbial communities and their interactions were identified
- Short HRT (6-12 h) enriched *Clostridiaceae-Lachnospiraceae-Enterobacteriaceae*
- Large HRT (18-24 h) negatively affected the performance of dark fermentation

The present chapter is a modified version of the article:

Palomo-Briones, R., Razo-Flores, E., Bernet, N., Trably, E. 2017. Dark-fermentative biohydrogen pathways and microbial networks in continuous stirred tank reactors: Novel insights on their control. *Applied Energy*, 198 77-87.

2.1 Summary

In the present work, the influence of the hydraulic retention time (HRT) on dark fermentation metabolism was evaluated through the operation and analysis of a series of four continuous stirred tank reactors (CSTR) at four HRT ranging from 6 h to 24 h. A maximum volumetric H₂ production rate (VHPR) of 2000 ± 149 mL H₂/L-d corresponding to a H₂ yield of 0.86 mol H₂/mol lactose was observed at 6 h HRT. In depth analysis of metabolite profiles and microbial communities showed that low values of HRT favored the emergence of a community dominated by *Clostridiaceae-Lachnospiraceae-Enterobacteriaceae*, which performed metabolic pathways co-producing H₂. In contrast, long HRT led to the establishment of *Sporolactobacillaceae-Streptococcaceae* microbial community that outcompeted H₂-producing bacteria and was responsible of lactate production. Results suggested that these two communities mutually excluded themselves and HRT can act as an operational parameter to control the microbial communities and consequently the related metabolic pathways.

Keywords: Biohydrogen; Dark fermentation; Hydrogen producing bacteria; Lactic acid bacteria (LAB); Metabolic network.

2.2. Introduction

Biohydrogen is worldwide considered as one of the most promising alternatives to substitute fossil fuels in a near future. Indeed, H₂ is not only characterized by its high density of energy (123 kJ/g ~ 2.75), but also the efficiency of its conversion to electric energy is relatively high, and its use does not generate any greenhouse gases. Amongst the technologies available to produce H₂, biological processes are environment friendly and can convert a wide variety of abundant organic biomass at low cost. In particular, biological production of H₂ by dark fermentation, so called biohydrogen, can be emphasized for its large use of sustainable substrates, the high H₂ production rates, and its simplicity of operation (Azwar et al., 2014). In contrast with the photo-fermentation processes, dark fermentation does not require light to occur, thus reactor design is simpler and its operation is not limited by light-darkness natural cycles.

In brief, a fermentation process is the biological oxidation of organic compounds where the same substrate molecule plays a role as a carbon source, an electron donor- and an electron-acceptor, *i.e.* a part of the molecule is oxidized while another part is reduced (Rittmann and McCarty, 2001). In particular, dark fermentation can be defined as the partial oxidation of organic substrates (mainly carbohydrates) without external electron acceptor. Dark fermentation leads to the production of low weight organic molecules (volatile fatty acids -VFA- and alcohols) altogether with H₂ generation. Such metabolic process can be carried out by mixed cultures of bacteria, the most representative members being related to *Prevotella*, *Lactobacillus*, *Clostridium*, *Selenomonas*, *Megasphaera* and *Enterobacter* genera (Etchebehere et al., 2016).

Metabolically, the maximum theoretical H₂ yield of dark fermentation is 4 mol of H₂ per mol of glucose consumed through the acetate pathway (Ghimire et al., 2015). In practice, H₂ yields reported for mesophilic cultures (Davila-Vazquez et al., 2009; Han et al., 2014; Mäkinen et al., 2012; Sivagurunathan et al., 2015) are about 1.3 mol H₂/mol glucose in average, while only few studies have reported H₂ yields beyond 3 mol H₂/mol hexose (Han et al., 2014). Low H₂ yields are probably linked to the complexity of microbial communities and metabolic pathways presented in dark fermentation.

In a dark fermentative community some members such as *Clostridium* and *Enterobacter* genera (H₂-producing bacteria, HPB) are efficient H₂ producers while others play different roles not necessarily linked to H₂ production, for instance, homoacetogens and LAB. On one hand, homoacetogens can use carbon dioxide or carbon monoxide and H₂ as sole carbon and energy sources under anaerobic conditions, along with the synthesis of acetate (Abubackar et al., 2016; Küsel and Drake, 2005; Luo et al., 2011; Massanet-

Nicolau et al., 2010). Previous studies showed homoacetogenesis as the cause of 36-56% of the total acetate observed in the fermentation media, resulting in H₂ productivities 45-90% lower than expected (Luo et al., 2011). Other authors reported that H₂ consumption by homoacetogens was equivalent to 250 mmol/d at 8 h of HRT in up-flow anaerobic sludge bed (UASB) reactors (Carrillo-Reyes et al., 2014). To avoid this type of metabolism, several strategies consisting in the reduction of H₂ accumulation have been suggested (*e.g.* gas sparkling, Bakonyi et al., 2017). On the other hand, LAB constitutes a microbial group commonly found in dark fermentative systems (*e.g.* Baghchehsaraee et al., 2010; Gomes et al., 2016; Kim et al., 2014; Noike et al., 2002; Park et al., 2016) which includes microorganisms of the families *Lactobacillaceae*, *Enterococcaceae*, *Streptococcaceae*, *Sporolactobacillus*, etc. Despite of their ubiquity, the role of LAB in dark fermentation has been scarcely studied (Sikora et al., 2013). Some authors argued that LAB compete with H₂ producers for carbon sources (Jo et al., 2007), while others have widely discussed that the excretion of bacteriocins could be the main cause of dark fermentation failure (Gomes et al., 2016; Noike et al., 2002).

Up to date, most of the reports in literature about LAB and other important microbial groups have been studied circumstantially. In consequence, there is still knowledge scarcity about their effects on fermentation performance, metabolic pathways and their roles in the microbial community of dark fermentation. A full understanding of these issues is fundamental to conduct better control and advance towards the implementation of the biohydrogen production technology at the industrial scale. In this direction, the study of the factors that determine the occurrence of these groups in dark fermentative systems is a pending task.

Therefore, throughout the experiments carried out in this work, HRT was evaluated as a potential factor to shape the metabolic pathways and microbial communities in continuous dark fermentative systems. Due to its simplicity and practicality in real life operation in comparison with other strategies, HRT could be of high importance for metabolic and microbial community control. Moreover, a microbial network analysis was used to reveal the interactions among the involved species. This methodology provides highly important information for the engineering and/or design of microbial communities, which is an alternative to enhance H₂ production.

2.3. Materials and methods

2.3.1. Inoculum source and substrate

Disaggregated anaerobic sludge from a full-scale municipal wastewater treatment plant (Marseille, France) was used as initial source of microorganisms. Before inoculation, the sludge was thermally treated by boiling during 2 hours. Seed sludge was added into a continuous stirred tank reactor (CSTR1) of 3.1 L total volume and 2L working volume, (APPLIKON Biotechnologies, USA) at a final concentration of 4.5 g/L of volatile suspended solids (VSS). The reactor was started in batch mode for 24 h, whereupon the bioreactor was operated in continuous mode for 25 d with a HRT of 6 h. When CSTR1 reached a stable state (lactose degradation efficiency, $46 \pm 2\%$; VHPR, 2448 ± 461 L H₂/L-d; H₂ yield, 0.89 mol H₂/mol lactose) 10 L of effluent were recovered and stored in 4 containers (2.5 L each) at -20 °C until their re-use as microbial inoculum for the subsequent experiments in reactors CSTR2, CSTR3, CSTR4 and CSTR5. A schematic representation of the experimental set-up is shown in Figure 2.1.

For all reactors, lactose was used as substrate at a concentration of 20 g/L. The fermentative medium was supplemented with the following components (mg/L): MgCl₂·6H₂O, 100; CuCl₂·H₂O, 1.25; MnCl₂ 4H₂O, 7; FeCl₂ 4H₂O, 19.1; NiCl₂ 6H₂O, 102.5; yeast extract, 500. Additionally, a phosphate buffer (KH₂PO₄-Na₂HPO₄, pH=5.9) was added at a final concentration of 50 mM.

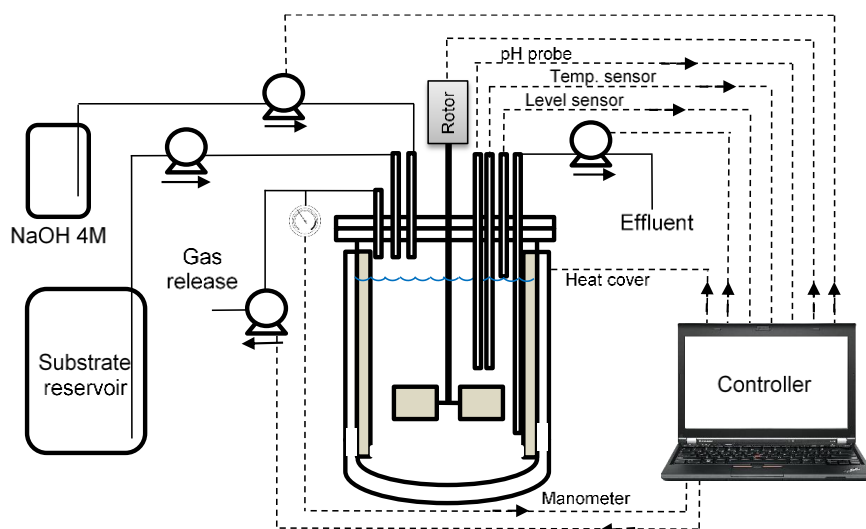


Figure 2.1. Schematic representation of the experimental set-up.

2.3.2. Experimental conditions

A series of 4 continuous stirred tank reactors (CSTR2 to CSTR5), 2 L working volume and 1.1 L of head space, were inoculated (same volume of 1L each, initial VSS 0.5 g/L for all cases) with frozen effluents from CSTR1. Reactors were first operated in batch mode for 24 h using lactose at a fixed concentration of 20 g_{lactose}/L. Thereafter, the reactors were operated at the following HRT: CSTR2, 6 h; CSTR3, 12 h; CSTR4, 18 h and CSTR5, 24 h for an equivalent time of 20 HRT, *i.e.* 120 h, 240h, 360h and 480h of operation, respectively. Stirring and temperature were set and regulated at 200 rpm and 37 °C, respectively, while the pH was automatically controlled at 5.9 by proper addition of 4 M NaOH.

2.3.3. Analytical methods

Gas production was monitored with a pressure control system that was configured to release the gas produced when pressure was above 1.1 bars. Gas composition (H₂ and CO₂) was determined through a gas chromatograph GC-8A equipped with a thermal conductivity detector (Shimadzu). Calibration was performed using three external gas standards: 5% CO₂ and 5% N₂ in methane, 20% CO₂ and 20% N₂ in methane, and 100% H₂, injected as 0.5 mL at 1 atm.

VFA and alcohols were quantified using high performance liquid chromatography (HPLC) coupled to a refractometer (Waters R410). Liquid samples were centrifuged at 13000 rpm for 15 min and filtered with 0.2 µm nylon filters. HPLC analysis was performed at a flow rate of 0.8 mL min⁻¹ using an Aminex HPX-87H, 300 x 7.8 mm (Bio-Rad) column at a temperature of 35 °C. H₂SO₄, 4 mM was used as mobile phase. COD and VSS were analyzed according to the standard methods (APHA/AWWA/WEF, 2012).

2.3.4. Microbial community analysis

DNA extraction was performed with the Fast DNA SPIN Kit for soil in accordance with the manufacturer's instructions (MP Biomedicals). PCR amplification of the bacterial 16S rRNA was conducted with Pfu Turbo DNA polymerase (Stratagene) and universal primers (5'-ACGGTCCAGACTCCTACGGG -3', *Escherichia coli* position F331; and 5'-TTACCGCGGCTGCTGGCAC -3', *E. coli* position R500) targeting the V3 region. The PCR conditions were as follows (Milferstedt et al., 2013): initial denaturation for 2 min at 94°C; 25 cycles of melting (1 min at 94°C), annealing (1 min at 61°C) and extension (1 min at 72°C); and a final extension step of 10 min at 72°C.

PCR products were analyzed by Capillary Electrophoresis Single Strand Conformation Polymorphism (CE-SSCP) in an ABI 3130 genetic analyzer (Applied Biosystems) according with a previous report (Rochex et al., 2008). The CE-SSCP profiles were aligned based on the ROX internal standard to take into account inter-sample electrophoretic variability and were normalized with the package *Statfingerprints* in R platform (R Development Core Team, 2011). From CE-SSCP fingerprints, Shannon's diversity index and Gini's coefficient were calculated as described previously (Cabrol et al., 2012).

In order to elucidate the identity of the microorganisms, a PCR-based 454-pyrosequencing was carried out. The PCR for 454 pyrosequencing was targeting the V4-V5 regions, using the universal primers 515-532F and 909-928R. The sequencing work was developed by the GeT PlaGe sequencing center of the genotoul life science network in Toulouse, France (get.genotoul.fr). The downstream sequences processing involved a chimeric analysis to validate the quality of the recovered sequences using an slightly modified version of the Standard Operation Procedure reported elsewhere (Kozich et al., 2013). The SILVA ribosomal RNA database (<https://www.arb-silva.de/>) was used for alignment and as taxonomic outline search of their taxonomic affiliation comparing to data bases.

2.3.5 Multivariate analysis and Pearson's correlations

Principal Components Analysis (PCA) was performed to determine possible relationships between microbial community, fermentation performance and operational parameters. The PCA was carried out using R software and *factoextra* package. As discussed elsewhere (Carrillo-Reyes et al., 2016; Ramette, 2007), PCA is a multivariate procedure which basically calculates new synthetic variables (principal components), which are mutually independent, uncorrelated, mathematically represented as a linear combinations of the original variables, and that account for as much of the variance of the original data as possible. To avoid overfitting, a second PCA was conducted considering a reduced number of factors selected on the basis of their weight.

Besides the multivariate analysis, a Pearson's correlation analysis was carried out with the information of microbial community, fermentation performances and operational parameters to give better insight on the different relationships occurring within the system. This analysis was performed in R software (R Development Core Team, 2011), using the *corrplot* package.

2.3.6 Microbial community networks

The network inference was performed following the protocol proposed by Faust et al. (Faust et al., 2015). In brief, four similarity measurements (Bray–Curtis and Kullback–Leibler dissimilarity, Pearson and Spearman correlation) were computed for a dataset composed by families with abundances >1% and observed in at least three samples. The p-value of each measurement was performed according with the permutation-renormalization and bootstrap (ReBoot) method (Faust et al., 2012). Measure-specific p-values were merged following the Brown's method. Finally, edges with merged p-values < 0.05 were kept. The whole network construction was performed within *Cytoscape* environment, using the *CoNet* application (Faust and Raes, 2016).

2.4. Results and discussion

2.4.1. HRT determines dark fermentation performances and metabolites distribution

A series of four CSTR fermentation reactors was operated for an equivalent time of 20 HRT each, using lactose at 20 g/L as substrate. Each CSTR was operated at a HRT value ranging from 6 to 24h (CSTR2, 6 h; CSTR3, 12h; CSTR4, 18h; CSTR5, 24h), at pH 5.9 and 37°C.

Results showed that HRT had an important impact on dark fermentation performances in terms of lactose consumption, H₂ yield, and VHPR (Figure 2.2). Overall, lactose degradation efficiency was enhanced by increasing the HRT, from 35% in CSTR2 (HRT = 6h) up to 82% in CSTR5 (HRT = 24h). In contrast, VHPR showed a gradual decrease from 2000 ± 149 mL H₂/L-d in CSTR2 to 604 ± 143 mL H₂/L-d in CSTR5. A maximum H₂ yield of 0.86 mol H₂/mol lactose was found in the CSTR2 at 6h HRT. The relationships observed between HRT and both VHPR and H₂ yields were consistent with previous studies where comparable trends were also reported, for instance, by employing halophilic bacteria (Zhang et al., 2013), using peach nectar and pulp as substrates (Diamantis et al., 2013), or when operated under reduced pressure (Lee et al., 2012). For the specific case of lactose, the results presented in this work were below the range of previous studies (Carrillo-Reyes et al., 2012; Davila-Vazquez et al., 2009; Rosa et al., 2014). Factor such as the composition of growth media or the source of inoculum could be among the possible causes of the relatively low VHPR. As discussed previously (Sivagurunathan et al., 2016a), it is widely accepted that short HRT improves the H₂-producing process by suppressing the growth of undesirable microorganisms unable to growth at high dilution rates. At the same time, short HRT is an effective

strategy for the establishment of stable H₂-producing microbial communities. A summary of literature studies in regard with HRT, metabolic and microbial community changes are shown in Table 2.1.

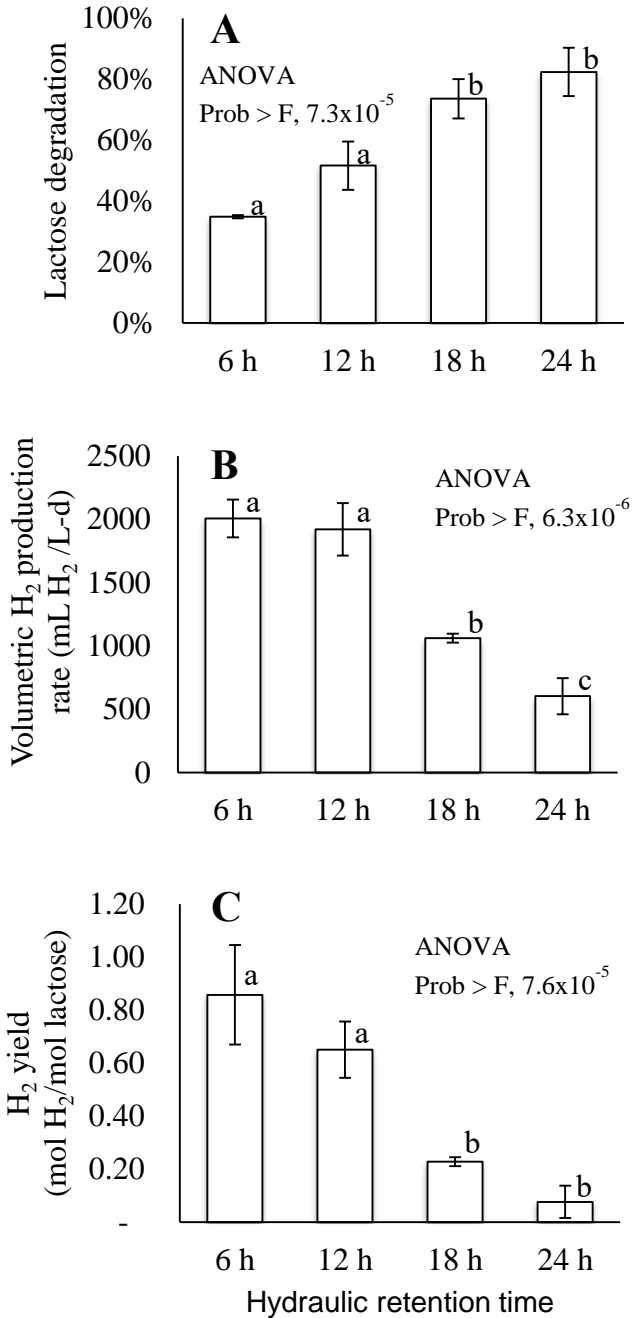


Figure 2.2. Summary of the influence of the hydraulic retention time on the performance of continuous stirred-tank reactors during dark fermentation. For each case, the three last samples were considered. Bars with the same lower case letter were not significantly different at a level 0.05 according with Tukey's tests.

Table 2.1. Selection of studies of biohydrogen production in continuous stirred-tank reactors.

Substrate	Inoculum	HRT ^a	VHPR ^b	HY ^c	Changes on the metabolic pathways	Changes on the microbial community	Microorganisms identified	Reference
Glucose	<i>Clostridium bifermentans</i>	6-24	3.8-5.5	0.7-1.1	- Lactate (HRT=18h) diminished H ₂ yield	-	<i>Clostridiaceae</i>	Zhang et al., 2013
Cheese whey	Anaerobic sludge	4-10	2.7-11.3	0.5-1.2	-	- <i>Clostridium</i> was dominant at HRT 10, 6 and 4 h - <i>Streptococcus</i> and <i>Enterococcus</i> presented at low HRT (6 & 4 h)	<i>Clostridiaceae</i> , <i>Enterococcaceae</i> <i>Streptococcaceae</i>	Davila-Vazquez et al., 2009
Sugarcane syrup	<i>Clostridium butyricum</i>	2-12	1.18-17.5	0.3-1.32	- High concentrations of lactate were observed at large HRT	- LAB (<i>Acatostipes</i>) disappeared with the decrease in HRT - Relative abundance was not assessed. - Shortening the HRT reduced the microbial diversity of the community	<i>Clostridium</i> , <i>Tetrasphaera</i> , <i>Flammeovirga</i> , <i>Tissierella</i> , <i>Butyrivibrio</i> , <i>Desulfobulbus</i> , <i>Olsenella</i> <i>Acotostipes</i>	Nualsri et al., 2016
Glucose	Anaerobic sludge	4-12	4.56-14.4	0.75-1.57	- Short HRT led to reduction of propionate production	- No further correlation was performed	<i>Clostridiaceae</i>	Wu et al., 2008
Sugarcane juice	<i>Clostridium butyricum</i>	4-36	0.13-1.81	0.05-1	- Short HRT led to reduction of propionate production	- <i>L. arbinses</i> and <i>C. butyricum</i> were dominant at all HRT	<i>Lactobacillus harbinensis</i> , <i>Klebsiella pneumoniae</i> , <i>Clostridium butyricum</i>	Zhang et al., 2006
Lactose	Anaerobic sludge	6-24	0.6-2	0.04-0.43	- Short HRT (6-12 h) were associated with H ₂ -producing pathways. - Large HRT (18-24h) were strongly associated with lactate in detriment of H ₂ production.	- The microbial community structure and interactions were driven by HRT. - LAB can be avoided at short HRT (6-12 h).	HPB^d consortium <i>Clostridiaceae</i> <i>Enterobacteriaceae</i> <i>Lachnospiraceae</i> LAB^e consortium <i>Sporolactobacillaceae</i> <i>Streptococcaceae</i>	This work

HRT: Hydraulic retention time (h)

^bVHPR: Volumetric H₂ production rate (L H₂/L-d)^cHY: H₂ yield (mol H₂/mol hexose equivalent)^dHPB: H₂-producing bacteria^eLAB: Lactic acid bacteria

Another important parameter worth to mention is the organic loading rate, which refers to the mass of substrate fed in a volume of reactor within a unit of time. OLR is function of both HRT and substrate concentration, thus the experiments performed for the present work also had different values of OLR; as lactose concentration was kept constant at 20 g lactose/L OLR ranged from 80 g lactose/L-d in CSTR2 to 20 g lactose/L-d in CSTR5. It was observed that OLR decline was accompanied by the decreases of VHPR and H₂ yield (Table 2.2) confirming that these parameters are strongly dependent on HRT and OLR.

A Pearson's correlation analysis revealed that, in terms of metabolites productivities (mmol per mol of substrate consumed), longer HRT favored the lactate pathway ($r = 0.96$, $p < 0.01$). In contrast, acetate was produced in higher proportion as well as other metabolites such as formate and ethanol under short HRT conditions ($r \sim -0.65$ for all cases, $p < 0.1$) (Figure 2.3). The analysis also showed that these three metabolites were strongly correlated to each other ($r > 0.9$, $p < 0.05$). An overview of significant Pearson's correlations is provided in supplementary material. In general, the information confirmed that the HRT was an effective factor that can shape dark fermentation towards two different stages: lactate type fermentation or acetate-formate-ethanol type fermentation.

Table 2.2. Summary of the performance of four continuous stirred-tank reactors operated at different values of hydraulic retention time.

HRT (h)	Time (# of HRT)	VHPR (mL H ₂ /L-d)	H ₂ yield (mol H ₂ /mol hexose)	Volatile fatty acids concentrations, mmol/L						
				S	L	F	A	P	E	B
6	2	414.1	0.2	0.3	0	9.2	4	0	6.6	1.4
6	6	559.9	0.3	0.9	0	23.7	10.9	0	20.3	0.8
6	12	1035.1	0.3	0.3	0	13.6	7.7	0	11.3	1.6
6	20	2007.4	0.9	0	0	7.3	7.1	0	4.0	2.9
12	2	1049	0.3	0	0	18.5	11.2	0	19.7	8.1
12	6	1352.6	1	0	0	3.9	11.4	0	6.9	11.3
12	12	2382.3	0.8	0	5.6	2.4	11.9	1.2	2.7	9.5
12	20	1920.4	0.7	0	10.8	2.7	8.1	2.4	2.3	6.0
18	2	807.1	0.5	0	5.5	12.5	7.0	0	17.8	14.9
18	6	907.5	0.3	0	0.5	9.8	3.4	4.7	8.8	3.8
18	12	771.2	0.2	0	30.9	4.8	11.5	7.8	1.5	12.3
18	20	1061.6	0.2	0	33.3	1.5	12.5	14.6	0	22.1
24	2	331.8	0.1	0	113.0	0	9.4	5.7	6.5	32.7
24	6	532.3	0.1	0	88.1	0	3.8	3.9	7.3	30.3
24	12	432.3	0.1	0	76.6	0	4.8	3.2	7.7	29.4
24	20	604.2	0.1	0	160.9	0	0	0	0	18.4

Volatile Fatty Acids: S, Succinate; L, Lactate; F, Formate; A, Acetate; P, Propionate; E, Ethanol; B, Butyrate. HRT: Hydraulic retention time; VHPR: Volumetric H₂ production rate.

For comparison purposes, the higher values of each column are colored in deep blue (■) while lower values are displayed in white (□).

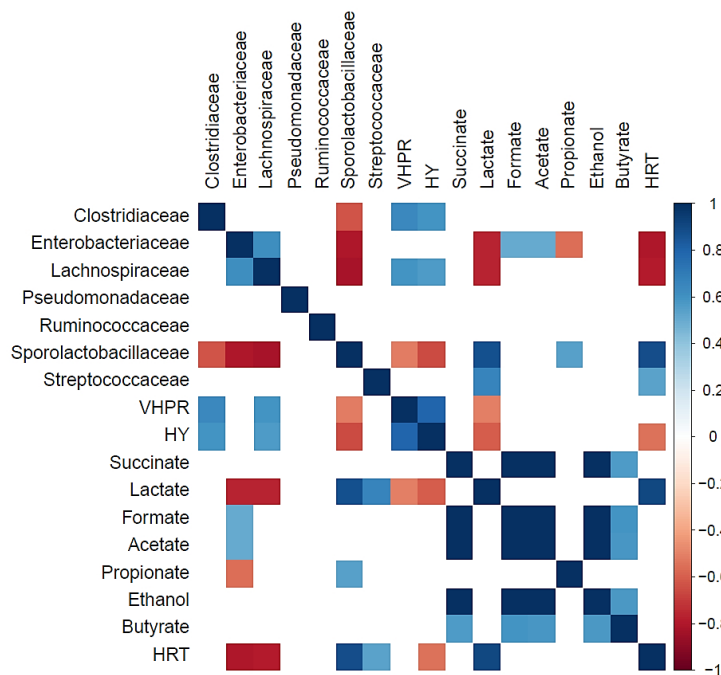


Figure 2.3. Matrix of Pearson's correlations obtained with the *corrplot* package in R environment. Only correlations with $p < 0.05$ are displayed. HY: H_2 yield (mol H_2 /mol lactose); VHPR: Volumetric hydrogen production rate (L H_2 /L-d); Formate, Acetate, Propionate, Lactate, Butyrate, Ethanol, Succinate and Propionate were considered as production yields (mmol VFA/mol lactose); HRT: hydraulic retention time (h). Microorganisms were analyzed in terms of their relative abundance from pyrosequencing results.

In addition, the COD-based analysis gives a clear overview of the metabolic shifts as consequence of the applied HRT (Figure 2.4). According to this analysis, a high percentage of substrate was directed to the synthesis of biomass and other unknown byproducts when HRT of 6, 12, and 18 h, were applied. Also, under such conditions, the percentage of substrate COD directed to H_2 was higher (8 and 6% COD basis) for HRT of 6 and 12 h in comparison with 18 and 24 h (1 and 3% COD basis), suggesting that the metabolic network resulted in efficient H_2 production. This finding is consistent with relatively high yields of ethanol, acetate and butyrate, all of them being metabolically linked to H_2 production. In contrast at the longest HRT, 24 h, most of the substrate (72% COD basis) ended as lactate.

VSS were experimentally determined, converted to COD using a theoretical equivalence of 1.42 g COD/g SSV (Rittmann and McCarty, 2001) and compared with COD percentages found for "biomass and others", especially in the first three cases (51, 67 and 63%). Through this procedure, it was confirmed that COD directed to biomass were 44, 54.9, 59, and 59%, for HRT of 6, 12, 18 and 24 h, respectively. Dark fermentative systems in CSTR have shown that about 30% of substrate is commonly directed to biomass, and in some cases, the percentage can reach near 50% of consumed COD. For instance, Jung et al. (2010) observed remarkable high biomass yields equivalent to 46% in a CSTR fed with the wastewater of a coffee drink manufacturer at a concentration of 20 g COD/L and 6 h of HRT (Jung et al., 2010). Lay et al. (2010) also showed biomass yields that accounted for 38% in a CSTR fed

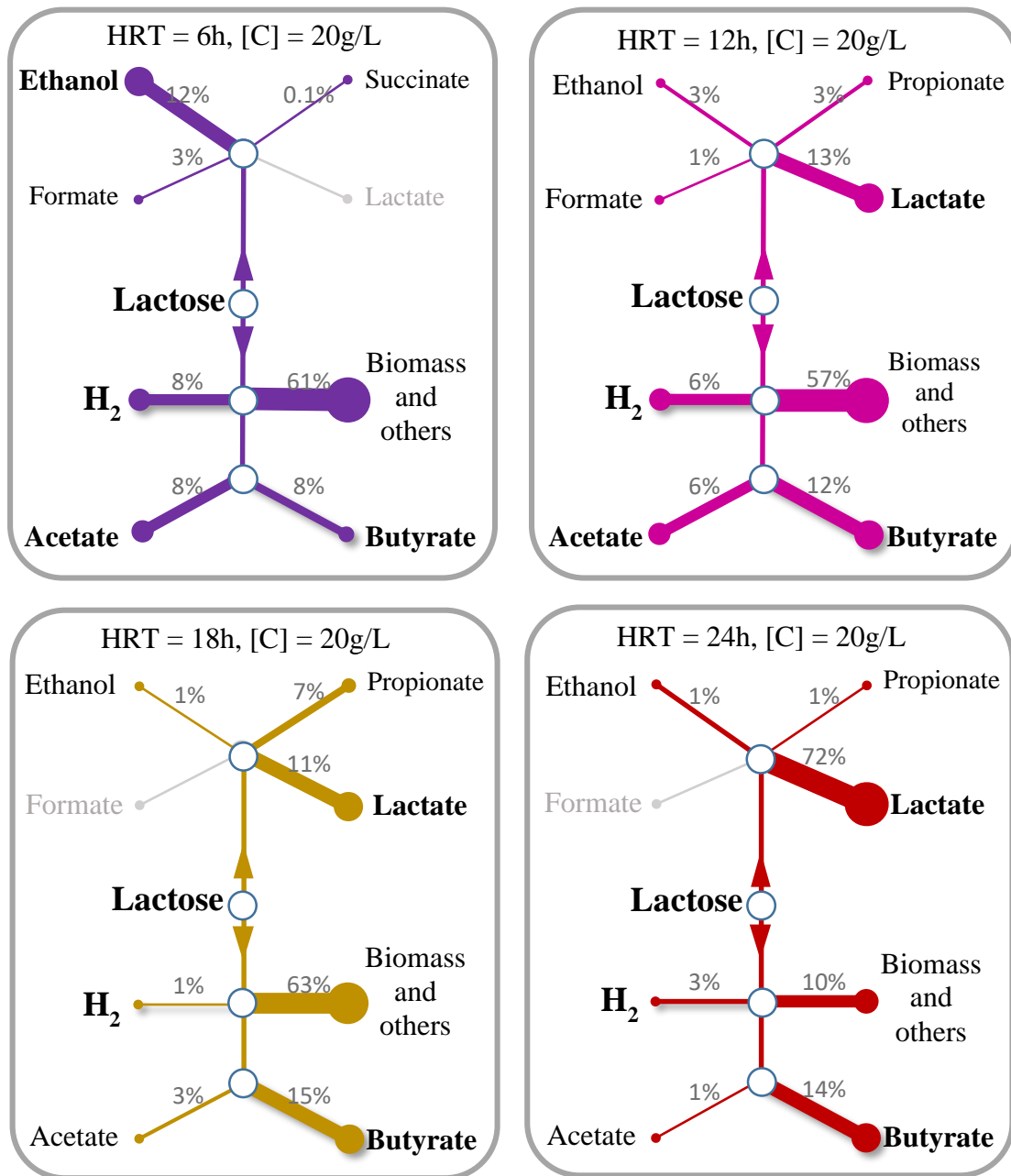


Figure 2.4. Summary of the influence of hydraulic retention time (HRT) on the metabolic pathways of dark fermentation based on the chemical oxygen demand. The balance was performed with the last 3 samples in the systems' operation.

with 40 g COD/L molasses at an HRT of 24 h (Lay et al., 2010). A possible reason of the high biomass yield can be that under short HRT (mainly 6 and 12 h), microorganisms directed a major fraction of the consumed substrate to maintain themselves in the system. If microorganisms do not direct an important fraction of COD to biomass synthesis under such conditions they would be washed out. There are other

factors that possible influence the percentage of COD directed to biomass, for example the specific growth rate of microorganisms which will be discussed later in this document.

2.4.2. HRT shapes the microbial community and modifies the metabolic pathways

A microbial community analysis through CE-SSCP was performed to characterize whether the changes towards high- or low-efficient states (described in previous section) was a consequence of metabolic shifts or changes in the microbial community structure. CE-SSCP profiles comparison clearly show that HRT had a great impact on the microbial community with regards to the relative abundance distribution of species (Figure 2.5). For instance, microorganisms numbered 170 and 390 were dominant at HRT of 6 h, while microorganisms at 560 and 690 were mainly present at HRT of 18 and 24 h. These observations were confirmed with a Bray-Curtis dissimilarity analysis and the corresponding cluster dendrogram (hierarchical clustering using Ward's method) (Figure 2.5, left-side). SSCP profiles were successfully grouped according with the HRT, being samples from the CSTR2 mostly at the bottom of the graph while samples taken from CSTR5 were placed at the top. Interestingly, samples from CSTR3 and CSTR4 were distributed according with the sampling time, being samples taken after 2 and 6 equivalents of HRT placed at the bottom, while those taken after 12 and 20 equivalents of HRT were located at the top. Such tendency suggests that microbial communities were dynamic and changed as function of the time of operation.

Further analysis of the CE-SSCP profiles revealed microbial diversity Shannon's indexes of 1.6 ± 0.4 in average, which can be considered low but consistent with literature. For example, similar indexes were reported for a CSTR system fed with 15 g/L of galactose at an HRT of 12 h (Sivagurunathan et al., 2016b). In contrast, values of the present work were lower than in granular systems. For instance, Cisneros-Pérez et al. (2015) reported Shannon indexes of 2.55 and 2.31 in two EGSB reactors operated about 96 days using heat shock and cell wash-out inocula, respectively. These differences are probably related to the strong selection of suspended-cell system in comparison with fixed-cell systems, a feature that is widely known. Indeed, the high Gini coefficients indicate that the community was dominated by only few organisms which confirms the highly selective conditions of the CSTR systems.

Furthermore, 16S-rRNA gene sequencing resulted in 382 OTUs, identified to the genus level against the SILVA database. OTUs unsuccessfully identified with the SILVA database were instead compared with *NCBI Transcript Reference Sequences* through its online service (<https://blast.ncbi.nlm.nih.gov/Blast.cgi>). Overall, only 9 families showed a relative abundance higher than 1% and were considered for further analysis (Figure 2.6). These families were identified as *Clostridiaceae*, *Enterobacteriaceae*,

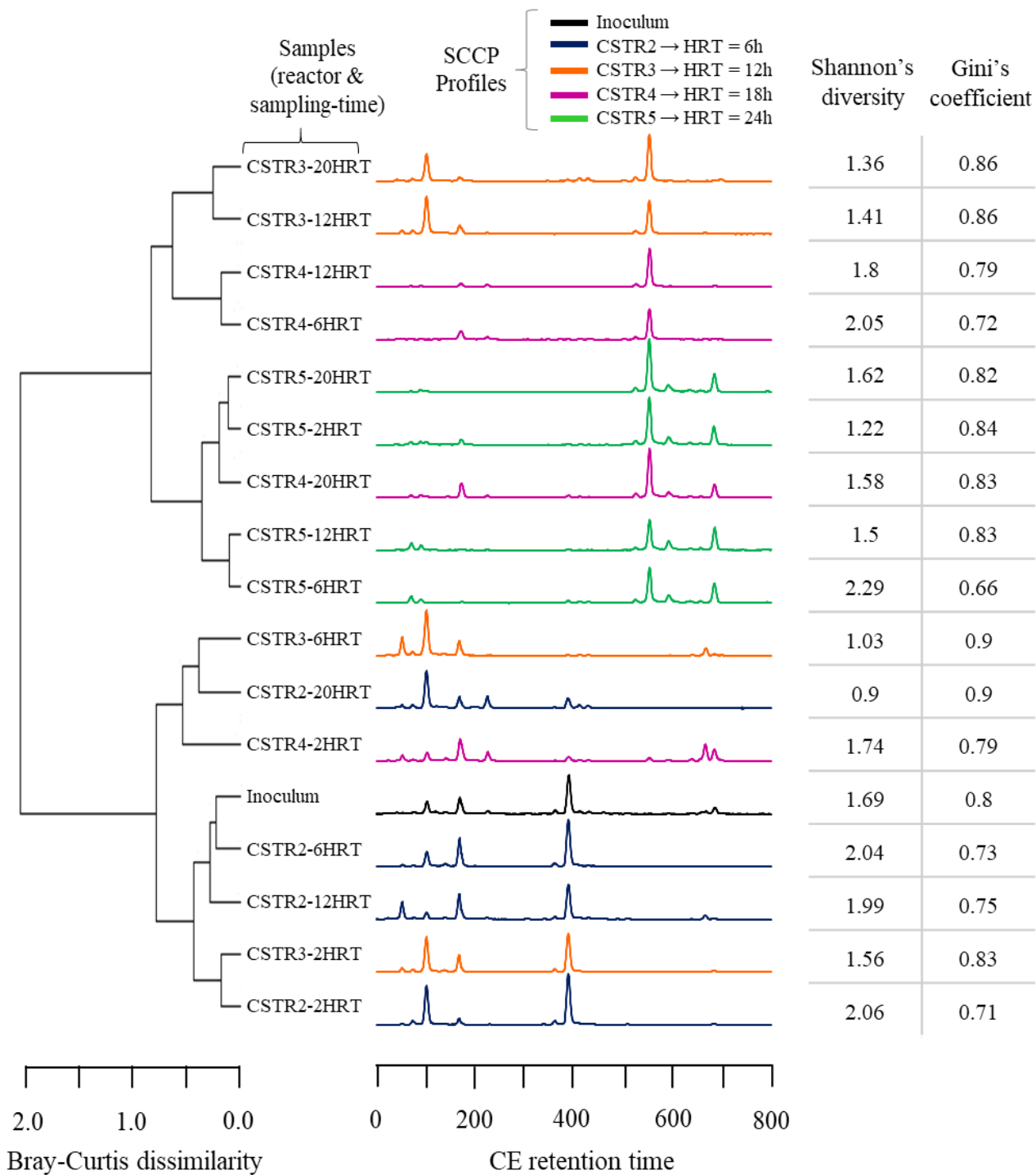


Figure 2.5. Capillary electrophoresis-based single-strand conformation polymorphism (CE-SSCP) fingerprints of samples from four continuous stirred-tank reactors (CSTR1 - CSTR4) operated under different hydraulic retention times (HRT) (6h, 12h, 18h and 24 h). Note that 4 samples (after 2, 6, 12 and 20 HRT) were analyzed for each condition. The CE-SSCP profiles were processed to compute Bray-Curtis dissimilarities and hierarchical clustered. Shannon's diversity index and Gini's coefficients for evenness were computed for each profile as well.

Sporolactobacillaceae, *Lachnospiraceae*, *Ruminococcaceae*, *Streptococcaceae*, *Pseudomonadaceae* and *Flavobacteriaceae*. In most cases, the sum of 2 and 3 families accounted for $\geq 60\%$ and $\geq 80\%$ of relative abundance, respectively. Such uneven distribution, foreseen from CE-SSCP profiles, is consistently found in H_2 -producing reactors (Etchebehere et al., 2016).

Altogether, CE-SSCP (Figure 2.5) and sequencing results (Figure 2.6) confirmed that HRT was a very important factor of microbial community selection. In other words, HRT acted as pressure of selection, by eliminating the microorganisms incapable to duplicate at higher velocity than HRT. To illustrate this mechanism, at the lowest value of HRT (6 h) only microorganisms with $\mu_{\max} > 0.115 \text{ h}^{-1}$ should remain, while at the highest HRT (24 h) the minimum μ_{\max} would be 0.028 h^{-1} .

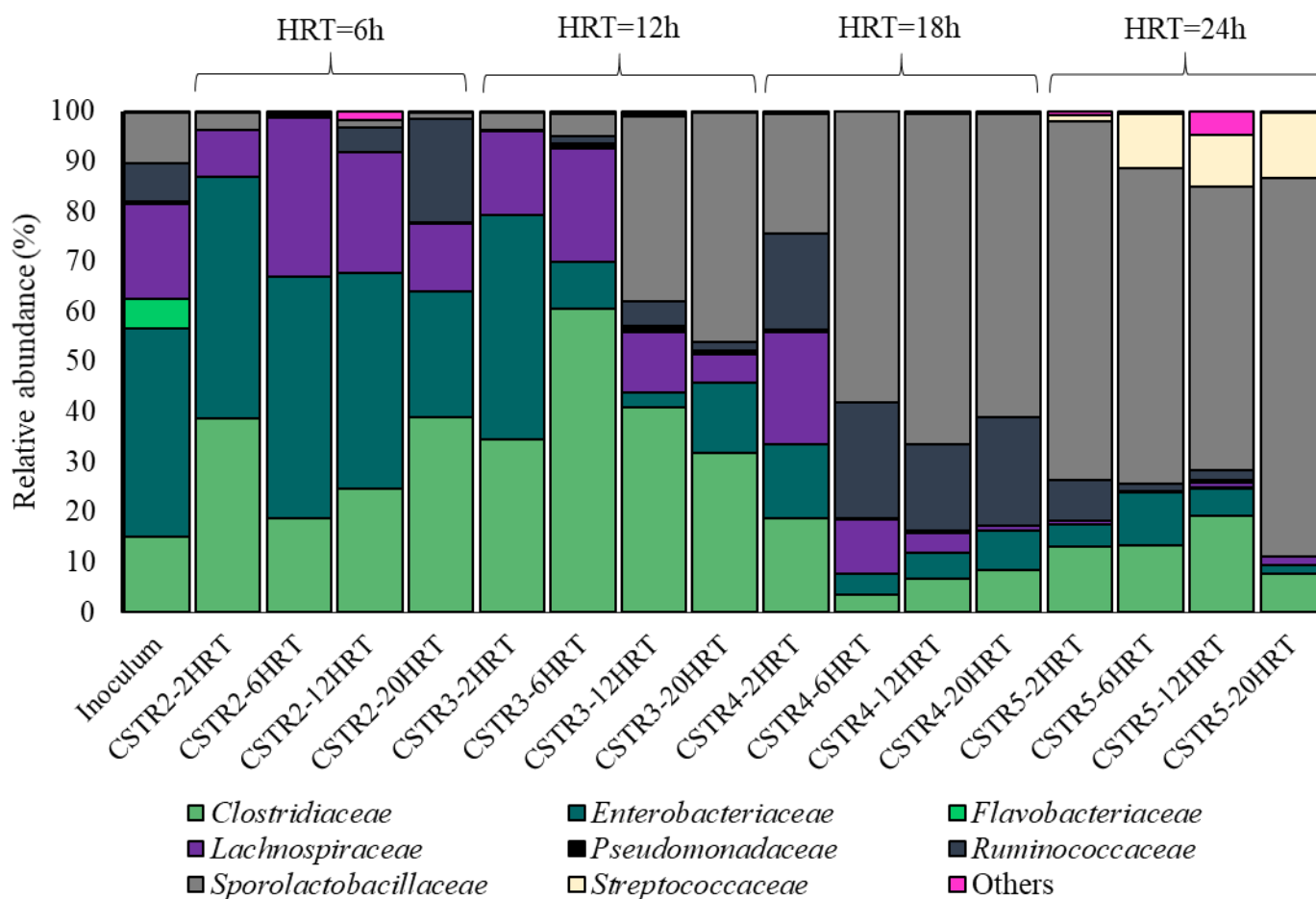


Figure 2.6. Relative abundance of bacteria families found from continuous stirred-tank reactors (CSTR) operated under different conditions of hydraulic retention time (HRT) (6h, 12h, 18h and 24 h). For each reactor, four samples were taken in different moments of the operation (after 2, 6, 12 and 20 HRT). Families with relative abundance $< 1\%$ were grouped as others.

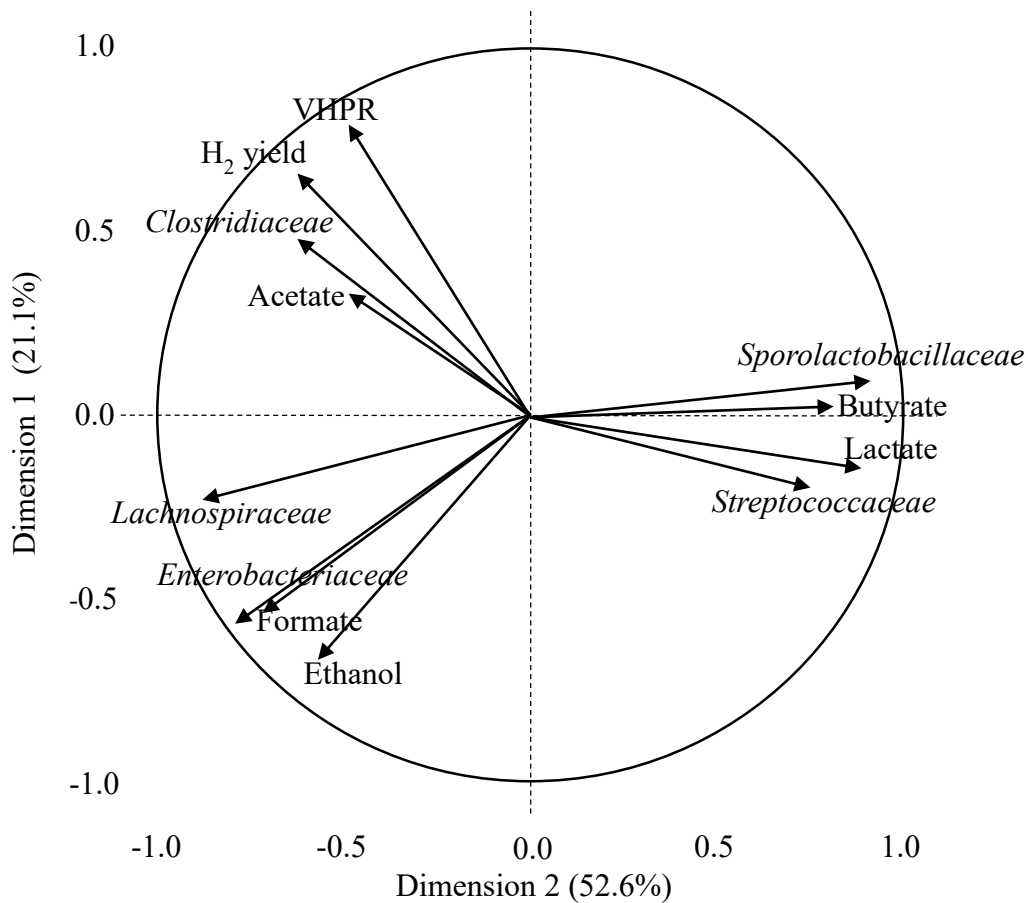


Figure 2.7. Principal components analysis for relative abundance of microbial families, metabolite yields and H₂ production performance. Samples considered were taken at times equivalent to 2, 6, 12 and 20 times the hydraulic retention time. VHPR: Volumetric H₂ production rate.

The changes observed among the microbial communities were consistent with growth rates reported for *Clostridiaceae* and *Enterobacteriaceae* bacteria, μ_{\max} of 0.5 and 4 h⁻¹, respectively (Chen et al., 2005; Tanisho, 1998). In comparison, appreciably lower μ_{\max} of 0.1 h⁻¹ has been reported for a *Sporolactobacillaceae* members (Zhao et al., 2010).

The variability in the relative abundance of microbial families, together with metabolites yields, and the reactor performance parameters were analyzed by principal components analysis with the aim to identify the relationships between the microbial groups and the metabolic pathways (Figure 2.7).

It was confirmed that short HRT (6 and 12h) favored the dominance of OTUs related to the families *Clostridiaceae* and *Enterobacteriaceae*. In contrast, samples from CSTR with larger HRT (18 and 24h) were dominated by bacteria from the *Sporolactobacillaceae* and *Streptococcaceae* families.

The PCA analysis also confirmed that the organisms issued from the family *Clostridiaceae* were closely related to the acetate pathway and system performances in terms of VHPR and H₂ yield. At the genus level, this family was mainly composed of *Clostridium* species, which is in agreement with higher H₂ production as found in the literature (Hung et al., 2011a).

Pathways leading to ethanol, formate and succinate were related to microorganisms from the *Lachnospiraceae* and *Enterobacteriaceae* families. In regard with *Enterobacteriaceae*, it is considered a family of H₂ producers although, metabolically, the maximum yield would be 2 mol H₂ per mol of hexose. Indeed, *Enterobacteriaceae* is associated with formate and ethanol production (Hallenbeck and Ghosh, 2009), which is in consistent with the PCA results. On the other hand *Lachnospiraceae* is a family known to much lesser extend in dark fermentative systems which has been associated to acetogenesis (Denman et al., 2015; Hung et al., 2011a). In our case this family was not significantly associated to acetate but more likely to production of succinate. Interestingly, *Lachnospiraceae* family has been observed in systems treating cheese whey as substrate with high percentage of lactose (Castelló et al., 2009; Davila-Vazquez et al., 2011).

Moreover, lactate pathway was linked to the presence of bacteria belonging to *Sporolactobacillaceae* and *Streptococcaceae* families, confirming that system performance under HRT of 24h was dominated by lactic-acid type fermentation. LAB have been widely found in dark fermentative systems but their implication remains controversial. In this study, longer HRT selected these organisms though reported μ_{\max} is about 0.1 h⁻¹ (Zhao et al., 2010). This value of μ_{\max} was possible remarkably lower since they were not present until HRT of 18 h (equivalent $\mu_{\max} = 0.038$ h⁻¹). Under such conditions LAB, specifically *Sporolactobacillaceae*, was a co-dominant group associated to the reduction of *Enterobacteriaceae* and *Clostridiaceae* which could be possible to the presence of bacteriocins as suggested in other studies (Hung et al., 2011a).

In conclusion it was demonstrated that HRT is a critical factor of selection that determines the shape of dark fermentation microbial community and subsequently the global metabolism.

Overall, short HRT selected microbial communities rich in *Clostridiaceae-Lachnospiraceae-Enterobacteriaceae* specialized in acetate, ethanol and succinate pathways, and strongly linked to better H₂ performances. On the contrary, long HRT selected *Sporolactobacillaceae-Streptococcaceae* families which are important LAB specialists in lactate synthesis.

2.4.3 A microbial interaction network displays an ecosystem dominated by mutual exclusive interactions

To identify the possible interactions existing among microorganisms in dark fermentative systems, a microbial network of interactions was constructed as described by Faust et al. (2015). The importance of this approach in the context of technology applicability relies on its possible usage for the design of synthetic microbial communities (Faust and Raes, 2012) or bioaugmentation strategies (Kumar et al., 2016), which have been identified as alternatives to improve H₂ productivities of dark fermentation. In both cases, it is necessary to identify the microbial groups, understand their capabilities and compatibilities with each other in order to successfully ensemble the desired community.

The resulting network (Figure 2.8) was composed by seven nodes corresponding to the families *Clostridiaceae*, *Enterobacteriaceae*, *Sporolactobacillaceae*, *Lachnospiraceae*, *Ruminococcaceae*, *Streptococcaceae*, and *Pseudomonadaceae* which were interconnected either positively or negatively by a total of thirteen edges. It is worth to note that more than 80% of the connections were mutual exclusive interactions, indicating that the microbial web was most probably dominated by competitive interactions

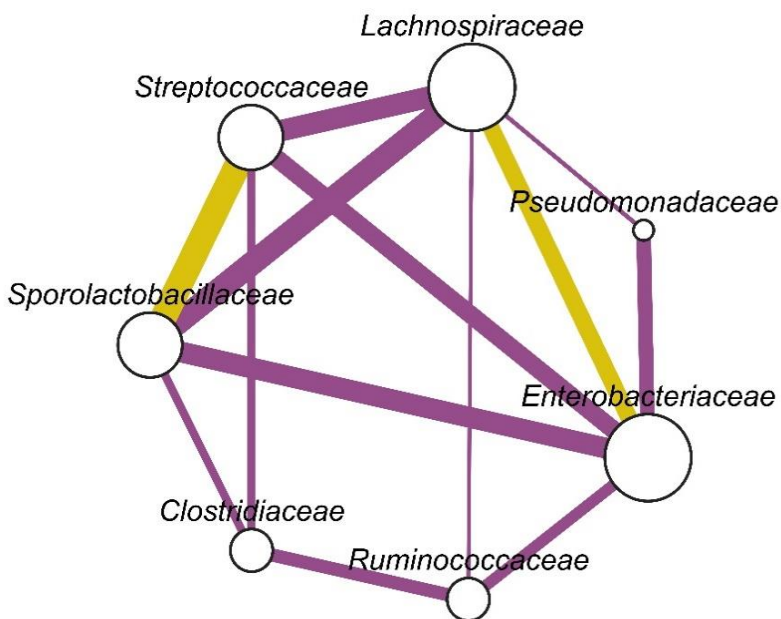


Figure 2.8. Network of interactions constructed from four different similarity measurements within Cytoscape environment, using the CoNet application (Faust and Raes, 2016). Only groups presented in at least three samples with > 1% relative abundance were considered. Edges represent strong connections ($p < 0.05$) between two microbial families (nodes). Yellow edges are positive interactions while purple edges represent a strong “exclusion” interaction. The width of the edges is shown proportional to the weight of the interaction between the microbial groups, while the size of the nodes is proportional to the number of interactions of the microbial group.

rather than cooperation. Interestingly, the two edges that corresponded with positive correlations were the pairs *Sporolactobacillaceae-Streptococcaceae* (both LAB families) and *Enterobacteriaceae-Lachnospiraceae*.

In regard with the positive relationship found between the two LAB families, this connection suggests that a sort of cooperation could be taking place. According with metabolic information on *Sporolactobacillaceae* members, most of them are unable to process lactose (Thamacharoensuk et al., 2015). Therefore, one possibility is that the organic carbon needed by *Sporolactobacillaceae* was provided by *Streptococcaceae* members or other organisms in the fermentation bulk, though the mechanism remains unclear.

As mentioned previously, the LAB families were predominant at relatively long HRT while *Enterobacteriaceae*, *Lachnospiraceae* and *Clostridiaceae* were dominant at low values of HRT. In this regard, the network analysis revealed that LAB had a strongly negative interaction with *Enterobacteriaceae*, *Lachnospiraceae* and *Clostridiaceae* families. This finding supports the possible existence of outcompeting mechanisms of LAB that are detrimental to dark-fermentative groups.

Altogether, the microbial network analysis indicates that two microbial community states can be distinguished all along the experiments, resulting from a competition between a group composed of *Enterobacteriaceae*, *Lachnospiraceae* and *Clostridiaceae* members and LAB. It is worth to mention that the network analysis considers only unique and direct interactions and cannot predict any direction of the interaction nor connections of the type “when x and y are present, z is also present”. Therefore, other approaches are required to fully characterize the possible implications of LAB in dark fermentative systems.

2.5. Conclusions

The effect of HRT on shaping metabolic pathways and microbial communities in dark fermentation was successfully investigated. A maximum VHPR of 2000 mL H₂/L-d corresponding to a H₂ yield of 0.86 mol H₂/mol lactose was reached with 6h HRT. It was found that short HRT (6-12 h) correlated with H₂ yield and led to microbial communities rich in *Clostridiaceae-Lachnospiraceae-Enterobacteriaceae* specialized in acetate-ethanol-formate pathways. Longer values of HRT (18-24 h) enriched the community in *Sporolactobacillaceae-Streptococcaceae* that strongly outcompeted HPB. Overall, it was demonstrated

that HRT is a critical factor of selection that determines the shape of microbial community and global metabolism in dark fermentation.

2.6. References

- Abubackar, H.N., Bengelsdorf, F.R., Dürre, P., Veiga, M.C., Kennes, C., 2016. Improved operating strategy for continuous fermentation of carbon monoxide to fuel-ethanol by clostridia. *Appl. Energy* 169, 210–217. <https://doi.org/10.1016/j.apenergy.2016.02.021>
- APHA/AWWA/WEF, 2012. *Standard Methods for the Examination of Water and Wastewater*, Standard Methods.
- Azwar, M.Y., Hussain, M. a., Abdul-Wahab, A.K., 2014. Development of biohydrogen production by photobiological, fermentation and electrochemical processes: A review. *Renew. Sustain. Energy Rev.* 31, 158–173. <https://doi.org/10.1016/j.rser.2013.11.022>
- Baghchehsaraee, B., Nakhla, G., Karamanev, D., Margaritis, A., 2010. Fermentative hydrogen production by diverse microflora. *Int. J. Hydrogen Energy* 35, 5021–5027. <https://doi.org/10.1016/j.ijhydene.2009.08.072>
- Bakonyi, P., Buitrón, G., Valdez-Vazquez, I., Nemesóthy, N., Bélafi-Bakó, K., 2017. A novel gas separation integrated membrane bioreactor to evaluate the impact of self-generated biogas recycling on continuous hydrogen fermentation. *Appl. Energy* 190, 813–823. <https://doi.org/10.1016/j.apenergy.2016.12.151>
- Cabrol, L., Malhautier, L., Poly, F., Lepeuple, A.-S., Fanlo, J.-L., 2012. Bacterial dynamics in steady-state biofilters: beyond functional stability. *FEMS Microbiol. Ecol.* 79, 260–71. <https://doi.org/10.1111/j.1574-6941.2011.01213.x>
- Carrillo-Reyes, J., Celis, L.B., Alatríste-Mondragón, F., Razo-Flores, E., 2014. Decreasing methane production in hydrogenogenic UASB reactors fed with cheese whey. *Biomass and Bioenergy* 63, 101–108. <https://doi.org/10.1016/j.biombioe.2014.01.050>
- Carrillo-Reyes, J., Celis, L.B., Alatríste-Mondragón, F., Razo-Flores, E., 2012. Different start-up strategies to enhance biohydrogen production from cheese whey in UASB reactors. *Int. J. Hydrogen Energy* 37, 5591–5601. <https://doi.org/10.1016/j.ijhydene.2012.01.004>
- Carrillo-Reyes, J., Trably, E., Bernet, N., Latrille, E., Razo-Flores, E., 2016. High robustness of a simplified microbial consortium producing hydrogen in long term operation of a biofilm fermentative reactor. *Int. J. Hydrogen Energy* 41, 2367–2376. <https://doi.org/10.1016/j.ijhydene.2015.11.131>
- Castelló, E., García y Santos, C., Iglesias, T., Paolino, G., Wenzel, J., Borzacconi, L., Etchebehere, C., 2009. Feasibility of biohydrogen production from cheese whey using a UASB reactor: Links between microbial community and reactor performance. *Int. J. Hydrogen Energy* 34, 5674–5682. <https://doi.org/10.1016/j.ijhydene.2009.05.060>
- Chen, W.-M., Tseng, Z.-J., Lee, K.-S., Chang, J.-S., 2005. Fermentative hydrogen production with *Clostridium butyricum* CGS5 isolated from anaerobic sewage sludge. *Int. J. Hydrogen Energy* 30, 1063–1070. <https://doi.org/10.1016/j.ijhydene.2004.09.008>
- Cisneros-Pérez, C., Carrillo-Reyes, J., Celis, L.B., Alatríste-Mondragón, F., Etchebehere, C., Razo-Flores, E., 2015. Inoculum pretreatment promotes differences in hydrogen production performance in EGSB reactors. *Int. J. Hydrogen Energy* 40, 6329–6339. <https://doi.org/10.1016/j.ijhydene.2015.03.048>
- Davila-Vazquez, G., Cota-Navarro, C.B., Rosales-Colunga, L.M., de León-Rodríguez, A., Razo-Flores, E., 2009. Continuous biohydrogen production using cheese whey: Improving the hydrogen production rate. *Int. J. Hydrogen Energy* 34, 4296–4304. <https://doi.org/10.1016/j.ijhydene.2009.02.063>

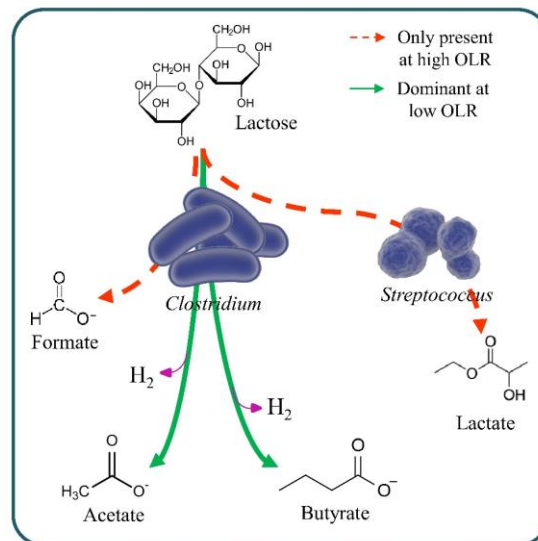
- Davila-Vazquez, G., de León-Rodríguez, A., Alatraste-Mondragón, F., Razo-Flores, E., 2011. The buffer composition impacts the hydrogen production and the microbial community composition in non-axenic cultures. *Biomass and Bioenergy* 35, 3174–3181. <https://doi.org/10.1016/j.biombioe.2011.04.046>
- Denman, S.E., Fernandez, G.M., Shinkai, T., Mitsumori, M., McSweeney, C.S., 2015. Metagenomic analysis of the rumen microbial community following inhibition of methane formation by a halogenated methane analog. *Front. Microbiol.* 6, 1–12. <https://doi.org/10.3389/fmicb.2015.01087>
- Diamantis, V., Khan, A., Ntougias, S., Stamatelatou, K., Kapagiannidis, A.G., Aivasidis, A., 2013. Continuous biohydrogen production from fruit wastewater at low pH conditions. *Bioprocess Biosyst. Eng.* 36, 965–974. <https://doi.org/10.1007/s00449-012-0832-z>
- Etchebehere, C., Castelló, E., Wenzel, J., del Pilar Anzola-Rojas, M., Borzacconi, L., Buitrón, G., Cabrol, L., Carminato, V.M., Carrillo-Reyes, J., Cisneros-Pérez, C., Fuentes, L., Moreno-Andrade, I., Razo-Flores, E., Filippi, G.R., Tapia-Venegas, E., Toledo-Alarcón, J., Zaiat, M., 2016. Microbial communities from 20 different hydrogen-producing reactors studied by 454 pyrosequencing. *Appl. Microbiol. Biotechnol.* 100, 3371–3384. <https://doi.org/10.1007/s00253-016-7325-y>
- Faust, K., Lima-Mendez, G., Lerat, J.-S., Sathirapongsasuti, J.F., Knight, R., Huttenhower, C., Lenaerts, T., Raes, J., 2015. Cross-biome comparison of microbial association networks. *Front. Microbiol.* 6, 1–13. <https://doi.org/10.3389/fmicb.2015.01200>
- Faust, K., Raes, J., 2016. CoNet app: inference of biological association networks using Cytoscape. *F1000Research* 5, 1519. <https://doi.org/10.12688/f1000research.9050.1>
- Faust, K., Raes, J., 2012. Microbial interactions: from networks to models. *Nat. Rev. Microbiol.* 10, 538–550. <https://doi.org/10.1038/nrmicro2832>
- Faust, K., Sathirapongsasuti, J.F., Izard, J., Segata, N., Gevers, D., Raes, J., Huttenhower, C., 2012. Microbial Co-occurrence Relationships in the Human Microbiome. *PLoS Comput. Biol.* 8, e1002606. <https://doi.org/10.1371/journal.pcbi.1002606>
- Ghimire, A., Frunzo, L., Pirozzi, F., Trably, E., Escudie, R., Lens, P.N.L., Esposito, G., 2015. A review on dark fermentative biohydrogen production from organic biomass: Process parameters and use of by-products. *Appl. Energy* 144, 73–95. <https://doi.org/10.1016/j.apenergy.2015.01.045>
- Gomes, S.D., Fuess, L.T., Mañunga, T., Feitosa de Lima Gomes, P.C., Zaiat, M., 2016. Bacteriocins of lactic acid bacteria as a hindering factor for biohydrogen production from cassava flour wastewater in a continuous multiple tube reactor. *Int. J. Hydrogen Energy* 41, 8120–8131. <https://doi.org/10.1016/j.ijhydene.2015.11.186>
- Hallenbeck, P.C., Ghosh, D., 2009. Advances in fermentative biohydrogen production: the way forward? *Trends Biotechnol.* 27, 287–97. <https://doi.org/10.1016/j.tibtech.2009.02.004>
- Han, H., Jia, Q., Wei, L., Shen, J., 2014. Influence of Cu²⁺ concentration on the biohydrogen production of continuous stirred tank reactor. *Int. J. Hydrogen Energy* 39, 13437–13442. <https://doi.org/10.1016/j.ijhydene.2014.04.022>
- Hung, C.-H., Chang, Y.-T., Chang, Y.-J., 2011. Roles of microorganisms other than *Clostridium* and *Enterobacter* in anaerobic fermentative biohydrogen production systems – A review. *Bioresour. Technol.* 102, 8437–8444. <https://doi.org/10.1016/j.biortech.2011.02.084>
- Jo, J.H., Jeon, C.O., Lee, D.S., Park, J.M., 2007. Process stability and microbial community structure in anaerobic hydrogen-producing microflora from food waste containing kimchi. *J. Biotechnol.* 131, 300–308. <https://doi.org/10.1016/j.jbiotec.2007.07.492>
- Jung, K.W., Kim, D.H., Shin, H.S., 2010. Continuous fermentative hydrogen production from coffee drink manufacturing wastewater by applying UASB reactor. *Int. J. Hydrogen Energy* 35, 13370–13378. <https://doi.org/10.1016/j.ijhydene.2009.11.120>

- Kim, D.H., Jang, S., Yun, Y.M., Lee, M.K., Moon, C., Kang, W.S., Kwak, S.S., Kim, M.S., 2014. Effect of acid-pretreatment on hydrogen fermentation of food waste: Microbial community analysis by next generation sequencing. *Int. J. Hydrogen Energy* 39, 16302–16309. <https://doi.org/10.1016/j.ijhydene.2014.08.004>
- Kozich, J.J., Westcott, S.L., Baxter, N.T., Highlander, S.K., Schloss, P.D., 2013. Development of a Dual-Index Sequencing Strategy and Curation Pipeline for Analyzing Amplicon Sequence Data on the MiSeq Illumina Sequencing Platform. *Appl. Environ. Microbiol.* 79, 5112–5120. <https://doi.org/10.1128/AEM.01043-13>
- Kumar, G., Bakonyi, P., Kobayashi, T., Xu, K.Q., Sivagurunathan, P., Kim, S.H., Buitr??n, G., Nemest??thy, N., B??lafi-Bak??, K., 2016. Enhancement of biofuel production via microbial augmentation: The case of dark fermentative hydrogen. *Renew. Sustain. Energy Rev.* 57, 879–891. <https://doi.org/10.1016/j.rser.2015.12.107>
- Küsel, K., Drake, H., 2005. Acetogenic Clostridia, in: *Handbook on Clostridia*. CRC Press, pp. 719–746. <https://doi.org/10.1201/9780203489819.ch32>
- Lay, C.-H., Wu, J.-H., Hsiao, C.-L., Chang, J.-J., Chen, C.-C., Lin, C.-Y., 2010. Biohydrogen production from soluble condensed molasses fermentation using anaerobic fermentation. *Int. J. Hydrogen Energy* 35, 13445–13451. <https://doi.org/10.1016/j.ijhydene.2009.11.128>
- Lee, K.-S., Tseng, T.-S., Liu, Y.-W., Hsiao, Y.-D., 2012. Enhancing the performance of dark fermentative hydrogen production using a reduced pressure fermentation strategy. *Int. J. Hydrogen Energy* 37, 15556–15562. <https://doi.org/10.1016/j.ijhydene.2012.04.039>
- Luo, G., Karakashev, D., Xie, L., Zhou, Q., Angelidaki, I., 2011. Long-term effect of inoculum pretreatment on fermentative hydrogen production by repeated batch cultivations: Homoacetogenesis and methanogenesis as competitors to hydrogen production. *Biotechnol. Bioeng.* 108, 1816–1827. <https://doi.org/10.1002/bit.23122>
- Mäkinen, A.E., Nissilä, M.E., Puhakka, J.A., 2012. Dark fermentative hydrogen production from xylose by a hot spring enrichment culture. *Int. J. Hydrogen Energy* 37, 12234–12240. <https://doi.org/10.1016/j.ijhydene.2012.05.158>
- Massanet-Nicolau, J., Guwy, A., Dinsdale, R., Premier, G., Esteves, S., 2010. Production of hydrogen from sewage biosolids in a continuously fed bioreactor: Effect of hydraulic retention time and sparging. *Int. J. Hydrogen Energy* 35, 469–478. <https://doi.org/10.1016/j.ijhydene.2009.10.076>
- Milferstedt, K., Santa-Catalina, G., Godon, J.-J., Escudié, R., Bernet, N., 2013. Disturbance Frequency Determines Morphology and Community Development in Multi-Species Biofilm at the Landscape Scale. *PLoS One* 8, e80692. <https://doi.org/10.1371/journal.pone.0080692>
- Noike, T., Takabatake, H., Mizunoc, O., Ohbab, M., 2002. Inhibition of hydrogen fermentation of organic wastes by lactic acid bacteria. *Int. J. Hydrogen Energy* 27, 1367–1371. [https://doi.org/10.1016/S0360-3199\(02\)00120-9](https://doi.org/10.1016/S0360-3199(02)00120-9)
- Nualsri, C., Kongjan, P., Reungsang, A., 2016. Direct integration of CSTR-UASB reactors for two-stage hydrogen and methane production from sugarcane syrup. *Int. J. Hydrogen Energy* 41, 17884–17895. <https://doi.org/10.1016/j.ijhydene.2016.07.135>
- Park, J.-H., Lee, S.-H., Ju, H.-J., Kim, S.-H., Yoon, J.-J., Park, H.-D., 2016. Failure of biohydrogen production by low levels of substrate and lactic acid accumulation. *Renew. Energy* 86, 889–894. <https://doi.org/10.1016/j.renene.2015.09.016>
- R Development Core Team, R., 2011. R: A Language and Environment for Statistical Computing, R Foundation for Statistical Computing. <https://doi.org/10.1007/978-3-540-74686-7>
- Ramette, A., 2007. Multivariate analyses in microbial ecology. *FEMS Microbiol. Ecol.* 62, 142–160. <https://doi.org/10.1111/j.1574-6941.2007.00375.x>

- Rittmann, B.E., McCarty, P.L., 2001. *Environmental Biotechnology: Principles and Applications*, McGraw-Hill Series in Water Resources and Environmental Engineering.
- Rochex, A., Godon, J., Bernet, N., Escudier, R., 2008. Role of shear stress on composition, diversity and dynamics of biofilm bacterial communities. *Water Res.* 42, 4915–4922. <https://doi.org/10.1016/j.watres.2008.09.015>
- Rosa, P.R.F., Santos, S.C., Sakamoto, I.K., Varesche, M.B.A., Silva, E.L., 2014. Hydrogen production from cheese whey with ethanol-type fermentation: Effect of hydraulic retention time on the microbial community composition. *Bioresour. Technol.* 161, 10–19. <https://doi.org/10.1016/j.biortech.2014.03.020>
- Sikora, A., Baszczyk, M., Jurkowski, M., Zielenkiewicz, U., 2013. Lactic Acid Bacteria in Hydrogen-Producing Consortia: On Purpose or by Coincidence?, in: *Lactic Acid Bacteria - R & D for Food, Health and Livestock Purposes*. InTech. <https://doi.org/10.5772/50364>
- Sivagurunathan, P., Kumar, G., Bakonyi, P., Kim, S.H., Kobayashi, T., Xu, K.Q., Lakner, G., T??th, G., Nemest??thy, N., B??lafi-Bak??, K., 2016a. A critical review on issues and overcoming strategies for the enhancement of dark fermentative hydrogen production in continuous systems. *Int. J. Hydrogen Energy* 41, 3820–3836. <https://doi.org/10.1016/j.ijhydene.2015.12.081>
- Sivagurunathan, P., Kumar, G., Park, J.H., Park, J.H., Park, H.D., Yoon, J.J., Kim, S.H., 2016b. Feasibility of enriched mixed cultures obtained by repeated batch transfer in continuous hydrogen fermentation. *Int. J. Hydrogen Energy* 41, 4393–4403. <https://doi.org/10.1016/j.ijhydene.2015.06.133>
- Sivagurunathan, P., Sen, B., Lin, C.Y., 2015. High-rate fermentative hydrogen production from beverage wastewater. *Appl. Energy* 147, 1–9. <https://doi.org/10.1016/j.apenergy.2015.01.136>
- Tanisho, S., 1998. Hydrogen Production by Facultative Anaerobe *Enterobacter aerogenes*, in: *BioHydrogen*. Springer US, Boston, MA, pp. 273–279. https://doi.org/10.1007/978-0-585-35132-2_35
- Thamacharoensuk, T., Kitahara, M., Ohkuma, M., Thongchul, N., Tanasupawat, S., 2015. *Sporolactobacillus shoreae* sp. nov. and *Sporolactobacillus spathodeae* sp. nov., two spore-forming lactic acid bacteria isolated from tree barks in Thailand. *Int. J. Syst. Evol. Microbiol.* 65, 1220–1226. <https://doi.org/10.1099/ijs.0.000084>
- WU, S., HUNG, C., LIN, C., LIN, P., LEE, K., LIN, C., CHANG, F., CHANG, J., 2008. HRT-dependent hydrogen production and bacterial community structure of mixed anaerobic microflora in suspended, granular and immobilized sludge systems using glucose as the carbon substrate. *Int. J. Hydrogen Energy* 33, 1542–1549. <https://doi.org/10.1016/j.ijhydene.2007.10.020>
- Zhang, S., Lee, Y., Kim, T.-H., Hwang, S.-J., 2013. Effects of OLRs and HRTs on hydrogen production from high salinity substrate by halophilic hydrogen producing bacterium (HHPB). *Bioresour. Technol.* 141, 227–232. <https://doi.org/10.1016/j.biortech.2012.12.056>
- Zhang, Z.-P., Show, K.-Y., Tay, J.-H., Liang, D.T., Lee, D.-J., Jiang, W.-J., 2006. Effect of hydraulic retention time on biohydrogen production and anaerobic microbial community. *Process Biochem.* 41, 2118–2123. <https://doi.org/10.1016/j.procbio.2006.05.021>
- Zhao, B., Wang, L., Li, F., Hua, D., Ma, C., Ma, Y., Xu, P., 2010. Kinetics of d-lactic acid production by *Sporolactobacillus* sp. strain CASD using repeated batch fermentation. *Bioresour. Technol.* 101, 6499–6505. <https://doi.org/10.1016/j.biortech.2010.03.069>

CHAPTER III

Hydrogen metabolic patterns driven by *Clostridium*-*Streptococcus* community shifts in a CSTR at different organic loading rates.



Highlights

- At $OLR \leq 44.1$ g lactose/L-d, the VHPR was in the range of 3.2-11.6 L H₂/L-d, while the H₂ yields were 1.84-2.14 mol H₂/mol hexose.
- At $OLR \geq 58.8$ g lactose/L-d the H₂ yield was 0.74-1.9 mol H₂/mol hexose while the VHPR was enhanced to 5.5-14.5 L H₂/L-d.
- High throughput sequencing revealed a low diverse and highly specialized *Clostridium*-*Streptococcus* microbial community that drove dark fermentation.
- Overall, a negative relationship between productivity and efficiency of dark fermentation was observed.

The present chapter is based on the article:

Palomo-Briones, Trably, E., López-Lozano, N.E., Celis, L.B., Méndez-Acosta, H.O., Bernet, N., Razo-Flores, E. 2018. Hydrogen metabolic patterns driven by *Clostridium*-*Streptococcus* community shifts in a continuous stirred tank reactor. *Applied Microbiology and Biotechnology*, 102 2465-2475.

3.1. Summary

The efficiency of hydrogen (H₂) production in dark fermentation systems is strongly dependent on the occurrence of metabolic pathways derived from the selection of microbial species that either consume molecular H₂ or outcompete hydrogenogenic bacteria for the organic substrate. In this study, the effect of organic loading rate (OLR) on the H₂ production performance, the metabolic pathways and the microbial community composition in a continuous system was evaluated. Two bacterial genera, *Clostridium* and *Streptococcus*, were dominant in the microbial community depending on the OLR applied. At low OLR (14.7 - 44.1 g lactose/L-d), *Clostridium sp.* was dominant and directed the system towards the acetate-butyrate fermentation pathway, with a maximum H₂ yield of 2.14 mol H₂/mol hexose obtained at 29.4 g lactose/L-d. Under such conditions, the volumetric H₂ production rate (VHPR) was between 3.2 - 11.6 L H₂/L-d. In contrast, relatively high OLR (58.8 and 88.2 g lactose/L-d) favored the dominance of *Streptococcus sp.* as co-dominant microorganism leading to lactate production. Under these conditions, the production of formate was also stimulated serving as a strategy to dispose the surplus of reduced molecules (e.g. NADH₂⁺), which theoretically consumed up to 5.72 L H₂/L-d. In such scenario, the VHPR was enhanced (13.7 – 14.5 L H₂/L-d) but the H₂ yield dropped to a minimum of 0.74 mol H₂/mol hexose at OLR = 58.8 g lactose/L-d. Overall, this research brings clear evidence of the intrinsic occurrence of metabolic pathways detrimental for biohydrogen production, *i.e.* lactic acid fermentation and production of formate, suggesting the use of low OLR as a strategy to control them.

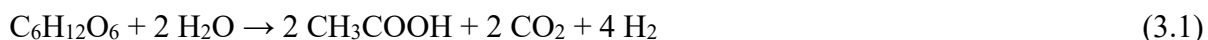
Keywords: Biohydrogen; Dark fermentation; Lactic acid bacteria (LAB); Hydrogen-producing bacteria (HPB); Microbial community

3.2. Introduction

The development of zero- and low-carbon technologies for energy production is an important milestone towards the mitigation of climate change. In this regard, biofuels have gained great attention due to the possibility to revalorize organic wastes generated by industrial, agricultural, and domestic sectors, and minimize the release of additional carbon into the atmosphere.

Biohydrogen is an energy carrier that can be distinguished among other fuels due to its high-energy content (120 kJ/g), highly efficient conversion to electric energy, and byproducts-free oxidation. The production of biohydrogen can be performed through four major biological processes: direct and indirect biophotolysis, photofermentation and dark fermentation. Among these, the dark fermentative technology has shown higher production rates and simpler operation than its counterparts. Moreover, dark fermentation is independent of light and the microbial communities have a remarkable metabolic flexibility that allow them to show good performance in spite to fluctuations of environmental conditions (Azwar et al., 2014).

Theoretically, the maximum H₂ metabolic yield of dark fermentative systems is four mol of H₂ per mol of glucose consumed (Agler et al., 2011). This yield is possible to achieve if only *Clostridium* species are involved in the fermentation by producing acetate as byproduct (Eq. 3.1).



In practice, H₂ yields are substantially lower than the theoretical value obtained from the ideal acetate fermentation (Nath and Das, 2004). This is mainly due to the diversity of metabolic routes, *i.e.*, the production of metabolites associated with low or none H₂ production. Such is the case of butyrate, propionate, ethanol, and lactate pathways, among others. Special focus has been paid to the lactate production, which is performed by LAB such as *Lactobacillus*, *Sporolactobacillus*, *Streptococcus*, etc. LAB outcompete hydrogenogenic microorganisms for the carbon source, but are also capable to produce growth-inhibitory compounds (Gomes et al., 2016; Noike et al., 2002; Sikora et al., 2013). In a previous report, it was informed that LAB co-dominated with *Clostridiaceae* microorganisms at relatively large HRT (18 and 24 h) in a continuous stirred tank reactors (CSTR) fed with lactose. On the contrary, short values of HRT (6 and 12 h) effectively selected *Clostridiaceae* species and prompted an efficient dark fermentation. Therefore, short HRT were suggested as a strategy to prevent the proliferation of LAB (Palomo-Briones et al., 2017). However, to the best of our knowledge, the effects of the OLR at fixed

HRT on LAB in a dark fermentative environment remain unexplored in CSTR systems. This issue is of high interest since the relationship between OLR and LAB can potentially affect the scaling up and economy of the process. On the other hand, H₂ yield can also be shortened due to H₂ consumption through the Wood-Ljungdahl pathway (WLP), which can be carried out by several *Clostridium* species (Diekert and Wohlfarth, 1994; Saady, 2013). In such pathway, H₂ and CO₂ are combined to produce acetyl-CoA and a diversity of other metabolites (Diekert and Wohlfarth, 1994; Schuchmann and Müller, 2014; Tracy et al., 2012).

Different authors have reported that LAB and WLP-hydrogenotrophic microorganisms are affected by environmental and operational conditions (*e.g.* Shanmugam et al. 2014; Carrillo-Reyes et al. 2014; Si et al. 2015). Nevertheless, most studies have been focused on the suppression of either LAB or WLP-hydrogenotrophic microorganisms, although these could be simultaneously present. In such scenario, the strategies aimed to suppress one of these groups could result in the enrichment of the second one, and *vice versa*. Therefore, this work aims to investigate the effect of OLR on the performance of H₂ production, metabolic pathways and microbial community in a lactose fed CSTR, with special focus on the potential co-occurrence of LAB and WLP-hydrogenotrophic microorganisms.

3.3. Materials and methods

3.3.1. Inoculum and substrate

Anaerobic granular sludge from a full-scale upflow anaerobic sludge blank reactor treating wastewater from a tequila factory was used as inoculum. Before inoculation, the sludge was disaggregated and heat pretreated at 90-95 °C for 2 hours to select spore-forming microorganisms. The inoculum was added at a final concentration of 4.5 g volatile suspended solids (VSS)/L. Cheese whey powder (Darigold, USA) with lactose content of 75.5% was used as substrate at concentrations ranging from 3.7 to 22.5 g_{lactose}/L. The feeding solution was supplemented with (mg/L): NH₄Cl, 2100; MgCl₂·6H₂O, 100; CuCl₂·H₂O, 1.25; MnCl₂ 4H₂O, 7; FeCl₂ 4H₂O, 19.1; NiCl₂ 6H₂O, 102.5. Additionally, phosphate buffer (KH₂PO₄-Na₂HPO₄, pH 5.9) was added to a final concentration of 100 mM.

3.3.2. Experimental setup

A bioreactor made of glass, with 1 L working volume and 0.3 L of head space (APPLIKON Biotechnologies, USA) was inoculated with the heat treated anaerobic sludge. The system was started-up

in batch mode for 24 h using cheese whey powder at a concentration of 22 g lactose/L. Afterward, the reactor was shifted to continuous operation at a HRT of 6 h (OLR of 88 g lactose/L-d). In subsequent stages, the OLR was decreased gradually from 88 to 15 g lactose/L-d by modifying the cheese whey powder concentration. Each OLR condition was maintained for at least 20 HRT (120 h) and until steady state was reached (VHPR variation < 10% in three consecutive measurements). Stirring, HRT, temperature and pH were set and controlled at 250 rpm, 6 h, 37 °C and 5.9, respectively.

3.3.3. Analytical methods

Liquid samples were collected in a regularly basis and used to determine biomass, chemical oxygen demand (COD), total carbohydrates and volatile fatty acids. Biomass (as volatile suspended solids, VSS) and soluble COD were quantified as described in the standard methods (APHA/AWWA/WEF, 2012). Total carbohydrates were determined by the phenol sulfuric method (Dubois et al., 1956). Volatile fatty acids were quantified from filtered (0.22 mm) samples by capillary electrophoresis (1600A, Agilent Technologies, Waldbronn, Germany) as reported elsewhere (Davila-Vazquez et al., 2008).

The volume of gas produced was measured through a liquid displacement device, and its composition (H₂ and CO₂) was determined through a gas chromatograph equipped with a thermal conductivity detector (6890N, Agilent Technologies, Waldbronn, Germany). All the gas volumes are reported at 1 atm and 273.15 K.

3.3.4. Capillary Electrophoresis - Single Strand Conformation Polymorphism (CE-SSCP)

The CE-SSCP was performed as described elsewhere (Palomo-Briones et al., 2017). In brief, the bacterial DNA was extracted using the ZR Fungal/Bacterial DNA MiniPrep extraction kit according to manufacturer's instructions (Zymo Research). The amplification of the V3 region of the 16S rRNA genes was performed with Pfu Turbo DNA polymerase (Stratagene, La Jolla, CA, USA) and the universal primers W49 5'-ACGGTCCAGACTCCTACGGG-3' and W104 5'-TTACCGCGGCTGCTGGCAC-3'. The PCR conditions were set as follows (Milferstedt et al., 2013): initial denaturation for 2 min at 94°C; 25 cycles of melting (1 min at 94°C), annealing (1 min at 61°C) and extension (1 min at 72°C); and a final extension step of 10 min at 72°C.

The PCR products were analyzed by CE-SSCP in an ABI 3130 genetic analyzer (Applied Biosystems, Foster City, CA, USA) as reported by Rochex et al. (2008). The resulting CE-SSCP profiles were aligned

with an internal standard (ROX) to consider the inter-sample electrophoretic variability and were normalized with the package *Statfingerprints* available on R platform (R Development Core Team, 2011).

The relative abundances of each peak on CE-SSCP profiles were computed with the spectroscopy functionality of OriginPro 8 (first derivative method, both directions, min height 1%, min width 1%). Subsequently, a Pearson's distances matrix was computed using CE-SSCP relative abundances, and it was displayed as a hierarchical cluster dendrogram. Such computing was carried out with the *corrplot*, *ggplot* and *ggdendro* packages under R environment (R Development Core Team, 2011).

3.3.5. Illumina sequencing and microbial community analysis

Illumina MiSeq 2x250 paired-end sequencing was performed following the manufacturers protocol (Illumina, USA). The V3-V4 regions of the rRNA gene (~450 bp) were amplified with the primers 341F (5'-CCTACGGGNGGCWGCAG) and 805R (5'-GACTACHVGGGTATCTAATCC) fused with Illumina adapters. The polymerase chain reaction (PCR) was performed using the Phusion High-Fidelity PCR Master Mix with HF Buffer (Thermo Scientific, USA) and the following conditions: initial denaturation step at 95 °C for 3 min, followed by 25 cycles (95 °C, 30 sec; 55 °C, 30 sec; 72 °C, 30 sec) and a final elongation step at 72 °C for 5 min. The PCR products were indexed with Nextera XT index primers in a second PCR (8 cycles) under identical conditions. The resulting amplicons were purified with Agencourt AMPure XP beads (Beckman Coulter, USA) and re-suspended in Illumina buffer. The Illumina sequencing work was carried out by the Unidad Universitaria de Secuenciación Masiva y Bioinformática, Instituto de Biotecnología, UNAM, Cuernavaca, Morelos, México.

The downstream sequence processing was performed using the Quantitative Insights into Microbial Ecology (QIIME) software (Caporaso et al., 2010). The analysis included the merging of the paired sequences with a minimum overlapping of 20 bp and zero errors in the overlapping region. The resulting sequences were quality filtered at a Phred score > Q20. Sequences with less than 350 pb were also eliminated. The chimeric sequences were filtered with the UCHIME 6.1 software (Edgar et al., 2011). Afterward, open OTU picking at a 97% sequence identity was carried out with the UCLUST algorithm (Edgar, 2010) using the SILVA RNA database (128 release) as reference (<https://www.arb-silva.de/download/archive/qiime/>). The sequences of this work were deposited in the NCBI BioProject PRJNA392772.

3.4. Results

3.4.1. Dark fermentation performance

The CSTR was operated during 80 days under controlled pH (5.9), temperature (37 °C) and HRT (6 h). The reactor was fed at six sequential OLR: 88, 59, 44, 29, 22, and 15 g lactose/L-d, referred from now on as Stage I, Stage II, Stage III, Stage IV, Stage V, and Stage VI, respectively. After the first six stages were carried out, an unexpected low performance was noticed in Stage II; thus, the OLR of 59 g lactose/L-d was applied again after Stage VI (15 g lactose/L-d). In total, the experiments consisted of seven experimental phases as shown in Figure. 3.1a.

The performance results show that the VHPR was directly linked with the OLR (Figure 3.1a). A maximal VHPR of 13.9 ± 2.2 L H₂/L-d (mean \pm SD) was observed in Stage I (OLR of 88.2 g lactose/L-d), while the lowest VHPR of 3.04 ± 0.9 L H₂/L-d was found in Stage VI (OLR of 14.7 g lactose/L-d). This confirmed that a successful hydrogenogenic fermentation was established. In terms of H₂ yield, the optimal value of 2.17 ± 0.29 mol H₂/mol hexose (mean \pm SD) was found at an OLR of 29.4 g lactose/L-d (Stage IV). Overall, the H₂ yields ranged between 0.67 and 2.17 mol H₂/mol hexose (Figure 3.1b).

To investigate the main metabolic pathways along the experiment, the volatile fatty acids were quantified. The analysis showed that steady state values of acetate and butyrate yields ranged within 0.13 - 0.53 mol acetate/mol hexose and 0.26 - 0.78 mol butyrate/mol hexose, respectively. On the other hand, the steady state values of formate and lactate were between 0.07 - 0.51 mol formate/mol hexose and 0.03 - 0.59 mol lactate/mol hexose, respectively. Further analysis of the steady states revealed positive correlations between the H₂ yield and the molar yields of acetate and butyrate (Figure 3.2 B and D). On the contrary, the molar yields of acetate and butyrate were negatively correlated with the OLR (Figure 3.2 F and H). Additionally, acetate and butyrate were produced in a roughly constant acetate/butyrate ratio of 0.7, independently of OLR, VHPR and H₂ yield. Moreover, the H₂ yield was negatively associated with lactate and formate yields (Figure 3.2 A and C). The data show that the metabolic routes associated with these two compounds seemed to be favored at relatively high OLR (59 and 88 g lactose/L-d) (Figure 3.2 E and G).

Considering that the synthesis of one mol of formate implies the direct or indirect consumption of one mol of H₂, the amount of H₂ depleted in such route was estimated. As result, the maximum amount of H₂ converted to formate was equivalent to 5.7 L H₂/L-d at an OLR of 88 g lactose/L-d (Stage I). In contrast,

the stage with the minimum production of formate was Stage IV (OLR = 29 g lactose/L-d) during which the equivalent amount of H₂ depleted was of 0.25 ± 0.08 L H₂/L-d. Consistently, the maximum H₂ yield was also presented at the same experimental stage (Table 3.1). Finally, it is worth to mention that biomass, residual lactose, volatile fatty acids and H₂ accounted between 84 and 97% of COD fed to the fermentation system (Figure 3.3).

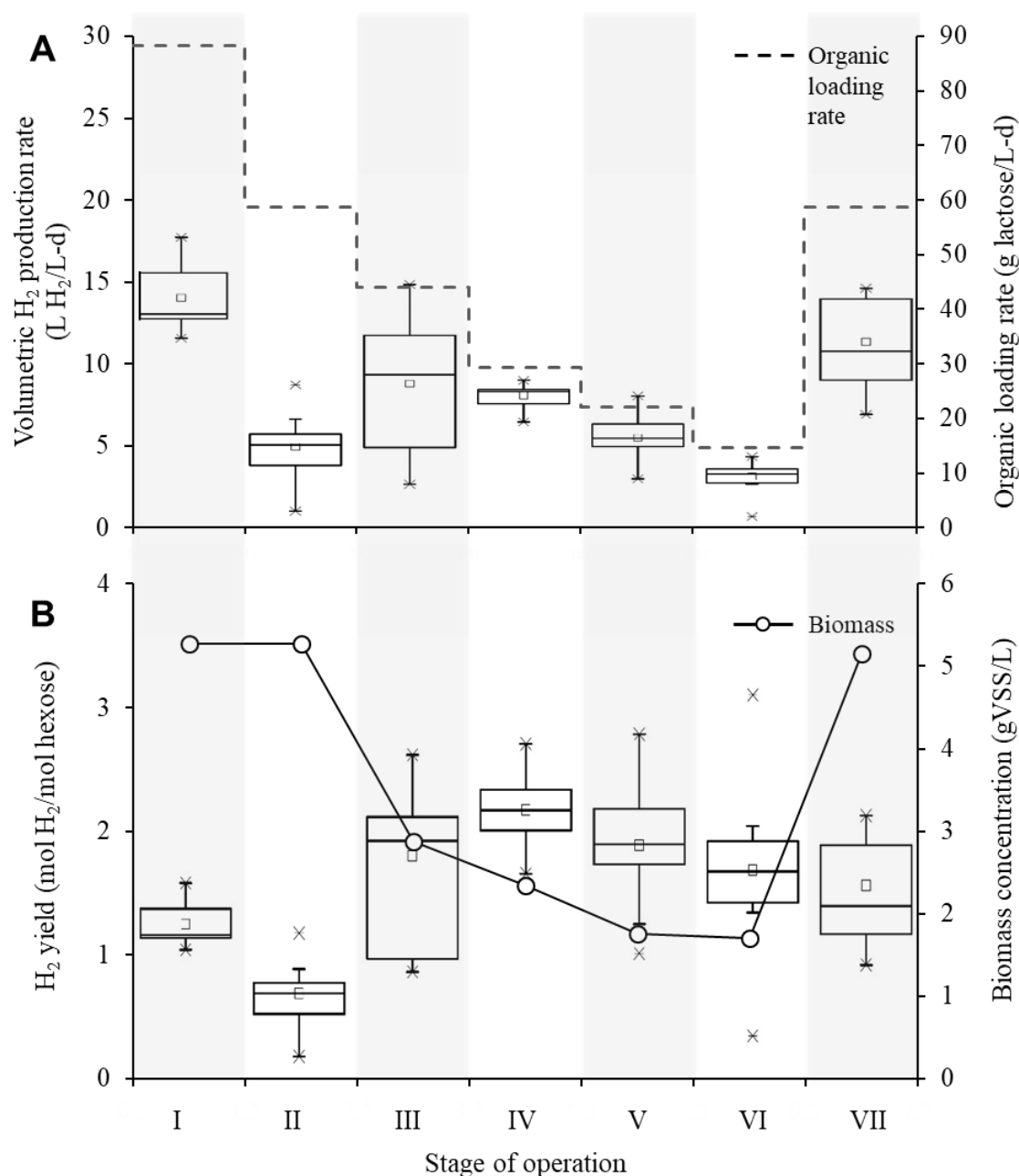


Figure 3.1. H₂ production performance of the continuous stirred-tank reactor operated at different values of organic loading rate. Box plots of the volumetric H₂ production rate (VHPR) and H₂ yield include all data of the corresponding periods. A) VHPR and OLR. B) H₂ yield and biomass concentration.

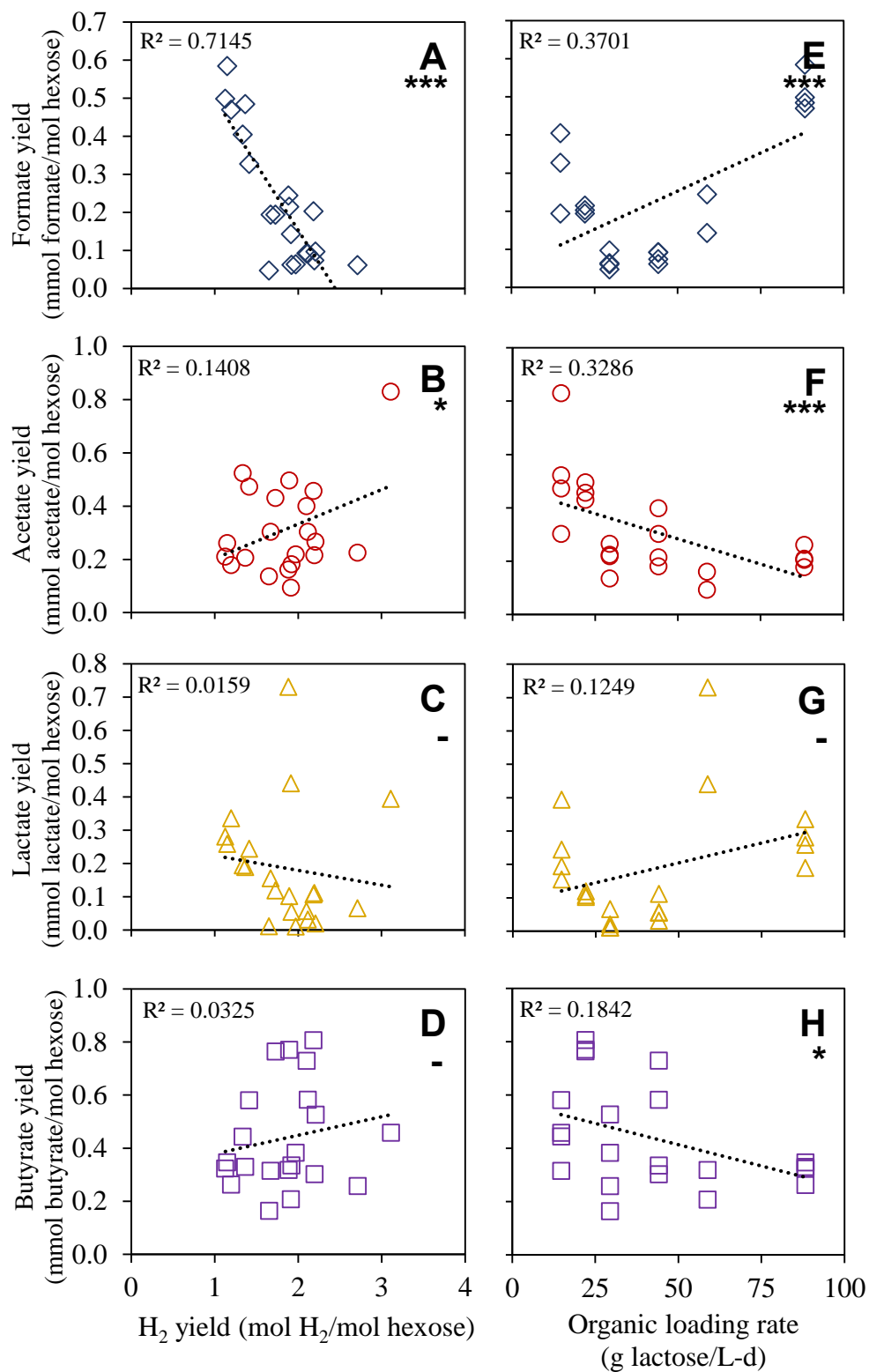


Figure 3.2. Linear correlations between: (A-D) H₂ yield and volatile fatty acids yields, (E-H) organic loading rate and volatile fatty acids yield. Statistical significance of the correlation is displayed according with the following legend: - Not significant, * p<0.10, ** p<0.05, *** p<0.01.

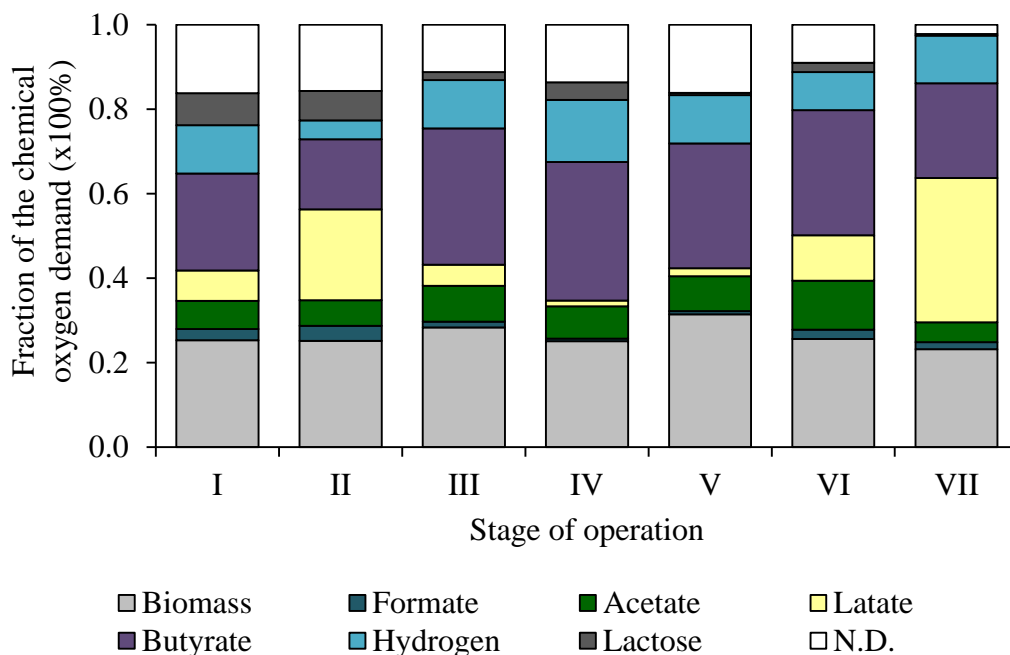


Figure 3.3. Balance of chemical oxygen demand (COD) of continuous stirred-tank reactor operation at different organic loading rates. The balance is based on the total COD of cheese whey powder fed into the bioreactor.

3.4.2. Microbial community analysis

16S-rRNA amplicons obtained at steady states were analyzed by CE-SSCP to characterize the microbial community structure and reveal the OLR-associated changes. The analysis showed that the microbial community was composed principally by three different microorganisms numbered 150, 224 and 910 in reference to the SSCP retention time (Figure 3.4B). Based on relative abundances, the microorganism numbered 910 was dominant at $OLR \geq 59$ g lactose/L-d. In contrast, two different organisms (150 and 224) dominated at $OLR \leq 44$ g lactose/L-d. An Unweighted Pair Group Method with Arithmetic Mean (UPGMA) analysis of the CE-SSCP profiles showed a clear association among stages I, II and VII, regardless of the amount of time separating such experimental stages (Figure 3.4A). On the other hand, stages III, IV, V and VI were also clustered with each other. Overall, two cohesive and OLR-dependent microbial community groups were unveiled.

To identify the microbial genera involved in the fermentation, the V3-V4 regions of 16S-rRNA gene were sequenced and compared with the Silva 16S RNA database to assign taxonomy. The 16S RNA sequencing resulted in 664101 ± 67239 high quality reads per sample, grouped in 14559 operational taxonomic units (OTU), identified up to the genus level. Overall, the results showed the presence of two main genera that

dominated all along the fermentation time, *Clostridium* and *Streptococcus* (Figure 3.5). To identify and characterize the link between CE-SSCP and 16S-rRNA sequencing, a correlation analysis was conducted. The results showed that *Clostridium* was well correlated with microorganisms numbered 150 ($R^2=0.96$, $p<0.01$) and 224 ($R^2=0.96$, $p<0.01$) while *Streptococcus* was strongly correlated with the microorganism numbered 910 ($R^2=0.98$, $p<0.01$). Therefore, 16S-rRNA sequencing results were used for microbial community analysis.

As shown in Figure 3.5, *Clostridium* and *Streptococcus* accounted for more than 88% of the relative abundance, while other microbial genera such as *Enterobacter*, *Escherichia*, *Lactobacillus*, *Lactococcus* and *Enterococcus*, remained subdominant. In general, the relative abundance of *Clostridium* was strongly associated with the reduction of the OLR, while the *Streptococcus* abundance was higher as the OLR increased (Figure 3.5B).

In order to better understand and visualize the relationship between the microbial community composition and the performance of the reactor (*i.e.* VHPR, OLR, H₂ yield, and metabolites yields), a Principal Components Analysis (PCA) was conducted (Figure 3.6). Two principal components accounted for more than 80 percent of the dataset variance. The results showed a clear relationship between *Clostridium* and the butyrate and acetate yields. On the other hand, *Streptococcus* was strongly linked to VHPR, OLR, and lactate yield. Interestingly, formate and H₂ yields showed negative influence on each other, confirming the aforementioned negative correlation between these two metabolic products. Nevertheless, no linear relationship was found between formate and H₂ yields with the *Clostridium* nor *Streptococcus* abundance.

3.5. Discussion

The continuous H₂ production from cheese whey powder was successfully established in a continuous reactor and was comparable to previous works under similar conditions (Cota-Navarro et al., 2011; Davila-Vazquez et al., 2009) demonstrating the reliability and reproducibility of dark fermentation with CSTR systems.

The sequencing analysis revealed that a low diverse and highly specialized microbial community composed mainly by *Clostridium* and *Streptococcus* species drove the lactose-based biohydrogen production. Low microbial diversity is considered as a common characteristic of H₂-producing bioreactors (Etchebehere et al., 2016). This feature becomes accentuated due to the strong pressure of selection that is typical of suspended-growth systems. Interestingly, the relative abundances of these genera were

negatively associated to each other, suggesting competitive interactions. In addition, the changes in the OLR had a critical impact on the microbial community distribution and subsequent metabolites production, including H₂. In this regard, two different OLR-dependent states of operation were identified.

Table 3.1. Summary of the steady state performance of dark fermentative continuous stirred-tank reactors operated under different organic loading rates.

Stage	OLR (g lactose/ L-d)	Theoretical VHPR ^a (L H ₂ /L-d)	Experimental VHPR (L H ₂ /L-d)	H ₂ yield ^b (mol H ₂ /mol hexose)	H ₂ consumed in formate synthesis ^c (L H ₂ /L-d)	Formate (mmol/L)	Acetate (mmol/L)	Lactate (mmol/L)	Butyrate (mmol/L)
I	88.2	46.2	13.7 ± 1.3	1.21 ± 0.11	5.72	63.9	26.8	33.4	39.6
II	58.8	30.8	5.5 ± 0.3	0.74 ± 0.04	2.01	22.5	19.3	34.1	23.2
III	44.1	23.1	11.6 ± 0.4	2.08 ± 0.12	0.44	5.0	16.9	3.9	30.1
IV	29.4	15.4	7.8 ± 1.1	2.14 ± 0.45	0.25	2.8	8.6	1.0	13.7
V	22.0	11.5	5.5 ± 0.7	1.93 ± 0.23	0.58	6.5	14.6	3.5	24.7
VI	14.7	7.7	3.2 ± 0.7	1.84 ± 0.73	0.54	6.0	8.0	3.7	7.1
VII	58.8	30.8	14.5 ± 0.1	1.90 ± 0.02	1.47	16.4	10.8	49.7	22.3

OLR: Organic loading rate; VHPR: Volumetric H₂ production rate.

^aTheoretical VHPR based on the theoretical yield of 4 mol H₂/mol hexose and lactose added; lactose was considered as 2 hexose equivalents.

^bCalculated on the base of hexose equivalents consumed.

^cBased on the assumption that formate was produced by the consumption of H₂: CO₂ + H₂ → CHOOH
Samples considered as steady state = 4, 4, 4, 4, 3, 5, and 3 for stages I-VII, respectively.

3.5.1. Highly efficient H₂-producing phase

The operation of dark fermentative CSTR at OLR ≤ 44.1 g lactose/L-d was found to favor the H₂ yield. At such conditions (Stages III-VI), the microbial community was clearly dominated by microorganisms from the *Clostridium* genus (Figure 3.5). These microorganisms have been widely found in dark fermentative systems and have been identified as highly desirable species for H₂ production (Cabrol et al., 2017). Theoretically, *Clostridium* species are capable to produce H₂ with a metabolic yield of 4 mol H₂/mol hexose following the acetate pathway (Eq. 3.1) and 2 mol H₂/mol hexose through the butyrate pathway (C₆H₁₂O₆ → CH₃-CH₂-CH₂-COOH + 2 CO₂ + 2H₂).

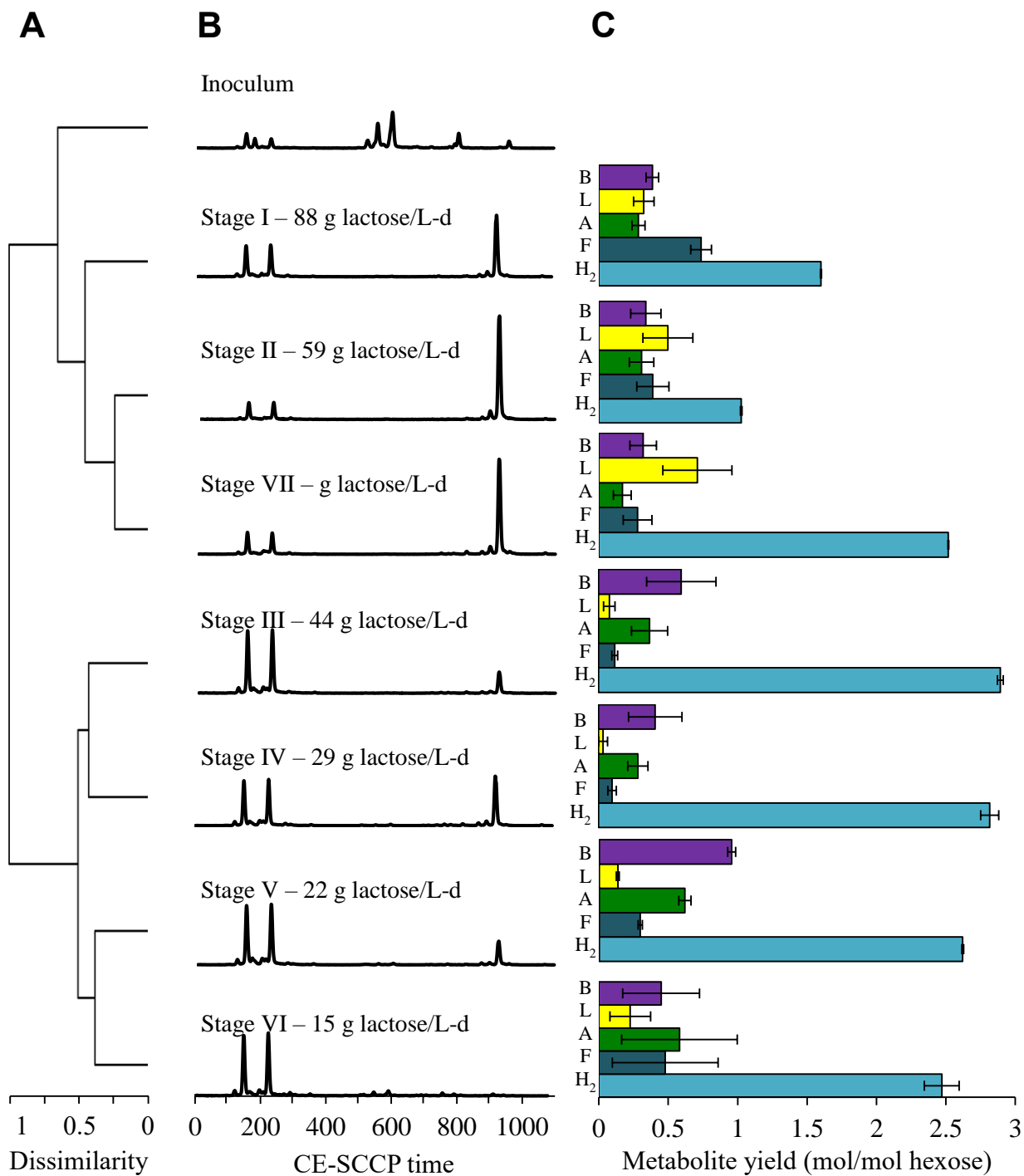


Figure 3.4. Microbial communities and metabolites productivities of dark fermentative systems under different values of organic loading rate (OLR). A) Ward D2 hierarchical cluster analysis based on Pearson distances; B) CE-SSCP profiles of microbial communities developed under different OLR; C) Volatile fatty acids and hydrogen yields from steady states. B, butyrate; L, lactate; A, acetate; F, formate.

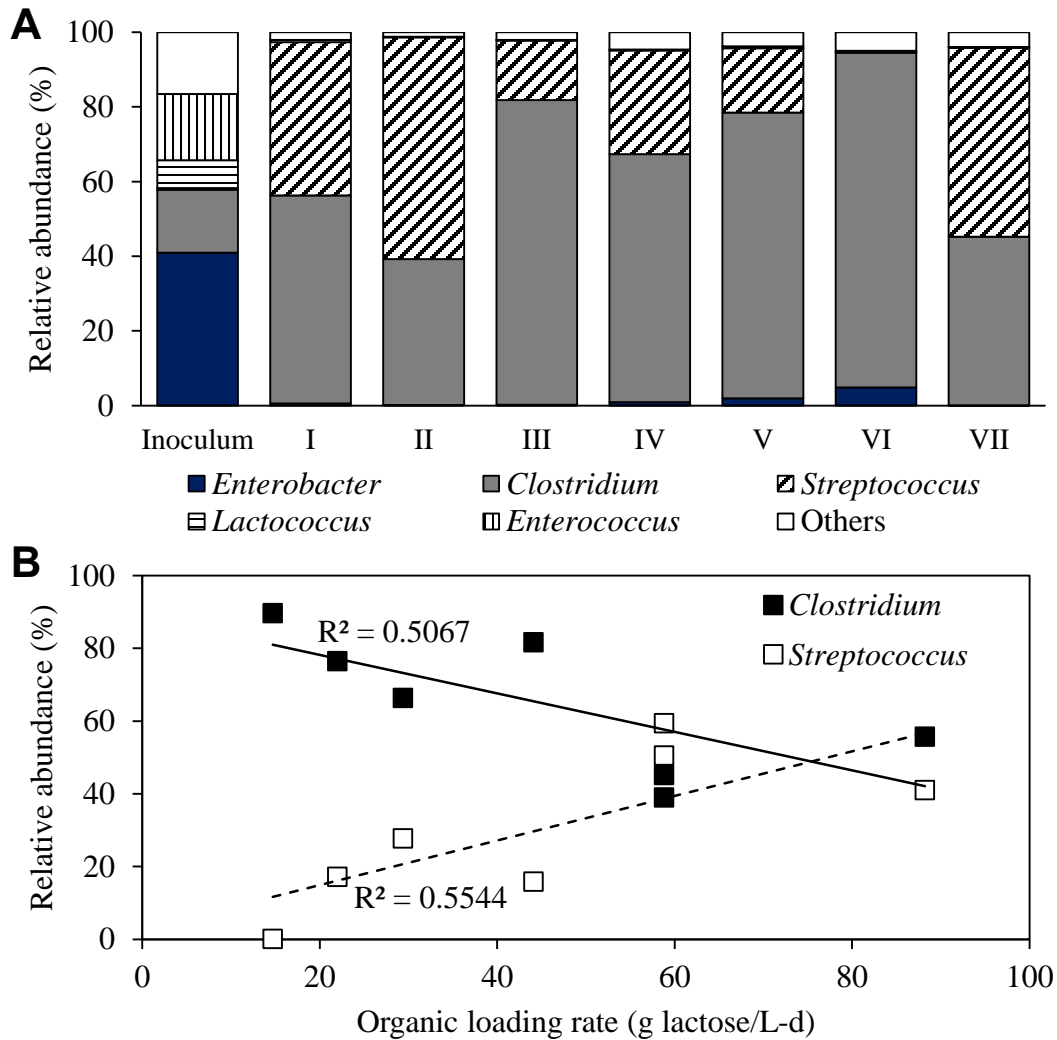


Figure 3.5. A) Profiles of the microbial communities from the operation of the continuous stirred-tank reactor at different conditions of organic loading rate (OLR) obtained by Illumina MiSeq analysis. B) Relationship between *Clostridium* and *Streptococcus* species with the OLR.

As expected, acetate and butyrate were the principal volatile fatty acids produced under the dominance of the *Clostridium* genus (Figure 3.4C) and the H_2 yield reached a maximum mean value of 2.14 mol H_2 /mol hexose (Stage IV). This is a remarkable achievement considering the metabolic limitation and that most of literature has reported about 1.3 mol H_2 /mol hexose.

3.5.2. Lactate and formate favored at high OLR

The operation of the CSTR at $OLR \geq 58.8$ g lactose/L-d caused an important increase in the VHPR (12.3 - 14.5 L H_2 /L-d) in detriment of the H_2 yield (1.21 - 1.9 mol H_2 /mol hexose). This seems to be a disjunction

point between productivity and efficiency of H₂ production. Such phenomenon could be explained by considering that, under high OLR conditions, H₂ is produced in such an amount that it is probably not transferred off the system with the required efficiency, *i.e.* the process is limited by mass transfer. Under such conditions, the microorganisms pursue alternative pathways to dispose the electrons gathered from the organic substrate and tend to produce less H₂ (Nath and Das, 2004). The results of this work clearly showed that such alternative metabolic routes were lactate and formate production.

The presence of lactate is a clear signal of the occurrence of lactic acid fermentation, which is usually found in dark fermentative systems (Baghchehsaraee et al., 2010; Etchebehere et al., 2016; Sikora et al., 2013). The lactic acid fermentation is generally associated to the ubiquitous LAB, whose appearance in dark fermentative systems is probably facilitated by operating under non-sterile conditions. *Streptococcus*, belonging to the LAB, was found as the main responsible of the lactate production (Figure 3.5). This microorganism has been previously found in hydrogenogenic granules where they presumably strengthen the granule structure (Hung et al., 2011b). Davila-Vazquez et al. (2009) also reported the presence of *Streptococcus* in a CSTR fed with cheese whey powder at an OLR of 92.4 and 138.6 g lactose/L-d. In a recent report, it was concluded that the HRT strongly affects the microbial community composition; it was shown that LAB (*Streptococcaceae* and *Sporolactobacillaceae*) can be controlled by operating at short HRT (6 h) (Palomo-Briones et al., 2017). In the present work, although the HRT was maintained at 6 h, the elimination of LAB was only possible at low OLR values.

The dynamics of the microbial community is often associated to the differences in growth capabilities of

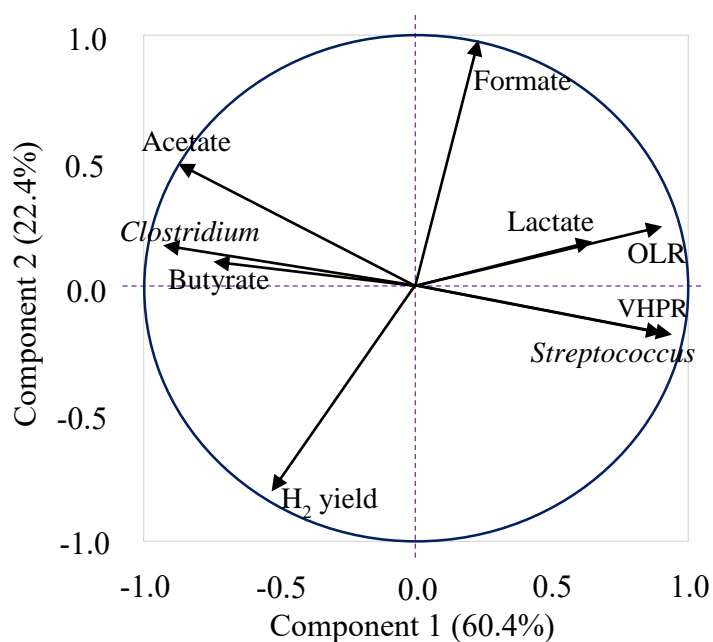


Figure 3.6. Principal Components Analysis of biohydrogen production under different organic loading rates. OLR: Organic loading rate; VHPR: Volumetric H₂ production rate.

the involved species. However, LAB and *Clostridium* have showed similar growth kinetics (e.g. Monod type) with lactose (Table 3.2); therefore, the community behavior is barely explained by kinetic differences. Rather, the community structure could possibly result from product inhibitory effects on the *Clostridium* population at high OLR that allowed LAB to better compete for the substrate uptake. In this regard, Napoli et al. (2011) reported that *Clostridium acetobutylicum* could be inhibited by the accumulation of acetate (26 mmol/L) and butyrate (34 mmol/L). In the present study, acetate and butyrate were in the range of the inhibitory concentrations reported by Napoli et al., (2011) and were strongly associated with the OLR (Table 3.1). Therefore, the inhibition phenomenon seems to be an important driver of the *Clostridium-Streptococcus* dynamics.

Table 3.2. Growth kinetic parameters of representative species of H₂ producing bacteria and lactic acid bacteria.

Microorganism	Kinetic conditions	μ_{max} , (1/h)	K_S , (g/L)	Reference
<i>Clostridium acetobutylicum</i>	Lactose, pH 5, 35 °C	0.95	1.34	Napoli et al., 2011
<i>Lactococcus casei</i>	Whey-lactose, pH 5.5, 37 °C	0.265	0.72	Altioek et al., 2006
<i>Lactobacillus bulgaricus</i>	pH 5.6, 42 °C	1.14	3.36	Burgos-Rubio et al., 2000
<i>Lactococcus lactis</i>	Lactose, pH 6.5, 30 °C	1.1	1.32	Boonmee et al., 2003
<i>Lactobacillus rhamnosus</i>	Glucose, pH 5.5, 40 °C,	0.45	0.30	Berry et al., 1999

In light of the microbial community results, the formate synthesis was probably produced by *Clostridium* species. This biochemical process can be catalyzed by the pyruvate:formate lyase (*pfl*) and the formate dehydrogenase (*fdh*). The former enzyme catalyzes the activation of pyruvate to acetyl-CoA with the concomitant production of formate and CO₂, while the later catalyzes the synthesis of formate from NADH₂⁺ and CO₂.

The *pfl* is broadly found in facultative anaerobes, but it has been also found in the genome of different *Clostridium* species such as *C. butyricum* , *C. acetobutylicum*, *C. beijirinkii*, *C. pasteurianum*, and *C. tyrobutyricum* (Kwok et al., 2014; Lee et al., 2016; Noar et al., 2014; Nolling et al., 2001; Pyne et al.,

2014). The gene of *fdh* enzyme has been reported as part of the genome of *Clostridium* species, such as *C. carboxidivorans* (Bruant et al., 2010), *C. ljungdahlii* (Köpke et al., 2010), *C. beijerinckii* (Milne et al., 2011), and *C. acetobutylicum* (Senger and Papoutsakis, 2008). *fdh* is also the first enzyme to participate in the WLP which leads to the synthesis of acetate (homoacetogenesis).

Considering the actual concentrations of volatile fatty acids, acetate and formate synthesis from H₂ and CO₂ are both favorable reactions (Table 3.3). Nevertheless, no evidence of autotrophic acetate (homoacetogenesis) was found in the experiments here reported. Therefore, formate was suggested as the main H₂ sink under the tested conditions.

Table 3.3. Gibbs' energy of acetate and formate autotrophic reactions.

	ΔG°	ΔG (Stage VI)	ΔG (Stage I)
$2 \text{HCO}_3^- + 2 \text{H}^+ + 4 \text{H}_2 \rightarrow \text{CH}_3\text{COO}^- + \text{H}^+ + 4 \text{H}_2\text{O}$	-144.4 kJ	-101.2 kJ	-98.15 kJ
$\text{HCO}_3^- + \text{H}^+ + \text{H}_2 \rightarrow \text{CHOO}^- + \text{H}^+ + \text{H}_2\text{O}$	-1.3 kJ	-35.7 kJ	-29.6 kJ

ΔG° were calculated at 25°C and standard concentrations.

ΔG were calculated at pH 5.9, 37°C and the following concentrations: $[\text{HCO}_3^-] = 0.05 \text{ M}$; $[\text{H}_2] = 0.05\text{M}$; $[\text{VFA}] = \text{Table 3.1}$. Gibbs' energy values were computed in accordance with Kleerebezem and Van Loosdrecht (2010).

To determine the exact mechanism of formate production will require further studies. However, as formate was OLR dependent, our hypothesis is that such conditions caused an excess of reduced equivalents (NADH_2^+ , Fd_{red}) that accumulated in the cell due to kinetic limitation at the hydrogenases (*hyd*) level. The primary method to dispose electrons is by the action of hydrogenases, but their activity is retro-inhibited at high concentrations of H₂. Thus, the production of formate was a possible strategy to dispose the excess of electrons gathered from the organic substrate, and maintain NAD^+/NADH and $\text{Fd}_{\text{ox}}/\text{Fd}_{\text{red}}$ equilibriums. Under this hypothesis, not only homoacetogenesis but also formic acid synthesis through either the *fdh* (*i.e.* WLP) or *pfl* route plays an important role in H₂ consumption that deserves to be studied with detail.

To overcome the detrimental consequences of formate synthesis and boost H₂ production, new ways to recover H₂ (and possibly CO₂ as well) as soon as it is produced should be developed and implemented. In this regard, different alternatives have been proposed with the aim to increase H₂ productivities. For example, Nasr et al. (2015) reported 22% increase of H₂ yield using KOH pellets to capture CO₂ *in situ*.

The capture of CO₂, as discussed by the authors, favored the shift of the hydrogenogenic reactions to the forward direction (*i.e.* production of H₂). Moreover, CO₂ sequestration also had an influence on the metabolic pathways, favoring acetate productivity while lowering butyrate production.

3.6. Conclusions

Overall, this research shows the results of continuous H₂ production in a CSTR from cheese whey powder as substrate. The microbial community was dominated by three bacterial phylotypes from two main genera, *Clostridium* and *Streptococcus*, whose relative abundances were strongly affected by the OLR. The shift in the microbial community composition also influenced the metabolic pathways performed. At low OLR (14.7-44.1 g lactose/L-d), *Clostridium* was the dominant genus and drove the system to a highly efficient acetate-butyrate fermentation. In contrast, high OLR (58.8 and 88.2 g lactose/L-d) caused an increase of acetate and butyrate concentrations, which possibly inhibited *Clostridium* growth and prompted the competition of LAB. In such scenario, *Streptococcus* aroused as the co-dominant microorganism and was successfully associated with the production of lactate. In consequence, the efficiency of H₂ production was negatively affected regardless of the higher VHPR observed. Moreover, it was found that H₂ was probably consumed through metabolic pathways leading to the production of formate as alternative to dispose the excess of reduced equivalents. Thus, not only homoacetogenesis but also formic acid synthesis plays an important role in H₂ consumption. A whole analysis of the results of this research revealed that the detrimental metabolisms of lactic acid fermentation and formate synthesis could be minimized at low OLR. Otherwise, the effective liberation of H₂ right after its production will be also required.

3.7. References

- Agler, M.T., Wrenn, B. a, Zinder, S.H., Angenent, L.T., 2011. Waste to bioproduct conversion with undefined mixed cultures: the carboxylate platform. *Trends Biotechnol.* 29, 70–78. <https://doi.org/10.1016/j.tibtech.2010.11.006>
- Altioek, D., Tokatli, F., Harsa, S., 2006. Kinetic modelling of lactic acid production from whey by *Lactobacillus casei* (NRRL B-441). *J. Chem. Technol. Biotechnol.* 81, 1190–1197. <https://doi.org/10.1002/jctb.1512>
- APHA/AWWA/WEF, 2012. Standard Methods for the Examination of Water and Wastewater, Standard Methods.
- Azwar, M.Y., Hussain, M. a., Abdul-Wahab, A.K., 2014. Development of biohydrogen production by photobiological, fermentation and electrochemical processes: A review. *Renew. Sustain. Energy Rev.* 31, 158–173. <https://doi.org/10.1016/j.rser.2013.11.022>
- Baghchehsaraee, B., Nakhla, G., Karamanev, D., Margaritis, A., 2010. Fermentative hydrogen production by diverse microflora. *Int. J. Hydrogen Energy* 35, 5021–5027. <https://doi.org/10.1016/j.ijhydene.2009.08.072>

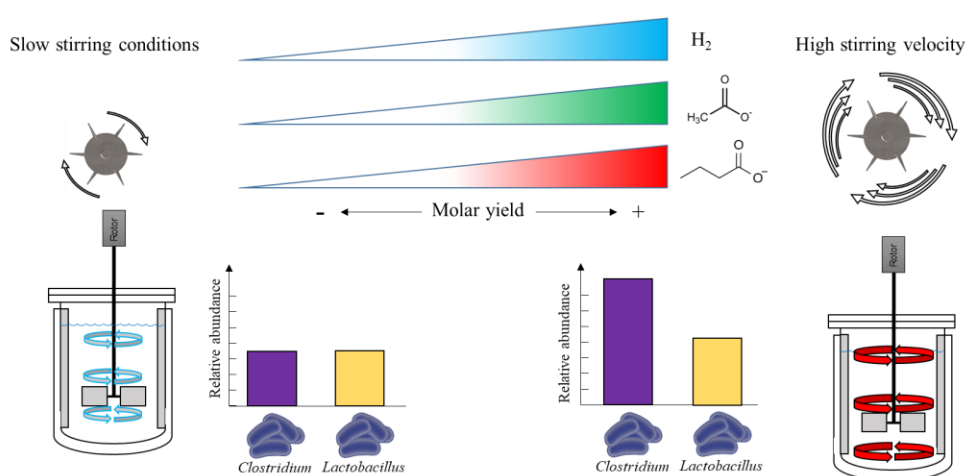
- Berry, A.R., Franco, C.M.M., Zhang, W., Middelberg, A.P.J., 1999. Growth and lactic acid production in batch culture of *Lactobacillus rhamnosus* in a defined medium. *Biotechnol. Lett.* 21, 163–167. <https://doi.org/10.1023/A:1005483609065>
- Boonmee, M., Leksawasdi, N., Bridge, W., Rogers, P.L., 2003. Batch and continuous culture of *Lactococcus lactis* NZ133: Experimental data and model development. *Biochem. Eng. J.* 14, 127–135. [https://doi.org/10.1016/S1369-703X\(02\)00171-7](https://doi.org/10.1016/S1369-703X(02)00171-7)
- Bruant, G., Lévesque, M.-J., Peter, C., Guiot, S.R., Masson, L., 2010. Genomic Analysis of Carbon Monoxide Utilization and Butanol Production by *Clostridium carboxidivorans* Strain P7T. *PLoS One* 5, e13033. <https://doi.org/10.1371/journal.pone.0013033>
- Burgos-Rubio, C.N., Okos, M.R., Wankat, P.C., 2000. Kinetic study of the conversion of different substrates to lactic acid using *Lactobacillus bulgaricus*. *Biotechnol. Prog.* 16, 305–314. <https://doi.org/10.1021/bp000022p>
- Cabrol, L., Marone, A., Tapia-Venegas, E., Steyer, J.-P., Ruiz-Filippi, G., Trably, E., 2017. Microbial ecology of fermentative hydrogen producing bioprocesses: useful insights for driving the ecosystem function. *FEMS Microbiol. Rev.* 41, 158–181. <https://doi.org/10.1093/femsre/fuw043>
- Caporaso, J.G., Kuczynski, J., Stombaugh, J., Bittinger, K., Bushman, F.D., Costello, E.K., Fierer, N., Peña, A.G., Goodrich, J.K., Gordon, J.I., Huttley, G.A., Kelley, S.T., Knights, D., Koenig, J.E., Ley, R.E., Lozupone, C.A., McDonald, D., Muegge, B.D., Pirrung, M., Reeder, J., Sevinsky, J.R., Turnbaugh, P.J., Walters, W.A., Widmann, J., Yatsunencko, T., Zaneveld, J., Knight, R., 2010. QIIME allows analysis of high-throughput community sequencing data. *Nat. Methods* 7, 335–336. <https://doi.org/10.1038/nmeth.f.303>
- Carrillo-Reyes, J., Celis, L.B., Alatríste-Mondragón, F., Razo-Flores, E., 2014. Decreasing methane production in hydrogenogenic UASB reactors fed with cheese whey. *Biomass and Bioenergy* 63, 101–108. <https://doi.org/10.1016/j.biombioe.2014.01.050>
- Cota-Navarro, C.B., Carrillo-Reyes, J., Davila-Vazquez, G., Alatríste-Mondragón, F., Razo-Flores, E., 2011. Continuous hydrogen and methane production in a two-stage cheese whey fermentation system. *Water Sci. Technol.* 64, 367–374. <https://doi.org/10.2166/wst.2011.631>
- Davila-Vazquez, G., Alatríste-Mondragón, F., de León-Rodríguez, A., Razo-Flores, E., 2008. Fermentative hydrogen production in batch experiments using lactose, cheese whey and glucose: Influence of initial substrate concentration and pH. *Int. J. Hydrogen Energy* 33, 4989–4997. <https://doi.org/10.1016/j.ijhydene.2008.06.065>
- Davila-Vazquez, G., Cota-Navarro, C.B., Rosales-Colunga, L.M., de León-Rodríguez, A., Razo-Flores, E., 2009. Continuous biohydrogen production using cheese whey: Improving the hydrogen production rate. *Int. J. Hydrogen Energy* 34, 4296–4304. <https://doi.org/10.1016/j.ijhydene.2009.02.063>
- Diekert, G., Wohlfarth, G., 1994. Metabolism of homocetogens. *Antonie Van Leeuwenhoek* 66, 209–21.
- Dubois, M., K.A.Gilles, J.K.Hamilton, P.A.Rebers, Fred.Smith, 1956. Colorimetric Method for Determination of Sugars and Related Substances. *Anal. Chem.* 28, 350–356. <https://doi.org/10.1021/ac60111a017>
- Edgar, R.C., 2010. Search and clustering orders of magnitude faster than BLAST. *Bioinformatics* 26, 2460–2461. <https://doi.org/10.1093/bioinformatics/btq461>
- Edgar, R.C., Haas, B.J., Clemente, J.C., Quince, C., Knight, R., 2011. UCHIME improves sensitivity and speed of chimera detection. *Bioinformatics* 27, 2194–2200. <https://doi.org/10.1093/bioinformatics/btr381>
- Etchebere, C., Castelló, E., Wenzel, J., del Pilar Anzola-Rojas, M., Borzacconi, L., Buitrón, G., Cabrol, L., Carminato, V.M., Carrillo-Reyes, J., Cisneros-Pérez, C., Fuentes, L., Moreno-Andrade, I., Razo-Flores, E., Filippi, G.R., Tapia-Venegas, E., Toledo-Alarcón, J., Zaiat, M., 2016. Microbial communities from 20 different hydrogen-producing reactors studied by 454 pyrosequencing. *Appl. Microbiol. Biotechnol.* 100, 3371–3384. <https://doi.org/10.1007/s00253-016-7325-y>

- Gomes, S.D., Fuess, L.T., Mañunga, T., Feitosa de Lima Gomes, P.C., Zaiat, M., 2016. Bacteriocins of lactic acid bacteria as a hindering factor for biohydrogen production from cassava flour wastewater in a continuous multiple tube reactor. *Int. J. Hydrogen Energy* 41, 8120–8131. <https://doi.org/10.1016/j.ijhydene.2015.11.186>
- Hung, C.-H., Cheng, C.-H., Guan, D.-W., Wang, S.-T., Hsu, S.-C., Liang, C.-M., 2011. Interactions between *Clostridium* sp. and other facultative anaerobes in a self-formed granular sludge hydrogen-producing bioreactor. *Int. J. Hydrogen Energy* 36, 8704–8711. <https://doi.org/10.1016/j.ijhydene.2010.06.010>
- Kleerebezem, R., Van Loosdrecht, M.C.M., 2010. A Generalized Method for Thermodynamic State Analysis of Environmental Systems. *Crit. Rev. Environ. Sci. Technol.* 40, 1–54. <https://doi.org/10.1080/10643380802000974>
- Köpke, M., Held, C., Hujer, S., Liesegang, H., Wiezer, A., Wollherr, A., Ehrenreich, A., Liebl, W., Gottschalk, G., Dürre, P., 2010. *Clostridium ljungdahlii* represents a microbial production platform based on syngas. *Proc. Natl. Acad. Sci.* 107, 13087–13092. <https://doi.org/10.1073/pnas.1004716107>
- Kwok, J.S.L., Ip, M., Chan, T.-F., Lam, W.-Y., Tsui, S.K.W., 2014. Draft Genome Sequence of *Clostridium butyricum* Strain NOR 33234, Isolated from an Elderly Patient with Diarrhea. *Genome Announc.* 2. <https://doi.org/10.1128/genomeA.01356-14>
- Lee, J., Jang, Y.S., Han, M.J., Kim, J.Y., Lee, S.Y., 2016. Deciphering *Clostridium tyrobutyricum* metabolism based on the whole-genome sequence and proteome analyses. *MBio* 7, 1–12. <https://doi.org/10.1128/mBio.00743-16>
- Milferstedt, K., Santa-Catalina, G., Godon, J.-J., Escudíé, R., Bernet, N., 2013. Disturbance Frequency Determines Morphology and Community Development in Multi-Species Biofilm at the Landscape Scale. *PLoS One* 8, e80692. <https://doi.org/10.1371/journal.pone.0080692>
- Milne, C.B., Eddy, J. a, Raju, R., Ardekani, S., Kim, P.-J., Senger, R.S., Jin, Y.-S., Blaschek, H.P., Price, N.D., 2011. Metabolic network reconstruction and genome-scale model of butanol-producing strain *Clostridium beijerinckii* NCIMB 8052. *BMC Syst. Biol.* 5, 130. <https://doi.org/10.1186/1752-0509-5-130>
- Napoli, F., Olivieri, G., Russo, M.E., Marzocchella Antonio, A., Salatino, P., 2011. Continuous lactose fermentation by *Clostridium acetobutylicum* - Assessment of acidogenesis kinetics. *Bioresour. Technol.* 102, 1608–1614. <https://doi.org/10.1016/j.biortech.2010.09.004>
- Nasr, N., Velayutham, P., Elbeshbishy, E., Nakhla, G., El Nagggar, M.H., Khafipour, E., Derakhshani, H., Levin, D.B., Hafez, H., 2015. Effect of headspace carbon dioxide sequestration on microbial biohydrogen communities. *Int. J. Hydrogen Energy* 40, 9966–9976. <https://doi.org/10.1016/j.ijhydene.2015.06.077>
- Nath, K., Das, D., 2004. Improvement of fermentative hydrogen production: Various approaches. *Appl. Microbiol. Biotechnol.* 65, 520–529. <https://doi.org/10.1007/s00253-004-1644-0>
- Noar, J., Makwana, S.T., Bruno-Bárcena, J.M., 2014. Complete Genome Sequence of Solvent-Tolerant *Clostridium beijerinckii* Strain SA-1. *Genome Announc.* 2. <https://doi.org/10.1128/genomeA.01310-14>
- Noike, T., Takabatake, H., Mizunoc, O., Ohbab, M., 2002. Inhibition of hydrogen fermentation of organic wastes by lactic acid bacteria. *Int. J. Hydrogen Energy* 27, 1367–1371. [https://doi.org/10.1016/S0360-3199\(02\)00120-9](https://doi.org/10.1016/S0360-3199(02)00120-9)
- Nolling, J., Breton, G., Omelchenko, M. V, Makarova, K.S., Zeng, Q., Gibson, R., Lee, H.M., Dubois, J., Qiu, D., Hitti, J., GTC Sequencing Center Production, Finishing, and B.T., Wolf, Y.I., Tatusov, R.L., Sabathe, F., Doucette-Stamm, L., Soucaille, P., Daly, M.J., Bennett, G.N., Koonin, E. V, Smith, D.R., 2001. Genome Sequence and Comparative Analysis of the Solvent-Producing Bacterium *Clostridium acetobutylicum*. *J. Bacteriol.* 183, 4823–4838. <https://doi.org/10.1128/JB.183.16.4823-4838.2001>

- Palomo-Briones, R., Razo-Flores, E., Bernet, N., Trably, E., 2017. Dark-fermentative biohydrogen pathways and microbial networks in continuous stirred tank reactors: Novel insights on their control. *Appl. Energy* 198, 77–87. <https://doi.org/10.1016/j.apenergy.2017.04.051>
- Pyne, M.E., Utturkar, S., Brown, S.D., Moo-Young, M., Chung, D.A., Chou, C.P., 2014. Improved Draft Genome Sequence of *Clostridium pasteurianum* Strain ATCC 6013 (DSM 525) Using a Hybrid Next-Generation Sequencing Approach. *Genome Announc* 2, 2–3. <https://doi.org/10.1128/genomeA.00790-14>
- R Development Core Team, R., 2011. R: A Language and Environment for Statistical Computing, R Foundation for Statistical Computing. <https://doi.org/10.1007/978-3-540-74686-7>
- Rochex, A., Godon, J., Bernet, N., Escudier, R., 2008. Role of shear stress on composition, diversity and dynamics of biofilm bacterial communities. *Water Res.* 42, 4915–4922. <https://doi.org/10.1016/j.watres.2008.09.015>
- Saad, N.M.C., 2013. Homoacetogenesis during hydrogen production by mixed cultures dark fermentation: Unresolved challenge. *Int. J. Hydrogen Energy* 38, 13172–13191. <https://doi.org/10.1016/j.ijhydene.2013.07.122>
- Schuchmann, K., Müller, V., 2014. Autotrophy at the thermodynamic limit of life: a model for energy conservation in acetogenic bacteria. *Nat. Rev. Microbiol.* 12, 809–821. <https://doi.org/10.1038/nrmicro3365>
- Senger, R.S., Papoutsakis, E.T., 2008. Genome-scale model for *Clostridium acetobutylicum*: Part I. Metabolic network resolution and analysis. *Biotechnol. Bioeng.* 101, 1036–1052. <https://doi.org/10.1002/bit.22010>
- Shanmugam, S.R., Chaganti, S.R., Lalman, J.A., Heath, D.D., 2014. Statistical optimization of conditions for minimum H₂ consumption in mixed anaerobic cultures: Effect on homoacetogenesis and methanogenesis. *Int. J. Hydrogen Energy* 39, 15433–15445. <https://doi.org/10.1016/j.ijhydene.2014.07.143>
- Si, B., Li, J., Li, B., Zhu, Z., Shen, R., Zhang, Y., Liu, Z., 2015. The role of hydraulic retention time on controlling methanogenesis and homoacetogenesis in biohydrogen production using upflow anaerobic sludge blanket (UASB) reactor and packed bed reactor (PBR). *Int. J. Hydrogen Energy* 40, 11414–11421. <https://doi.org/10.1016/j.ijhydene.2015.04.035>
- Sikora, A., Baszczyk, M., Jurkowski, M., Zielenkiewicz, U., 2013. Lactic Acid Bacteria in Hydrogen-Producing Consortia: On Purpose or by Coincidence?, in: *Lactic Acid Bacteria - R & D for Food, Health and Livestock Purposes*. InTech. <https://doi.org/10.5772/50364>
- Tracy, B.P., Jones, S.W., Fast, A.G., Indurthi, D.C., Papoutsakis, E.T., 2012. Clostridia: the importance of their exceptional substrate and metabolite diversity for biofuel and biorefinery applications. *Curr. Opin. Biotechnol.* 23, 364–381. <https://doi.org/10.1016/j.copbio.2011.10.008>

CHAPTER IV

Enhancement of mass transfer conditions to increase the productivity and efficiency of dark fermentation



Highlights

- H₂ production and yield were increased due to the enhancement of hydrogen mass transfer properties.
- The enhancement of hydrogen mass transfer was associated with the increase of acetate and butyrate production yields.
- The microbial community composition of dark fermentation was controlled by the mass transfer conditions.
- It was showed that H₂ producing biomass is also capable to consume it; such consumption was successfully modelled through the Gompertz equation

The present chapter is based on the article:

Palomo-Briones, R., Celis, L.B., Méndez-Acosta, H.O., Bernet, N., Trably, E., Razo-Flores, E. 2018. Enhancement of mass transfer conditions to increase the productivity and efficiency of dark fermentation. To be submitted to *Fuels*.

4.1. Summary

Hydrogen (H₂) produced by dark fermentation is an alternative to fulfill the requirements of the transportation sector and to be a complementary source in the forthcoming electricity grid. However, the dark fermentative H₂ production is limited by the accumulation of H₂ in the fermentation broth. In continuous stirred-tank reactors (CSTR), such phenomenon is associated with poor mass transfer conditions. Nevertheless, this parameter has been scarcely considered to enhance H₂ production. In this work, The relationship between H₂ mass transfer conditions and performance of dark fermentation was evaluated using a series of continuous stirred-tank reactors fed with cheese whey and operated at H₂ mass transfer coefficients (k_{La}) ranging from 1.04 to 4.23 1/h. The results showed that volumetric hydrogen production rates and H₂ yields increased 74 and 78%, respectively, due to enhanced mass transfer conditions. More specifically, a maximum hydrogen production of 7.66 L/L-d with a H₂ yield of 1.1 mol H₂/mol hexose was obtained at a $k_{La} = 4.23$ 1/h. Furthermore, 16S-DGGE analysis and sequencing revealed that *Clostridium* and *Lactobacillus* were the dominant microorganisms. In particular, *Clostridium* increased its occurrence at k_{La} of 2.72-4.23 1/h as a response to lower dissolved H₂ concentrations. The novelty of this work relies on the demonstration that mass transfer conditions controls H₂ accumulation and enhances the reactor performance for H₂ production.

Keywords: CSTR, biohydrogen, dark fermentation, mass transfer.

4.2. Introduction

The diversification of energy sources is a critical keystone in the contemporaneous vision of sustainable development. In this regard, biofuels are expected to play a relevant role to fulfill future requirements of the transportation sector and to be a complementary source in the forthcoming electricity grid. In this context, molecular hydrogen (H_2) has been underlined due to its high energy content (120 kJ/g) and the highly efficient conversion to electricity through the H_2 fuel-cell technology. Moreover, H_2 can be produced from a wide range of residual biomass through dark fermentation, which also makes it an attractive option in waste valorization scenarios.

The production of H_2 through dark fermentation is achieved by anaerobic microorganisms that use two principal metabolic routes: the pyruvate formate lyase and the pyruvate ferredoxin oxydoreductase pathways (Cabrol et al., 2017). These routes are associated with maximum theoretical metabolic yields of 2 and 4 mol H_2 /mol hexose, respectively. However, most studies in literature report H_2 yields generally below these values.

The low H_2 production depends on multiple factors, including the microbial community composition, the operational conditions and the efficiency of mass transfer. It is well known that gas to liquid mass transfer is a common limiting step in fermentations, dark fermentation may not be the exception because the efficiency of H_2 release from the liquid to the gas is expected to play a key role in the fermentation performance. The importance of this topic relies on the fact that the dissolved H_2 concentration in the fermentation broth can exert a thermodynamic control on the H_2 -associated metabolic pathways. For instance, as H_2 accumulates ($P_{H_2} > 60$ Pa), the H_2 synthesis from ferredoxin becomes theoretically unfeasible. As a consequence, the maximum H_2 yield decreases from 4 to 2 mol H_2 /mol hexose (Angenent et al., 2004). Further accumulation of H_2 in the liquid phase ($P_{H_2} > 500$ Pa) leads to the occurrence of homoacetogenesis, which is the metabolism that synthesizes acetate from H_2 and CO_2 (Demirel and Scherer, 2008; Liu et al., 2016; Saady, 2013).

Different alternatives have been proposed to enhance H_2 transfer from the liquid to the gas phase in dark fermentative systems, including gas sparging (Bakonyi et al., 2017; Chang et al., 2012; Kim et al., 2006), reduced pressure (Kisielewska et al., 2015; Lee et al., 2012), different bioreactor configurations (Contreras-Dávila et al., 2017) and mechanical stirring (Beckers et al., 2015). The latter strategy can be highlighted due to its low-cost and ease of implementation. Using mechanical stirring in batch and semi-continuous systems, Beckers et al. (2015) successfully showed that the H_2 yield was positively linked to

the increase of the volumetric mass transfer coefficient (k_{LA}) controlled in turn by the stirring velocity and gas sparging.

In a continuous regime, it can moreover be hypothesized that different steady states of performance could arise as a function of the k_{LA} (*i.e.* stirring regime) with concomitant changes in metabolic pathways and microbial community composition. Therefore, the aim of this work was to compare steady state performances of dark fermentative systems under different conditions of mechanical stirring (associated with different k_{LA}) with a special focus on the potential shifts in metabolic pathways and microbial communities.

4.3. Materials and methods

4.3.1. Inoculum and fermentation medium

The seed sludge was obtained from a full-scale UASB reactor treating wastewater from a tequila factory (Casa Herradura, Jalisco, Mexico). Before its utilization, the sludge was heat treated at 105 °C for 24 h, pulverized in a mortar, and sieved through 0.5 mm mesh. The resulting powder was added to the reactor at a total solids (TS) concentration of 4.5 g TS/L for the startup of CSTR I (See section 2.2).

In all the fermentation experiments, cheese whey powder (CWP) (Darigold, USA) with a lactose content of 75.5% was used as substrate at a fixed inlet concentration of 15 g lactose/L. The fermentation medium was supplemented with the following components as described previously (mg/L) (Palomo-Briones et al., 2017): NH_4Cl , 2110; $\text{MgCl}_2 \cdot 6\text{H}_2\text{O}$, 100; $\text{CuCl}_2 \cdot \text{H}_2\text{O}$, 1.25; $\text{MnCl}_2 \cdot 4\text{H}_2\text{O}$, 7; $\text{FeCl}_2 \cdot 4\text{H}_2\text{O}$, 19.1; $\text{NiCl}_2 \cdot 6\text{H}_2\text{O}$, 102.5. In addition, a phosphate buffer (KH_2PO_4 - Na_2HPO_4 , pH 5.9) was added to reach a final concentration of 100 mM.

4.3.2. Bioreactors set-up and operational conditions

A series of five CSTR (Applikon Biotechnologies, USA) with a working volume of 1 L (internal diameter of 70.88 cm²) was set up as shown in Figure 4.1. The bioreactors were equipped with a stirrer and two Rushton-type impellers symmetrically positioned along the depth of the reactor working-volume.

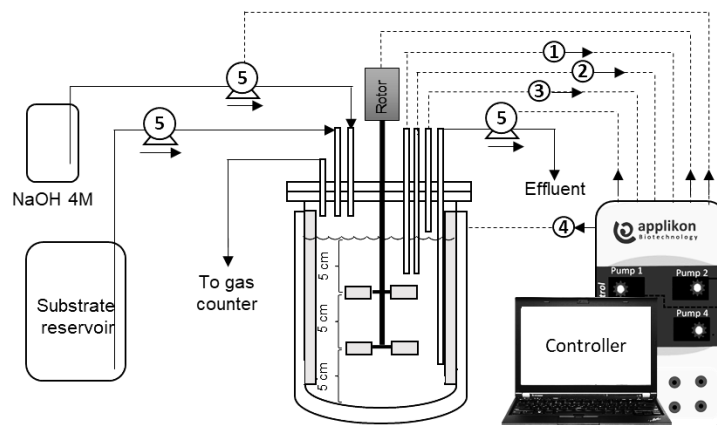


Figure 4.1. Schematic representation of the experimental set-up. 1, pH probe; 2, temperature sensor; 3, level sensor; 4, heat cover; 5, peristaltic pump.

CSTR I was inoculated with the pretreated anaerobic sludge (section 4.3.1) at a concentration of 4.5 g TS/L and started-up in batch mode for 24 h with an initial substrate concentration of 15 g lactose /L. The stirring, temperature and pH were controlled at 250 rpm, 37 °C and 5.9, respectively. Thereafter, the reactor was switched to continuous mode with a fixed hydraulic retention time (HRT) of 6 h. The reactor was monitored for a minimum of 20 HRT equivalents, *i.e.* 5 days, and until a steady state was reached in terms of volumetric hydrogen production rate (VHPR). The steady state was defined as the phase where the variation of three consecutive measurements was less than 10% of the VHPR. In such state, enough volume of effluent was recovered and centrifuged at 3500 rpm for 10 min at 4°C. The resulting pellets were re-suspended in mineral medium without substrate, characterized in terms of volatile suspended solids (VSS) and stored at -4 °C until their use as inoculum in four more reactors CSTR II to V.

CSTR II - V were inoculated with the recovered biomass from CSTR I at a concentration of 0.45 g VSS/L. The start-up strategy and operational conditions were maintained identical to CSTR I, except for the stirring velocity, which was set at 100, 200, 300 and 400 rpm in CSTR II, CSTR III, CSTR IV and CSTR V, respectively. Similarly to CSTR I, the four bioreactors were operated and monitored for a minimum of 20 HRT and until stable VHPR was observed.

4.3.3. Analytical methods

Liquid samples were collected on a regular basis and used to determine the concentrations of biomass, soluble chemical oxygen demand (COD), total carbohydrates and short-chain volatile fatty acids (VFA). The biomass concentration (as volatile suspended solids, VSS) and soluble COD were quantified as

described in the standard methods (APHA/AWWA/WEF, 2012). Total carbohydrates concentrations were determined by the phenol sulfuric method (Dubois et al., 1956). The VFA were quantified from filtered (22 μm) samples by capillary electrophoresis (1600A, Agilent Technologies, Waldbronn, Germany) as reported elsewhere (Davila-Vazquez et al., 2008). All H_2 and VFAs yields were calculated considering the amount of hexose consumed

The gas production in the CSTR experiments was measured through a liquid displacement device (SEV. Puebla, Mexico), and its composition (H_2 and CO_2) was determined through a gas chromatograph equipped with a thermal conductivity detector (6890N, Agilent Technologies, Waldbronn, Germany). The gas volumes are reported at 1 atm and 273.15 K.

4.3.4. Determination of k_{LA} and dissolved H_2 concentration

To determine H_2 mass transfer coefficients (k_{LA} , 1/h) in the CSTR, a series of O_2 desorption experiments were performed at 50, 100, 200, 300 and 400 rpm using the gas-out method described elsewhere (Beckers et al., 2015).

In brief, the reactor vessel was filled with mineral medium without substrate and inoculum. Stirring, temperature and pH were set to 50-400 rpm, 37 °C and 5.9, respectively. The system was assembled with an electrode to measure and record the dissolved oxygen (DO) concentration. For each experiment, the system was first degassed with N_2 and then flushed with pure oxygen until the dissolved O_2 concentration reached >100%. Afterwards, the O_2 sparging was ceased and the decrease of the dissolved gas concentration until equilibrium was recorded. The obtained data were normalized and adjusted to the following desorption equation:

$$[DO(t)] = [DO]_{t=0} * e^{-\{k_{\text{L}}a\}_{\text{O}_2} * t} \quad (4.1)$$

Where t (h) represents the elapsed time and $\{k_{\text{L}}a\}_{\text{O}_2}$ is the volumetric mass transfer coefficient of O_2 . The resulting $\{k_{\text{L}}a\}_{\text{O}_2}$ value altogether with the oxygen and hydrogen diffusivities (D_{O_2} and D_{H_2} , respectively) were used to compute the $\{k_{\text{L}}a\}_{\text{H}_2}$ considering the following relationship (Beckers et al., 2015):

$$\{k_{\text{L}}a\}_{\text{H}_2} = \{k_{\text{L}}a\}_{\text{O}_2} * \left(\frac{D_{\text{H}_2}}{D_{\text{O}_2}} \right)^{1/2} \quad (4.2)$$

Where D_{H_2} and D_{O_2} were 5.91×10^{-5} and 2.62×10^{-5} cm²/s at 40 and 37 °C, respectively (Ferrell and Himmelblau, 1967; Han and Bartels, 1996).

Furthermore, to estimate the dissolved H₂ concentration under the different stirring conditions, it was first considered that the mass transfer of H₂ from the liquid to the gas phase (Q_{H_2} , in mol_{H2}/L-h) can be described as follows:

$$Q_{H_2} = \{k_L a\}_{H_2} * (C_{H_2,liq} - p_{H_2,gas} * H^{cp}) \quad (4.3)$$

Where $\{k_L a\}_{H_2}$ (1/h) is the volumetric mass transfer coefficient for H₂, $C_{H_2,liq}$ (mol/L) is the concentration of dissolved H₂, $p_{H_2,gas}$ (atm) is the H₂ partial pressure of the headspace, and H^{cp} (mol/L-atm) is the Henry's coefficient of H₂ (8.47×10^{-4} mol/L-atm at 37°C, Sander, 2015).

Solving the equation for $C_{H_2,liq}$ (Eq. 4), we obtain an expression with two known constants (*i.e.* $k_L a$ and H^{cp}) and two variables that can be derived from bioreactors operation (*i.e.* Q_{H_2} and $p_{H_2,gas}$).

$$C_{H_2,liq} = \frac{Q_{H_2}}{\{k_L a\}_{H_2}} + p_{H_2,gas} * H^{cp} \quad (4.4)$$

4.3.5. Microbial community analysis

To investigate the microbial community structure and identify potential changes in response to stirring speed, a PCR-DGGE approach was followed as described previously (Carrillo-Reyes et al., 2012). DNA was extracted from biomass recovered after 24h of batch cultivation (start-up phase) and at the end of each stage using a DNA extraction kit (Zymo-Research). The 16S rRNA gene was amplified by PCR using the 27F (5'-AGAGTTTGATCCTGGCCAG) and 1492R (5'-GGTACCTTGTACGACTT) universal primers for bacteria. A nested PCR was conducted with amplicons from the previous stage and primers 357F-GC (5'-CGCCCGCCGCGCGCGGGCGGGGCGGGGCGGGGGCACGGGGGGCCTACGGAGGCAGCAG-3') and 907R (5'-CCGTCAATTCMTTTGAGTTT) to amplify the V3 - V5 regions. The PCR products were loaded in polyacrylamide gels (8%) with a denaturing gradient (urea-formamide) that ranged from 30 to 60 %. The DGGE electrophoresis conditions were 70 V for 20 h at 60 °C. After electrophoresis, the gel was fixed with acetic acid (10%), treated with a AgNO₃ solution (1 g/L) and revealed with a Na₂CO₃ (23.3 g/L) solution. The gel bands were photographed under visible light with a digital camera. The DGGE images were analyzed with the BioNumeric bioinformatics software (Applied

Maths, Belgium) to create a presence-absence matrix from which Euclidean distances were calculated. The distances between the DGGE profiles were visualized through a UPGMA dendrogram computed in the R environment.

Moreover, the selected DNA bands were cut, reamplified by PCR using 341F (without GC-clamp) and 907R primers and sequenced by the dideoxynucleotides method in a 3130 Genetic Analyzer (Applied Biosystems). The sequences were edited to remove low quality nucleotides with the BioEdit software (Ibis Therapeutics, USA). Edited sequences were compared with the reference 16S-rRNA database of NCBI to find the closest relatives.

4.3.6. Hydrogen consumption

With the aim to evaluate the homoacetogenic activity under the different mass transfer conditions tested, the following mass balance on H₂, acetate and butyrate was performed as suggested elsewhere (Arooj et al., 2008; Luo et al., 2011):

$$\text{Homoacetogenic acetate} = (2 \cdot \text{Acetate} + 2 \cdot \text{Butyrate} - \text{Propionate} - \text{H}_2) / 6 \quad (4.5)$$

Where carboxylic acids and H₂ are given in mol/d.

To confirm and characterize the H₂ consumption capacity of the microbial community, a series of H₂ consumption experiments was also carried out. These experiments were conducted in 120 mL serum bottles with a working volume of 80 mL, using biomass harvested from the CSTR III (200 rpm) as inoculum. For this purpose, enough volume of effluent was recovered from CSTR III and centrifuged at 3500 rpm for 10 min at 4°C. The resulting pellets were re-suspended in mineral medium (composition shown in section 2.1), characterized in terms of VSS, and stored at -4 °C until their use. The experiments were prepared with an initial concentration of 2 g VSS/L using the mineral medium with the composition described in section 2.1 and supplemented with 560 mg/L of NaHCO₃. No organic substrate was added. The serum bottles were hermetically sealed and the headspace displaced first with N₂ and then with pure H₂. A second set of experiments was identically prepared, but H₂ was pressurized at 1.4 atm. Two additional microcosms bottles were prepared, one without biomass and the other without H₂, to serve as physicochemical and endogenous controls, respectively. All the experiments were incubated at 37 °C. The H₂ consumption was computed from the decrease of the system pressure and headspace composition.

The cumulative H₂ consumption was modelled utilizing the Gompertz model (Ginkel et al., 2001; Zwietering et al., 1990):

$$H_{2_{cumulative}}(t) = H_{max} \cdot \exp \left\{ -\exp \left[\frac{2.71828 \cdot R_{max}}{H_{max}} (\lambda - t) + 1 \right] \right\} \quad (4.6)$$

Where $H_{2_{cumulative}}(t)$ (mmol) is the cumulative H₂ consumed at time t, H_{max} (mmol) is the maximum amount of H₂ consumed in the experiment, R_{max} (mmol/h) is the maximum rate of H₂ consumption, and λ (h) is the lag time before the H₂ consumption.

4.3.7. Statistic analysis

To evaluate the effects of mass transfer conditions on the different response variables of this study, an analysis of variance was conducted. The effect was considered to be significant at a p value lower than 0.05. The response variable was verified to be normally distributed through graphical inspection (q-q plot). The heteroscedasticity was also verified with residual plots. Variables not normally distributed were transformed previously to the analysis. Alternatively, the non-parametric test of Kruskal-Wallis was used. All statistical analysis were conducted with R software (R Development Core Team, 2011).

4.4. Results and discussion

4.4.1. k_{La} determination in dark fermentative system

The $\{k_{La}\}_{H_2}$ coefficients, named here “ k_{La} ” for simplicity, were determined in accordance with previously reported methodology (Beckers et al., 2015). The k_{La} values were in the range of 0.58 - 4.23 1/h and function of the stirring velocity (Table 4.1). Such values are specific for the configuration, geometry and specific transfer area of the reactor. Nevertheless, these results are consistent to similar systems as reported elsewhere (Beckers et al., 2015; de Kok et al., 2013). The subsequent biological experiments were conducted under $\text{rpm} \geq 100$ rpm to avoid possible stagnation at lower speeds.

4.4.2. The k_{La} as key mechanism controlling the productivity and the efficiency of dark fermentation

CSTR I was operated for an equivalent time of 34 HRT (8.5 days) at an organic loading rate (OLR) of 60 g lactose/L-d with the main objective of producing seed-biomass for the subsequent experiments (CSTR II - V). The performance of CSTR I was relatively stable in terms of productivity and efficiency, with an average VHPR of 7.1 ± 1.0 L/L-d and H₂ yield of 0.94 ± 0.1 mol H₂/mol hexose. Under similar OLR (55.4

g lactose/L-d), Davila-Vazquez et al. (2009) reported a VHPR of 8.8 L/L-d and an H₂ yield of 1.2 mol H₂/mol hexose, which was similar to the results showed in the present work. The stability of H₂ production and the similarity with previous reports were clear indications of a successful establishment of the dark fermentative H₂ production. Thus, the biomass was then recovered to serve as inoculum in the following experiments.

Table 4.1. Volumetric mass transfer coefficients at different stirring velocities in stirred-tank reactors.

Reactor details	Stirring velocity (rpm)	k _{LA} O ₂ (1/h)	k _{LA} H ₂ (1/h)	References
Stirred-tank 1 L	50	0.38	0.58	This study
Only mechanical stirring	100	0.69	1.04	
with Rushton impellers	200	1.09	1.64	
T = 37 °C	300	1.81	2.72	
pH = 5.9	400	2.81	4.23	
A = 0.071/cm				
Stirred-tank 1 L	100	-	0.95	de Kok et al., 2013
Mechanical stirring*	400	-	3.49	
T = 30 °C				
pH = 5.5				
Stirred-tank 2.3 L	0	0.061	0.08	Beckers et al., 2015
Only mechanical stirring	100	0.191	0.25	
with Rushton impellers	400	0.524	0.77	
T = 30 °C				
A = 0.05/cm				

A: specific transfer area

* Nitrogen was sparged in the headspace

CSTR II to V were independently operated with stirring velocities ranging from 100 to 400 rpm, associated with k_{LA} values within a range of 1.04 to 4.23 1/h (Table 4.1). The results showed that the mass transfer coefficient strongly affected dark fermentation in terms of VHPR (F_{3, 50}=13.05, p<0.05) and H₂ yield (F_{3, 50}=13.04, p<0.05) (Figure 4.2). At the lowest k_{LA} tested (1.04 1/h at 100 rpm), the VHPR was 4.4 ± 1.3 L/L-d with an H₂ yield of 0.6 ± 0.15 mol H₂/mol hexose. In contrast, at the highest value of k_{LA} (4.23 1/h at 400 rpm), an average VHPR of 7.66 ± 1.42 L/L-d was obtained with an H₂ yield of 1.08 ± 0.21 mol H₂/mol hexose. These results represent an increase of 74% in terms of VHPR and 78% in terms of H₂ yield.

The extent of improvement, in both VHPR and H₂ yield, achieved in this work was consistent with previous reports that focused on H₂ mass transfer (Table 4.2). For instance, Beckers et al. (2015) reported an improvement of approximately 89 and 19 % in terms of H₂ production rate and H₂ yield, respectively, in an anaerobic stirred tank reactor after having increased the stirring conditions from 0 to 400 rpm. Using CO₂ sparging, Kim et al. (2006) were able to increase the VHPR and H₂ yield in a CSTR by 56% and 118%, respectively. Nevertheless, such an approach resulted in H₂ dilution, which is not convenient for practical applications. This issue was solved by Bakonyi et al. (2017) recirculating the CO₂ produced in the fermentation. Through that strategy, the VHPR and the H₂ yield increased by 25 % and 10%, respectively, in comparison with the control fermentation experiment.

In comparison, with optimized mixed conditions reported in the present work, remarkable increases in the VHPR and H₂ yield were reached, avoiding the utilization of additional gases and, therefore, the H₂ produced remains concentrated.

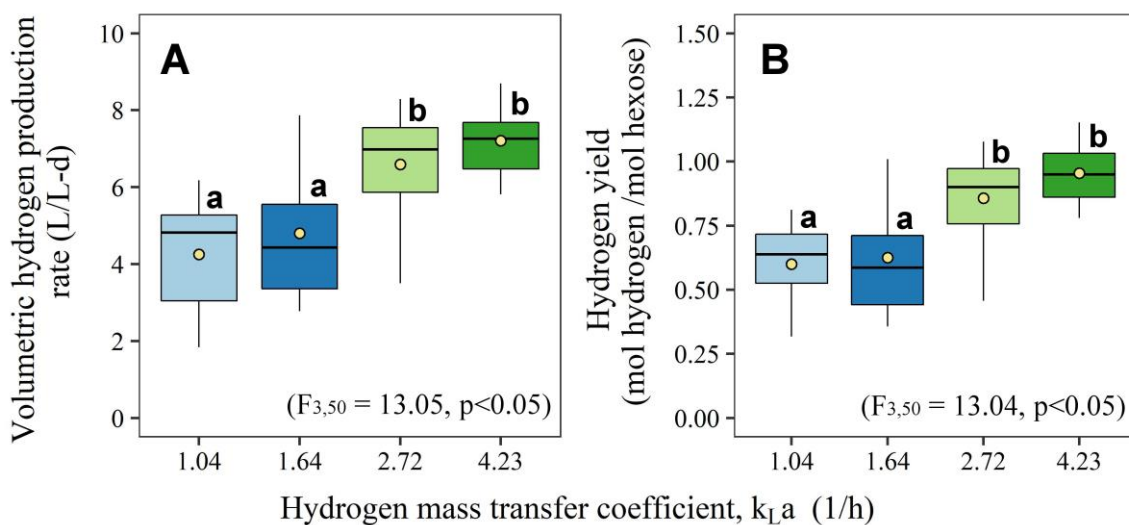


Figure 4.2. Summary of the effects of k_{La} on A) the volumetric H₂ production rate and B) the H₂ yield. Boxes with same letters are not significant different at $p < 0.05$ in accordance with the Tukey test.

Table 4.2. Selection of literature works aiming the improvement of H₂ transfer conditions of dark fermentation systems.

Strategy	Reaction mode	Extent of improvement	Reference
Gas sparging	CSTR	25% increase of VHPR (7.35 to 9.2 L/L-d) 10% increase of H ₂ yield (1.60 to 1.76 mol H ₂ /mol hexose)	Bakonyi et al., 2017
	CSTR	56% increase of VHPR (3.52 to 5.5 L/L-d) 118% increase of H ₂ yield (0.77 to 1.68 mol H ₂ /mol hexose)	Kim et al., 2006
Reduced pressure	UASB	107% increase of VHPR (0.68 to 1.42 L/L-d) 63% increase of H ₂ yield (2.8 to 4.55 mol H ₂ /g COD)	Kisielewska et al., 2015
Stirring	AnSBR	89% increase of H ₂ rate (140 to 264 mL H ₂ /h) 19% increase of H ₂ yield (1.58 to 1.88 mol H ₂ /mol hexose)	Beckers et al., 2015
	CSTR	13.5% decrease of H ₂ yield (1.48 to 1.28 mol H ₂ /mol hexose with sparging in the headspace)	de Kok et al., 2013
	CSTR	74% increase of VHPR (4.39 to 7.66 L/L-d) 78% increase of H ₂ yield (0.66 to 1.08 mol H ₂ /mol hexose)	This study

4.4.3. The enhancement of k_La intensifies the metabolic routes leading to H₂ production.

To investigate the influence of the k_La on metabolic pathways, the main VFA (*i.e.* formate, acetate, butyrate and lactate) concentrations were determined at the different conditions of stirring velocities. The analysis revealed that the enhancement of hydrogen mass transfer performance (Figure 4.2) was accompanied by an increase of the VFA molar yield. In particular, significant differences in acetate and butyrate production yields (Figure 4.3A) were observed in parallel with the enhancement of the H₂ transfer

conditions. In CSTR II, with k_{La} of 1.04 1/h (100 rpm), the production of acetate and butyrate was 0.29 and 0.31 mol/mol hexose, respectively. Meanwhile, in CSTR V, with k_{La} of 4.23 1/h (400 rpm), the acetate and butyrate yields increased up to 0.44 and 0.5 mol/mol hexose, respectively. This finding is consistent with the fact that the acetate and butyrate pathways are the most efficient routes in terms of hydrogen production by dark fermentation.

On the other hand, the estimated H_2 concentrations in the fermentation broth (Figure 4.3C) clearly indicated that the increase of acetate and butyrate yields were associated with the change of mass transfer conditions and the subsequent decrease of dissolved H_2 . The theoretical H_2 concentrations in the fermentation liquid were in the range of 7.5 to 3.4 mmol H_2/L , with the lowest value at the stirring velocity of 400 rpm.

Nevertheless, considering the results of VFA and dissolved H_2 concentration, as well as the VHPR and H_2 yield (Figure 4.2), it seemed that mass-transfer did not affect H_2 metabolism beyond a k_{La} of 2.6 1/h, *i.e.*

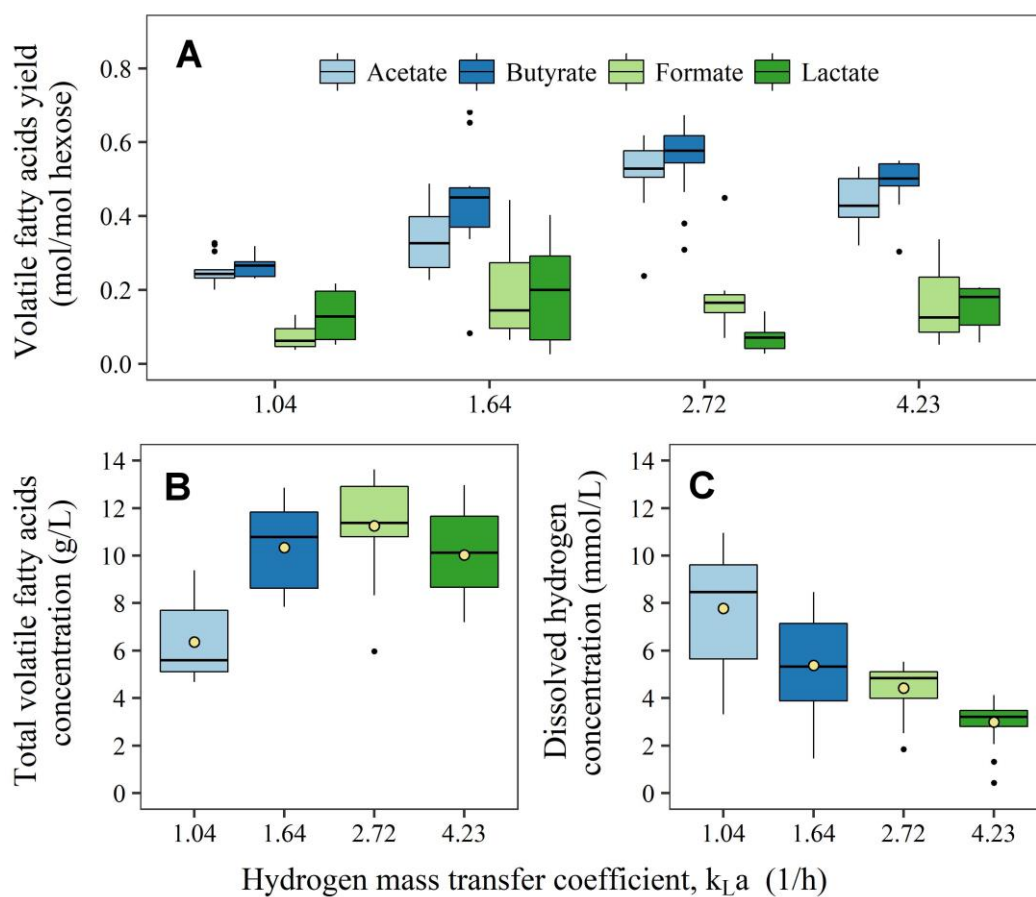


Figure 4.3. Effect of k_{La} on A) the yield of volatile fatty acids, B) total volatile fatty acids concentration, and C) dissolved H_2 concentrations.

300 rpm. Thus, the operation at 300 rpm was considered as the most suitable stirring velocity for this type of reactor.

4.4.4. Microbial community

The analysis of the 16S rRNA-DGGE (Figure 4.4) and the sequencing results (Table 4.3) showed that the microbial community was mainly composed of *Clostridium* and *Lactobacillus* species. These two genera have been previously reported to play important roles in dark fermentative systems (Palomo-Briones et al., 2018, 2017). *Clostridium spp.* are mostly related to hydrogen producing bacteria and are widely found in dark fermentative systems associated with high efficiencies (e.g. Cabrol et al., 2017; Etchebehere et al., 2016). In contrast, *Lactobacillus spp.* correspond to lactic acid bacteria that have been identified as substrate competitors of hydrogen producers during the fermentation of cheese whey (Ferreira Rosa et al., 2016). Moreover, it was shown that the abundance of lactic acid bacteria increased under relatively high organic loading rates (58.8 and 88.2 g lactose/L-d), and it was likely associated with the accumulation of H₂ in the fermentative medium (Palomo-Briones et al., 2018).

Interestingly, the DGGE analysis showed that *Lactobacillus* (band at DGGE relative distance ~ 68) was more abundant in the samples taken at the end of CSTRs operation (Figure 4.4), suggesting that these microorganisms were enriched during the hydrogen production process. The DGGE profiles also revealed that the bands associated with *Clostridium* (two bands at DGGE relative distances of 45 and 50,

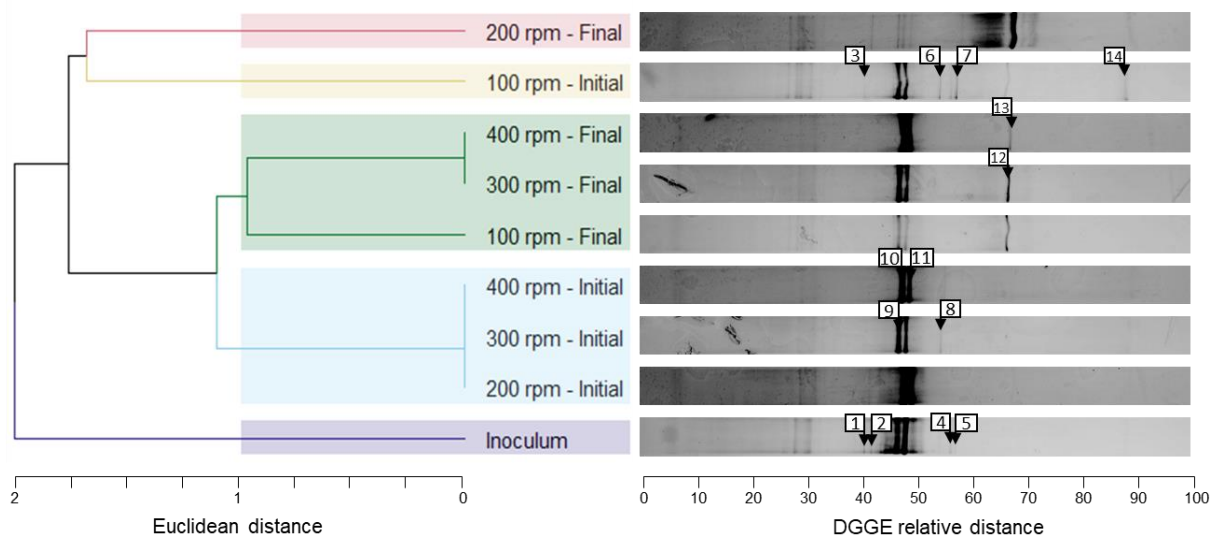


Figure 4.4. Denaturing gradient gel electrophoresis (DGGE) profiles from dark fermentation systems operated under different mass transfer conditions. The band numbers indicate samples that were sequenced (see Table 4.3).

approximately) were less intense in the samples taken at the end of CSTR II and CSTR III (100 and 200 rpm) than those taken in CSTR IV and CSTR V (300 and 400 rpm). Altogether, these findings indicate that the H₂ transfer conditions did not only affect the productivity, efficiency and metabolism in dark fermentative systems, but have also important implications on shaping the microbial communities.

Table 4.3. Affiliation of DGGE bands from samples taken under different mass transfer conditions.

Band	Closest relative (order/family/genus/species)	Identity	Accession No.
1	<i>Clostridiales/Clostridiaceae/Clostridium/ C. butyricum</i>	549/551 (99%)	NR_113244.1
2	<i>Clostridiales/Clostridiaceae/Clostridium/ C. butyricum</i>	551/551 (100%)	NR_113244.1
3	<i>Clostridiales/Clostridiaceae/Clostridium/ C. butyricum</i>	438/441 (99%)	NR_113244.1
4	<i>Clostridiales/Ruminococcaceae/Caproiciproducens/ C. galactitolivorans</i>	470/478 (98%)	NR_145929.1
5	<i>Clostridiales/Ruminococcaceae/Caproiciproducens/ C. galactitolivorans</i>	336/352 (95%)	NR_145929.1
6	<i>Bacillales/Sporolactobacillaceae/ Sporolactobacillus/ S. nakayamae</i>	339/352 (96%)	NR_114001.1
7	<i>Clostridiales/Clostridiaceae/Clostridium/ C. jeddahense</i>	549/553 (99%)	NR_144697.1
8	<i>Bacillales/Sporolactobacillaceae/Sporolactobacillus/ S. terrae</i>	457/470 (97%)	NR_112772.1
9	<i>Clostridiales/Clostridiaceae/Clostridium/ C. butyricum</i>	555/562 (99%)	NR_113244.1
10	<i>Clostridiales/Clostridiaceae/Clostridium/ C. butyricum</i>	542/548 (99%)	NR_113244.1
11	<i>Clostridiales/Clostridiaceae/Clostridium/ C. butyricum</i>	551/551 (100%)	NR_113244.1
12	<i>Lactobacillales/Lactobacillaceae/ Lactobacillus/ L. paracasei</i>	543/543 (100%)	NR_113337.1
13	<i>Lactobacillales/Lactobacillaceae/ Lactobacillus/ L. paracasei</i>	546/547 (99%)	NR_113337.1
14	<i>Enterobacterales/Enterobacteriaceae/Klebsiella/ K. variicola</i>	528/529 (99%)	NR_025635.1

4.4.5. The dual capacity of hydrogenogenic biomass

As largely reported, several dark fermentative species issued from the *Clostridium* genus have the capacity to consume H₂ through the homoacetogenesis pathway in response to high dissolved H₂ concentrations. To quantify this activity in mixed cultures, previous studies reported an approach based on balancing the acetate, butyrate and hydrogen productivities (Arooj et al., 2008; Luo et al., 2011). In accordance with this method, it was found that the acetate production rate ranged from 31.1 to 68.6 mol acetate/L-d. In terms of percentage, the acetate produced by homoacetogenesis was 32-46 % of the total acetate quantified in the systems (Table 4.4). Similar values were reported elsewhere by Luo et al. (2011) at different conditions of pH, temperature and sludge pretreatment. Also, in UASB reactors, Carrillo-Reyes et al. (2014) reported homoacetogenic productivities that represented about 50% of the total acetate observed. In regard to homoacetogenesis estimation, it is important to mention that its theoretical evaluation is subjected to uncertainties that are difficult to control. These uncertainties can be summarized in two issues:

Table 4.4. Theoretical determinations of H₂ consumption by homoacetogenesis.

Stirring (rpm)	kLa (1/h)	VHPR (L/L-d)	H ₂ yield (mol H ₂ /mol hexose)	Homoacetogenesis			
				(mol acetate/L-d)	% of total acetate	(L H ₂ -eq/L-d) ^a	% of theoretical H ₂ ^b
100	1.04	4.40	0.61	31.1	32	2.79	39%
200	1.64	5.60	0.73	61.1	46	5.47	49%
300	2.72	7.67	1.00	68.6	38	6.15	44%
400	4.23	7.66	1.08	45.8	33	4.10	35%

VHPR: Volumetric H₂ production rate

^a Accounts the amount of H₂ consumed in the synthesis of homoacetogenic acetate

^b Estimates the % of H₂ that is lost by the homoacetogenic route

1) homoacetogenesis is carried out through a metabolic pathway (the Wood-Ljungdahl pathway) that could theoretically lead to other not considered metabolites such as butyrate and formate, and 2) the mass balance assumes that acetate is associated with a hydrogen molar yield of 4 mol H₂/mol hexose, which is not accurate in most of the cases.

In this study, the biomass harvested from a hydrogen-producing reactor (CSTR III) was used to perform experiments to study the consumption of hydrogen, confirm the dual characteristics of the dark fermentative microorganisms and propose a method to avoid uncertainties in the estimation of homoacetogenesis. These experiments can be further considered as an initial approach to determine the kinetic parameters associated with the homoacetogenic activity of dark fermentative cultures.

The results showed that the H₂ consumption profile was successfully modelled with the Gompertz equation (Figure 4.5). The corresponding kinetic parameters are presented in Table 4.5. Interestingly, the system with an initial pressure of 1.4 atm showed remarkably higher velocity of H₂ uptake in comparison with the system at 1 atm. This finding suggests that H₂ accumulation controls the metabolism leading to its own consumption. Furthermore, the capillary electrophoresis analysis revealed that acetate was the main metabolite, produced at final concentrations of 94.8 ± 39 and 175 ± 46 mg/L in the system with an initial pressure of 1 and 1.4 atm, respectively.

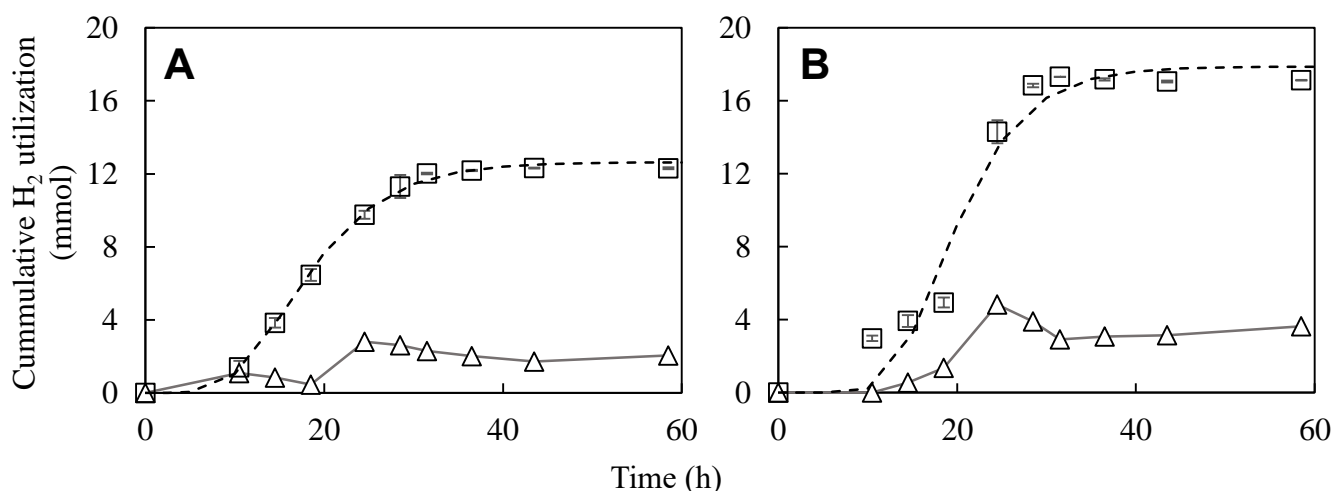


Figure 4.5. H₂ consumption profiles using hydrogenogenic biomass harvested from the continuous stirred-tank reactor III. Experimental points (\square), physicochemical control ($-\Delta-$) and gompertz model ($- -$). A) Experiment performed at an initial P_{H₂} of 1 atm. B) Experiment performed at an initial P_{H₂} of 1.4 atm.

Table 4.5. Summary of H₂ consumption experiments. For both experimental conditions, two additional serum bottles were set-up to account for the inoculum activity (without addition of H₂ gas) and the contribution of physicochemical phenomena (*e.g.* mass transfer).

Experiment	Initial pressure (Atm)	Gompertz parameters			pH final	Acetate concentration (mg/L)
		H _{max} (mmol _{H₂})	R _{max} (mmol H ₂ /h)	λ (h)		
A (n=3)	1	12.64	0.75	9.49	5.47 ± 0.02	94.9 ± 39
B (n=3)	1.4	17.87	1.24	12.52	5.44 ± 0.19	175 ± 46

4.5. Conclusions

This research demonstrates that the dark fermentation pathways and the related microbial communities can be controlled by improving the hydrogen mass transfer conditions. It was found that the increase of the mass transfer coefficient, $k_{L,a}$, enhanced the VHPR from 4.4 ± 1.3 L/L-d at a $k_{L,a}$ of 1.04 1/h (100 rpm) to 7.6 ± 1.4 L/L-d at $k_{L,a}$ of 4.23 1/h (400 rpm), which is equivalent to a 74 % increase. Similarly, the H₂ yield shifted from 0.6 ± 0.15 mol_{H₂}/mol hexose to 1.08 ± 0.21 mol H₂/mol hexose, *i.e.* an increment of

78%. The improvement in mass transfer conditions produced lower concentrations of dissolved H₂, which favored the dominance of *Clostridium sp.* over *Lactobacillus sp.*, which led to an enhancement of H₂ production through the acetate and butyrate pathways. The dual capability of the hydrogenogenic biomass was confirmed through microcosm studies that allowed to develop a first approach towards the characterization of H₂ consuming mixed cultures. Overall, it was demonstrated that the dark fermentation could be successfully controlled by mass transfer conditions.

4.6. References

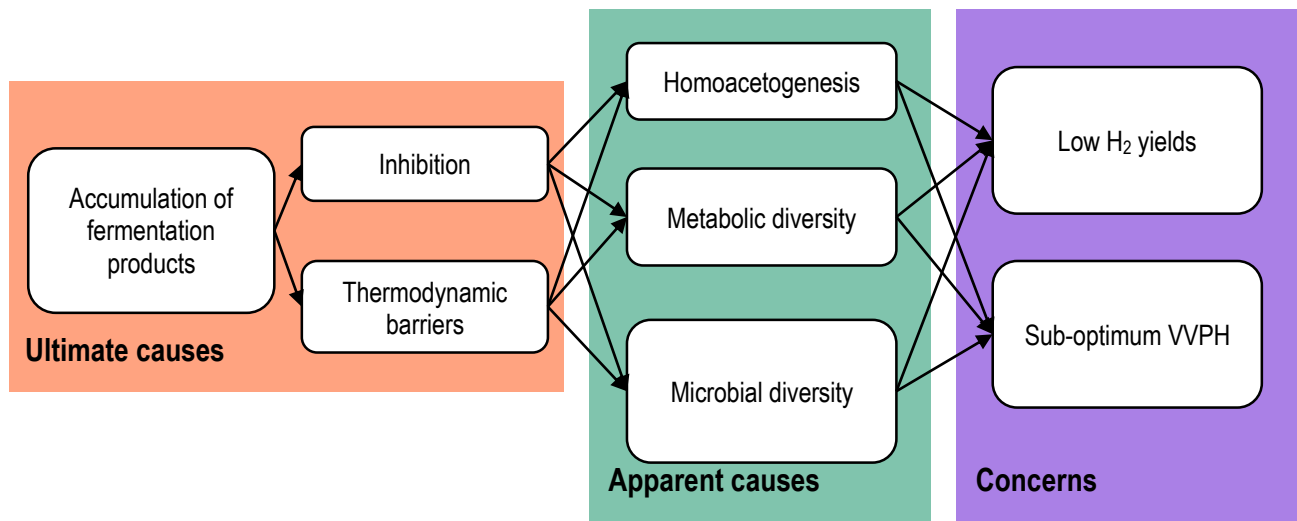
- Angenent, L.T., Karim, K., Al-Dahhan, M.H., Wrenn, B. a., Domínguez-Espinosa, R., 2004. Production of bioenergy and biochemicals from industrial and agricultural wastewater. *Trends Biotechnol.* 22, 477–485. doi:10.1016/j.tibtech.2004.07.001
- APHA/AWWA/WEF, 2012. *Standard Methods for the Examination of Water and Wastewater*, Standard Methods.
- Arooj, M., Han, S., Kim, S., Kim, D., Shin, H., 2008. Continuous biohydrogen production in a CSTR using starch as a substrate. *Int. J. Hydrogen Energy* 33, 3289–3294. doi:10.1016/j.ijhydene.2008.04.022
- Bakonyi, P., Buitrón, G., Valdez-Vazquez, I., Nemestóthy, N., Bélafi-Bakó, K., 2017. A novel gas separation integrated membrane bioreactor to evaluate the impact of self-generated biogas recycling on continuous hydrogen fermentation. *Appl. Energy* 190, 813–823. doi:10.1016/j.apenergy.2016.12.151
- Beckers, L., Masset, J., Hamilton, C., Delvigne, F., Toye, D., Crine, M., Thonart, P., Hiligsmann, S., 2015. Investigation of the links between mass transfer conditions, dissolved hydrogen concentration and biohydrogen production by the pure strain *Clostridium butyricum* CWBI1009. *Biochem. Eng. J.* 98, 18–28. doi:10.1016/j.bej.2015.01.008
- Cabrol, L., Marone, A., Tapia-Venegas, E., Steyer, J.-P., Ruiz-Filippi, G., Trably, E., 2017. Microbial ecology of fermentative hydrogen producing bioprocesses: useful insights for driving the ecosystem function. *FEMS Microbiol. Rev.* 41, 158–181. doi:10.1093/femsre/fuw043
- Carrillo-Reyes, J., Celis, L.B., Alatríste-Mondragón, F., Razo-Flores, E., 2014. Decreasing methane production in hydrogenogenic UASB reactors fed with cheese whey. *Biomass and Bioenergy* 63, 101–108. doi:10.1016/j.biombioe.2014.01.050
- Carrillo-Reyes, J., Celis, L.B., Alatríste-Mondragón, F., Razo-Flores, E., 2012. Different start-up strategies to enhance biohydrogen production from cheese whey in UASB reactors. *Int. J. Hydrogen Energy* 37, 5591–5601. doi:10.1016/j.ijhydene.2012.01.004
- Chang, S., Li, J., Liu, F., Yu, Z., 2012. Effect of different gas releasing methods on anaerobic fermentative hydrogen production in batch cultures. *Front. Environ. Sci. Eng.* 6, 901–906. doi:10.1007/s11783-012-0403-1
- Contreras-Dávila, C.A., Méndez-Acosta, H.O., Arellano-García, L., Alatríste-Mondragón, F., Razo-Flores, E., 2017. Continuous hydrogen production from enzymatic hydrolysate of *Agave tequilana* bagasse: Effect of the organic loading rate and reactor configuration. *Chem. Eng. J.* 313, 671–679. doi:10.1016/j.cej.2016.12.084
- Davila-Vazquez, G., Alatríste-Mondragón, F., de León-Rodríguez, A., Razo-Flores, E., 2008. Fermentative hydrogen production in batch experiments using lactose, cheese whey and glucose: Influence of initial substrate concentration and pH. *Int. J. Hydrogen Energy* 33, 4989–4997. doi:10.1016/j.ijhydene.2008.06.065

- Davila-Vazquez, G., Cota-Navarro, C.B., Rosales-Colunga, L.M., de León-Rodríguez, A., Razo-Flores, E., 2009. Continuous biohydrogen production using cheese whey: Improving the hydrogen production rate. *Int. J. Hydrogen Energy* 34, 4296–4304. doi:10.1016/j.ijhydene.2009.02.063
- de Kok, S., Meijer, J., van Loosdrecht, M.C.M., Kleerebezem, R., 2013. Impact of dissolved hydrogen partial pressure on mixed culture fermentations. *Appl. Microbiol. Biotechnol.* 97, 2617–25. doi:10.1007/s00253-012-4400-x
- Demirel, B., Scherer, P., 2008. The roles of acetotrophic and hydrogenotrophic methanogens during anaerobic conversion of biomass to methane: a review. *Rev. Environ. Sci. Bio/Technology* 7, 173–190. doi:10.1007/s11157-008-9131-1
- Dubois, M., K.A.Gilles, J.K.Hamilton, P.A.Rebers, Fred.Smith, 1956. Colorimetric Method for Determination of Sugars and Related Substances. *Anal. Chem.* 28, 350–356. doi:10.1021/ac60111a017
- Etchebehere, C., Castelló, E., Wenzel, J., del Pilar Anzola-Rojas, M., Borzacconi, L., Buitrón, G., Cabrol, L., Carminato, V.M., Carrillo-Reyes, J., Cisneros-Pérez, C., Fuentes, L., Moreno-Andrade, I., Razo-Flores, E., Filippi, G.R., Tapia-Venegas, E., Toledo-Alarcón, J., Zaiat, M., 2016. Microbial communities from 20 different hydrogen-producing reactors studied by 454 pyrosequencing. *Appl. Microbiol. Biotechnol.* 100, 3371–3384. doi:10.1007/s00253-016-7325-y
- Ferreira Rosa, P.R., Carrer Gomes, B., Amâncio Varesche, M.B., Luiz Silva, E., 2016. Characterization and antimicrobial activity of lactic acid bacteria from fermentative bioreactors during hydrogen production using cassava processing wastewater. *Chem. Eng. J.* 284, 1–9. doi:10.1016/j.cej.2015.08.088
- Ferrell, R.T., Himmelblau, D.M., 1967. Diffusion coefficients of hydrogen and helium in water. *AIChE J.* 13, 702–708. doi:10.1002/aic.690130421
- Ginkel, S. Van, Sung, S., Lay, J.-J., 2001. Biohydrogen Production as a Function of pH and Substrate Concentration. *Environ. Sci. Technol.* 35, 4726–4730. doi:10.1021/es001979r
- Han, P., Bartels, D.M., 1996. Temperature Dependence of Oxygen Diffusion in H₂O and D₂O †. *J. Phys. Chem.* 100, 5597–5602. doi:10.1021/jp952903y
- Kim, D.H., Han, S.K., Kim, S.H., Shin, H.S., 2006. Effect of gas sparging on continuous fermentative hydrogen production. *Int. J. Hydrogen Energy* 31, 2158–2169. doi:10.1016/j.ijhydene.2006.02.012
- Kisielewska, M., Dębowski, M., Zieliński, M., 2015. Improvement of biohydrogen production using a reduced pressure fermentation. *Bioprocess Biosyst. Eng.* 38, 1925–1933. doi:10.1007/s00449-015-1434-3
- Lee, K.-S., Tseng, T.-S., Liu, Y.-W., Hsiao, Y.-D., 2012. Enhancing the performance of dark fermentative hydrogen production using a reduced pressure fermentation strategy. *Int. J. Hydrogen Energy* 37, 15556–15562. doi:10.1016/j.ijhydene.2012.04.039
- Liu, R., Hao, X., Wei, J., 2016. Function of homoacetogenesis on the heterotrophic methane production with exogenous H₂/CO₂ involved. *Chem. Eng. J.* 284, 1196–1203. doi:10.1016/j.cej.2015.09.081
- Luo, G., Karakashev, D., Xie, L., Zhou, Q., Angelidaki, I., 2011. Long-term effect of inoculum pretreatment on fermentative hydrogen production by repeated batch cultivations: Homoacetogenesis and methanogenesis as competitors to hydrogen production. *Biotechnol. Bioeng.* 108, 1816–1827. doi:10.1002/bit.23122
- Palomo-Briones, R., Razo-Flores, E., Bernet, N., Trably, E., 2017. Dark-fermentative biohydrogen pathways and microbial networks in continuous stirred tank reactors: Novel insights on their control. *Appl. Energy* 198, 77–87. doi:10.1016/j.apenergy.2017.04.051
- Palomo-Briones, R., Trably, E., López-Lozano, N.E., Celis, L.B., Méndez-Acosta, H.O., Bernet, N., Razo-Flores, E., 2018. Hydrogen metabolic patterns driven by Clostridium-Streptococcus community shifts in a continuous stirred tank reactor. *Appl. Microbiol. Biotechnol.* 102, 2465–2475. doi:10.1007/s00253-018-8737-7

- R Development Core Team, R., 2011. R: A Language and Environment for Statistical Computing, R Foundation for Statistical Computing. doi:10.1007/978-3-540-74686-7
- Saad, N.M.C., 2013. Homoacetogenesis during hydrogen production by mixed cultures dark fermentation: Unresolved challenge. *Int. J. Hydrogen Energy* 38, 13172–13191. doi:10.1016/j.ijhydene.2013.07.122
- Sander, R., 2015. Compilation of Henry's law constants (version 4.0) for water as solvent. *Atmos. Chem. Phys.* 15, 4399–4981. doi:10.5194/acp-15-4399-2015
- Zwietering, M.H., Jongenburger, I., Rombouts, F.M., van 't Riet, K., 1990. Modeling of the bacterial growth curve. *Appl. Environ. Microbiol.* 56, 1875–81. doi:0099-2240/90/061875-07\$02.00/0

CHAPTER V

Strategies of control of microbial communities during dark fermentation: Conclusions and perspectives



Highlights

- Homoacetogenesis is a concomitant phenomenon of H₂ production in mixed culture fermentations
- Short HRT (6 h), low OLR (≤ 44.1 g lactose/L-d), and appropriate stirring velocity ($kLa \geq 2.72$ 1/h) were identified as the most suitable conditions for efficient H₂ production.
- Extractive fermentation arises as an alternative to overcome the thermodynamic and inhibitory effects caused by the high concentrations of metabolites at highly productive conditions.

5.1 General discussion and conclusions

In accordance with the literature review, three main challenges of dark fermentative systems have been identified (Chapter I): homoacetogenesis, LAB and mass transfer limitations. The results of the present thesis revealed that such phenomena are significantly affected by the HRT, substrate concentration and H₂ transfer conditions.

On the one hand, it was demonstrated that the HRT serves as a selection pressure upon the microbial community and metabolic pathways (Chapter II). At short values of HRT (6-12 h), the dominance of H₂-producing bacteria, *Clostridiaceae* and *Enterobacteriaceae*, was favored. In contrast, large values of HRT (18-24 h) promoted the appearance of microorganisms belonging to the families of *Sporolactobacillaceae* and *Streptococcaceae*, two well-known groups of LAB. It was suggested that short HRT values selected a H₂-producing community on the basis of microbial growth differences; this hypothesis was supported by growth kinetic parameters that have been reported elsewhere for *Sporolactobacillus* (Zhao et al., 2010). In such study, it was showed that *Sporolactobacillus* can grow at a maximum specific rate (μ_{\max}) of 0.117 1/h. Considering a steady state in the chemostat, where $d[\text{biomass}]/dt = 0$ (Rittmann and McCarty, 2001), the minimum HRT to keep a stable *Sporolactobacillus* population must be 8.5 h. Thus, the operation of the CSTR at HRT values of 6 h effectively maintained such detrimental group of microorganisms out of the system while H₂-producing bacteria became dominant.

In addition, it was found that the establishment of *Sporolactobacillaceae* was concomitant to the appearance of microorganisms belonging to the *Streptococcaceae* family. Interestingly, the members of this later family can actually grow at appreciably higher specific rates (Bibal et al., 1988; Poolman and Konings, 1988; Rogers et al., 1978); *i.e.* they can grow at HRT of 6 h. However, their appearance was only possible when *Sporolactobacillaceae* was also present. This observation was a clear indicative of a positive interaction between the two families that was confirmed by the microbial network analysis (Figure 2.8). Based on the *Sporolactobacillaceae* inability to metabolize lactose (Thamacharoensuk et al., 2015), it was hypothesized that the substrate required by *Sporolactobacillaceae* was possibly provided by *Streptococcaceae* members or other organisms in the fermentation broth.

Further research work revealed that the interesting dynamic between H₂-producing bacteria and LAB was controlled not only by the HRT but also by the inlet substrate concentration (Chapter III). Specifically, the high-throughput sequencing analysis showed that the *Clostridium* genus was the dominant

microorganism at $OLR \leq 44.1$ g lactose/L-d. On the contrary, at $OLR \geq 58.8$ g lactose/L-d, *Streptococcus* sp. arose as co-dominant bacteria with a maximum relative abundance of 59%.

The metabolic yields were in close association with the microbial community observations. Consistently, a strong relationship was observed between the *Streptococcus* relative abundance and the lactate concentration, while the dominance of the *Clostridium* genus was parallel to the increase of butyrate and acetate yields. Interestingly, although the maximum H_2 yield was found under the dominance of *Clostridium*, no correlation was found between the H_2 yield and the relative abundance of *Clostridium*. Indeed, the PCA analysis showed that *Clostridium* and the H_2 yield were orthogonal to each other (Figure 3.4) indicating that the variance of H_2 yield was barely explained by the *Clostridium* abundance. At first, this finding seems counterintuitive given the fact that H_2 production and efficiency are usually associated with the *Clostridium* genus. However, it was showed that *Clostridium* species could carry out metabolic pathways detrimental for H_2 production. Specifically, it was suggested that the formic acid observed along the CSTR operation could be result of H_2 and CO_2 consumption through the Wood-Ljungdahl pathway. This metabolic feature was hypothesized as a strategy to re-oxidize electron carriers needed for a stable and continuous fermentation.

In the light of the above results, it was established that stages with higher VHPR were among the less efficient in terms of H_2 yield. Furthermore, such stages were characterized by diverse metabolic routes and bacterial populations. To explain this phenomenon, it was proposed that the increase of the VHPR caused an increase of the dissolved H_2 concentration that could have negative effects on the continuous H_2 production yield, promoted the consumption of H_2 , and relesed an ecological niche in benefit of LAB.

In alignment with these ideas, the impacts of the H_2 mass transfer conditions on dark fermentation performance, metabolic pathways and microbial community were further investigated (Chapter IV). For such attempt, the fermentation was performed at different values of the H_2 mass transfer coefficient (1.04-4.23 1/h) by changing the velocity of mechanical stirring (100-400 rpm). The results demonstrated that the improvement of the H_2 mass transfer rate had positive effects on the H_2 yield and VHPR. Moreover, it was shown that such mechanism decreased the dissolved H_2 concentration that derived in a less diverse microbial community and higher acetate, butyrate and H_2 yields.

Beyond the impacts of HRT, OLR and mass transfer conditions on dark fermentation performance, the present thesis approached the emergent concern of homoacetogenesis. In general, the experimental evidence indicated that homoacetogenesis is a concomitant phenomenon of H_2 production in mixed culture

fermentations. As demonstrated in Chapter IV, this fact is probably the natural consequence of the dual capability of several *Clostridium* species that possess the genetic potential to conduct the Wood-Ljungdahl pathway. Indeed, from a biochemical perspective, it has been suggested that homoacetogenesis is a mechanism required to overcome the inhibition of the hydrogenases, which are in turn needed to re-oxidize the electron acceptors and maintain the equilibrium of electron carriers. Moreover, it is important to point out that the consumption of H₂ through the Wood-Ljungdahl pathway does not necessarily end in the acetate formation. Depending on multiple factors such as the concentrations of H₂, CO₂ and carboxylic acids, other molecules can be synthesized. In Chapter IV, it was proposed that the production of formate can be a result of the H₂ consumption metabolism.

An important contribution of this thesis was the finding that decreasing the H₂ concentration in the fermentation broth can control such metabolism. In turn, this can be done by 1) limiting the amount of organic substrate fed into the system (Chapter III) or 2) enhancing the H₂ mass transfer rate (Chapter IV). In the former proposition, the H₂ produced is also limited and its accumulation in the fermentation broth can be successfully controlled. As a result, the H₂ consumption decreased while the efficiency of dark fermentation (*i.e.* the H₂ yield) was enhanced. Such approach, however, is trivial and opposite to the objectives of the H₂ production biotechnology that aims to maximize the volumetric productivities. In the second proposition, the H₂ is promptly released from the liquid while its consumption by homoacetogenesis is minimized. This method is preferred over the previous one because it does not compromise the H₂ production. Still, the use of this method could be associated to major costs due to extra energy requirements that should be considered in future efforts to scale up the technology.

Overall, short HRT (6 h), low OLR (≤ 44.1 g lactose/L-d), and appropriate stirring velocity ($k_{La} \geq 2.72$ 1/h) were identified as the most suitable conditions for efficient H₂ production, avoiding excessive diversification of microbial communities and controlling low rates of H₂ consumption by homoacetogenesis and other metabolic routes.

5.2 Perspectives

5.2.1 The way forward in H₂ research

Despite of the considerable effort towards the enhancement of H₂ yields of dark fermentation and (therefore) the H₂ productivities, the biotechnology is still suboptimal in such terms. The theoretical H₂ yield of 4 mol H₂/mol hexose is far to be reached. Up to date, only few studies have reported efficiencies

above 2 mol H₂/mol hexose, while in terms of productivity, VHPR are rarely above 10 L H₂/L-d. What are the causes of this congestion? To answer this question, a brief overview of the research strategies can be of utility.

Traditionally, research on dark fermentation has focused on the improvement and optimization of pH, temperature, substrate concentrations, retention time, organic load, inoculum source, etc. For example, it has been showed that H₂ production from cheese whey can be increased at HRT of 6 h and OLR of 138.6 g lactose/L-d, obtaining a VHPR of 25 L H₂/L-h with a H₂ yield of 1.4 mol H₂/mol hexose (Davila-Vazquez et al., 2009). Other researchers have evaluated the pH and found that values about 5.5-6.0 are optimum for H₂ production (Fan et al., 2006). Using hydrolysates of agave bagasse, Contreras-Dávila et al. (2017) also reported better results when implementing pH of about 5.5. An extensive review on the effects of operational parameters is provided in Chapter I. What is important to highlight from this approach is that, due to multiple reasons, dark fermentation has been considered as a black box, with little or none importance on the real players of the process. The main contribution of this type of research was the establishment of environmental conditions suitable to carry out dark fermentation.

In the past two decades, a second wave of research focused on the study of microbial communities aiming to open the black box and get new insights that could be helpful to control H₂-producing systems. For instance, it was showed that different microbial communities can develop in accordance with the inoculum pretreatment (Carrillo-Reyes et al., 2016; Cisneros-Pérez et al., 2017, 2015). Authors argued that such effect is temporary and H₂-producing communities tend to converge towards a similar structure, giving more relevance to the operational conditions. More recently, the use of high-throughput technologies allowed characterizing the microbial community structure with a definition not seen before. In this regard, it has been revealed that the microbial communities developed in dark fermentation systems are more complex than usually assumed (Castelló et al., 2011; Etchebehere et al., 2016; Ratti et al., 2015; Tapia-Venegas et al., 2015). Nevertheless, such complexity is mostly observed in bioreactors where the solids retention time is decoupled from HRT, such is the case of fixed-biomass reactors and long-HRT systems. In suspended growth bioreactors operated at relatively short HRT (< 24 h), the microbial communities of dark fermentation are subjected to a strict biokinetic control; thus, the microbial diversity is dramatically diminished. In some cases, two groups of bacteria can account for more than 90% of biomass in the system (*e.g.* Chapter III). The simplicity in terms of microbial diversity has facilitated the understanding of the ecological interactions between the microbial community members and brought to the spotlight the wide metabolic capacities of dark fermentative bacteria.

Due to these novel methodologies, an interesting discussion has been developed from the microbial ecology and metabolic points of view (*e.g.* Cabrol et al., 2017; Elbeshbishy et al., 2017; Hung et al., 2011a; Saady, 2013). Eventually, it was recognized that *Clostridium* can also perform H₂ consumption if environmental conditions are appropriate (Dash et al., 2016; Saady, 2013). One of the contributions of the present thesis was to define some environmental conditions where homoacetogens and LAB have less intense effects on dark fermentation.

Considering the outlook described in these lines, the missing perspective towards the increase of H₂ efficiency and productivity is probably the general disregard on the control of thermodynamic barriers. These barriers, computed and described in accordance with the laws of thermodynamics (Goldberg and Alberty, 2010; Kleerebezem and Van Loosdrecht, 2010), can occur due to carboxylic acids, CO₂ and H₂ accumulation; all products of dark fermentation. In fact, the inhibition phenomena in dark fermentation is widely known and well documented (Bundhoo and Mohee, 2016; Elbeshbishy et al., 2017; Van Ginkel and Logan, 2005). Nevertheless, scarce efforts have been done to solve it. It was just recently that the removal of H₂ as a way to avoid homoacetogenesis brought the topic to the light (*e.g.* Bakonyi et al., 2017; Beckers et al., 2015; Chang et al., 2012; Kim et al., 2006; Kisielewska et al., 2015; Lee et al., 2012). In this regard, Chapter IV of this thesis addressed part of its relevance. Still, more research is needed to explore more alternatives to efficiently remove not only H₂ but also the rest of metabolites of dark fermentation.

A promising alternative to overcome the thermodynamic and inhibitory effects caused by the high concentrations of metabolites at highly productive conditions is the development and implementation of extractive fermentation schemes. This strategy aims to remove metabolic products in situ to reduce their concentrations, thus, limiting their detrimental effects on the fermentation performance. Extractive fermentations have been successfully implemented for the production of butanol (Xue et al., 2017), lactic acid (Othman et al., 2017) and other metabolic compounds. However, the use of extractive fermentation has been barely considered for H₂-producing systems (Jones et al., 2017, 2015; Kidanu et al., 2017; Massanet-Nicolau et al., 2016; Redwood et al., 2012). Most of them have been only tested in batch systems and/or under states of low productivity.

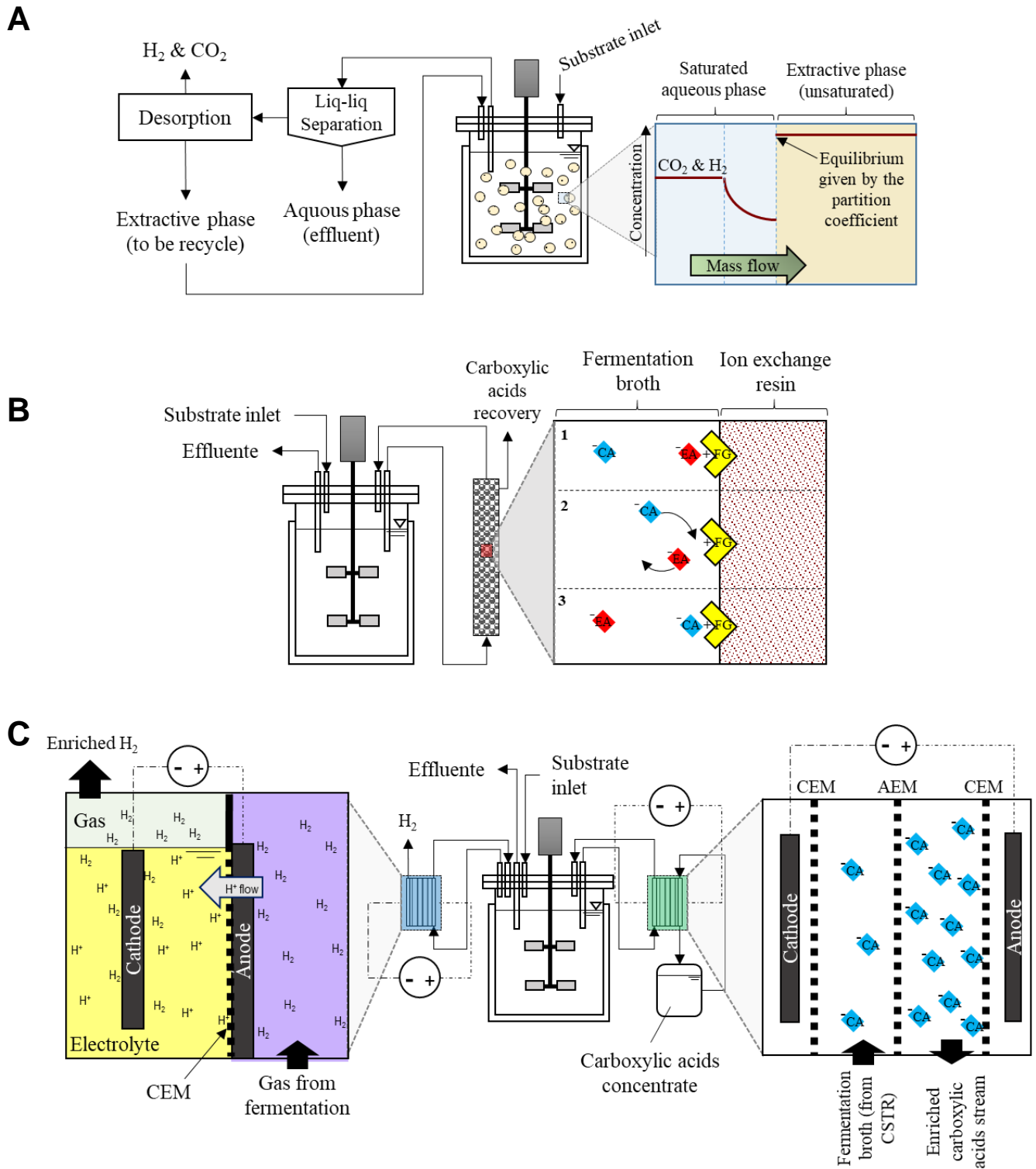


Figure 5.1. Schemes for extractive dark fermentation. A) Liquid-liquid extraction, B) ion exchange, and C) electrodialysis. CA: Carboxylic acid; EA: Exchanged anion; FG: Functional group; CEM: Cation exchange membrane; AEM: Anion exchange membrane.

Therefore, a foreseen way forward in the field is the development of extractive dark fermentation systems. Specific solutions such as liquid-liquid extraction, ion exchange, and electrodyalisis are worth to be explored. In the case of liquid-liquid extraction, the targeted compounds are H₂ and CO₂. For this case, an insoluble absorbent liquid (with affinity for the H₂ and CO₂) is added to the bioreactor. In such a way, the H₂ and CO₂ are constantly transferred to the absorbent keeping their concentrations low. To implement this extractive method, the productive system must be modified to include a unit for desorption and recovery of the spent absorbent (Figure 5.1A). In the case of ion exchange, functionalized materials are used to recover compounds of interest, in this case VFA, based on their electric charge. To do so, an exchange column must be implemented in a closed loop to keep the VFA concentration continuously below some specific value (Figure 5.1B). Finally, electrodyalisis methods are based on the simultaneous use of an electric field and ionic selective membranes to separate compounds taking advantage of their ionic properties. To perform the separation in situ, the membrane module must be arranged as shown in Figure 5.1C.

Finally, it is worth to mention that any of the configurations described in the previous lines is an opportunity to recover purified compounds that could be of the industrial interest economically. This is an important step towards the complete valorization of organic residues which is necessary to make the whole waste treatment process economically feasible. Indeed, such biorefinery perspective is considered as the way forward of research on biohydrogen production.

Altogether with the implementation of extractive fermentation, the development of novel strategies of control of dissolved H₂, volatile fatty acids ratios and microbial composition can also be of utility. In the case of dissolved H₂, the on-line measurement of dissolved H₂ concentration through specialized microsensors (*e.g.* Unisense® hydrogen sensors) can be incorporated as feedback to adjust the mixing conditions of CSTR, and therefore the dissolved H₂ concentration. This strategy would require to set a critical value of dissolved hydrogen concentration beyond which, the mixing of the bioreactor will be intensified through the proper actuator. Considering the research presented in chapter IV, a suitable set value would be about 3.4 mmol H₂/L. If H₂ is accumulated beyond the setpoint, even under efficient mixing conditions, a second response could be focused on reducing the loading rate. Through this strategy, derived from observations of Chapter III, the production of H₂ could be maximized and at the same time controlling homoacetogens and other metabolic pathways.

Control schemes based on monitoring H₂ concentrations in the liquid phase are mainly found for anaerobic digestion control (e.g Björnsson et al., 2001; Cord-Ruwisch et al., 1997; Giovannini et al., 2016). Nevertheless, to the best of my knowledge, this is an unexplored field in dark fermentation control.

5.2.2 Going back to homoacetogenesis

About methods

The present work was developed with focus on the interesting phenomenon of homoacetogenesis, the H₂ and CO₂ consumption to produce acetate. The evidence compiled along the present thesis revealed that H₂ concentration is a main driver of such process. The H₂ concentration can also control other metabolisms and the appearance of undesired populations as well.

The process can be evaluated in different ways, including mass balance, H₂-consumption kinetics, and gene-targeted tools.

The mass balance method, described by Arooj et al. (2008) and Luo et al. (2011), assumes the following:

1. H₂ is only produced through acetate and butyrate pathways (Figure 1.1). Thus the formation of acetate and butyrate in the fermentation broth will be associated with the production of 2 and 4 mol of H₂, respectively. For the sake of clarity, we will refer to this metabolites-base amount of H₂ as theoretical H₂.
2. The difference between the theoretical H₂ and the experimental H₂ can be explained by its consumption through propionate and homoacetogenesis. One mol of propionate is associated with the consumption of 1 mol of H₂, while homoacetogenesis is linked with the consumption of 4 mol of H₂.

In sum, the mass balance is summarized in the equation below:

$$H_2 = 2Butyrate + 2Acetate - Propionate - 4Acetate_{homoacetogenesis} \quad (5.1)$$

However, the estimation of homoacetogenesis through equation 5.1 does not consider that the Wood-Ljungdahl pathway can also produce other products apart of acetate. For example, *Clostridium ljungdahlii* possess the enzymatic machinery required to produce ethanol from 2 mol of CO₂ and 6 mol of H₂ (Köpke et al., 2010). Other metabolites such as formate, butyrate, and butanol are also possible to be produced depending on the *Clostridium* species as well as the fermentation conditions (Oswald et al., 2018; Schiel-

Bengelsdorf and Dürre, 2012). Considering this, there is not a simple way to discriminate between metabolites produced in the fermentation and metabolites produced through the Wood-Ljungdahl pathway.

Moreover, H₂ (in the form of NADH) can be used on membrane translocation of cations (H⁺ or Na⁺) that aims to build up an electrochemical gradient that can be used to drive the phosphorylation of ADP (Buckel and Thauer, 2013). Furthermore, NADH is also consumed in the synthesis of fatty acids and other compounds required for cell biosynthesis.

Therefore, homoacetogenesis conclusions based on Eq. 5.1 have to be taken with caution. In this thesis (Chapter IV), batch tests were proposed as an alternative to confirm the H₂ consumption capacities of hydrogenogenic cultures. Such tests do not replicate the environmental conditions of H₂-producing systems and, therefore, kinetic parameters do not represent the actual activity of homoacetogenesis in the analyzed CSTR fermentation. Still, the kinetic information obtained through this method can be used to infer and compare the H₂ consumption potentials of the mixed cultures under investigation.

The third and most effective alternative to evaluate homoacetogenesis consists on the implementation of molecular techniques targeting the presence (DNA-based) and expression (mRNA-based) of genes of the WLP. The DNA-based strategy has been successfully used to assess acetogens in natural environments and anaerobic reactors (Gagen et al., 2010; Leaphart and Lovell, 2001; Ryan et al., 2008; Xu et al., 2009); however, DNA-based methods only tell if the capacity to perform homoacetogenesis is present, not if it is actually taking place. Thus, only mRNA-based techniques can be used to make inferences about the homoacetogenic activity in systems of study. In this respect, few studies have reported this type of analysis (Tan et al., 2013; Wan et al., 2016; Xu et al., 2015). As the interest on homoacetogens increases (not only for H₂ production but also in syngas fermentation), it is possible that mRNA-based methods to search for homoacetogens will rise in popularity.

5.3. References

- Arooj, M., Han, S., Kim, S., Kim, D., Shin, H., 2008. Continuous biohydrogen production in a CSTR using starch as a substrate. *Int. J. Hydrogen Energy* 33, 3289–3294. doi:10.1016/j.ijhydene.2008.04.022
- Bakonyi, P., Buitrón, G., Valdez-Vazquez, I., Nemestóthy, N., Bélafi-Bakó, K., 2017. A novel gas separation integrated membrane bioreactor to evaluate the impact of self-generated biogas recycling on continuous hydrogen fermentation. *Appl. Energy* 190, 813–823. doi:10.1016/j.apenergy.2016.12.151
- Beckers, L., Masset, J., Hamilton, C., Delvigne, F., Toye, D., Crine, M., Thonart, P., Hilgsmann, S., 2015. Investigation of the links between mass transfer conditions, dissolved hydrogen concentration and biohydrogen production by the pure strain *Clostridium butyricum* CWBI1009. *Biochem. Eng. J.* 98, 18–28. doi:10.1016/j.bej.2015.01.008

- Bibal, B., Goma, G., Vayssier, Y., Pareilleux, A., 1988. Influence of pH, lactose and lactic acid on the growth of *Streptococcus cremoris*: a kinetic study. *Appl. Microbiol. Biotechnol.* 28, 340–344. doi:10.1007/BF00268192
- Björnsson, L., Murto, M., Jantsch, T.G., Mattiasson, B., 2001. Evaluation of new methods for the monitoring of alkalinity, dissolved hydrogen and the microbial community in anaerobic digestion. *Water Res.* 35, 2833–2840. doi:10.1016/S0043-1354(00)00585-6
- Buckel, W., Thauer, R.K., 2013. Energy conservation via electron bifurcating ferredoxin reduction and proton/Na⁺ translocating ferredoxin oxidation. *Biochim. Biophys. Acta - Bioenerg.* 1827, 94–113. doi:10.1016/j.bbabi.2012.07.002
- Bundhoo, M.A.Z., Mohee, R., 2016. Inhibition of dark fermentative bio-hydrogen production: A review. *Int. J. Hydrogen Energy* 41, 6713–6733. doi:10.1016/j.ijhydene.2016.03.057
- Cabrol, L., Marone, A., Tapia-Venegas, E., Steyer, J.-P., Ruiz-Filippi, G., Trably, E., 2017. Microbial ecology of fermentative hydrogen producing bioprocesses: useful insights for driving the ecosystem function. *FEMS Microbiol. Rev.* 41, 158–181. doi:10.1093/femsre/fuw043
- Carrillo-Reyes, J., Cortés-Carmona, M.A., Bárcenas-Ruiz, C.D., Razo-Flores, E., 2016. Cell wash-out enrichment increases the stability and performance of biohydrogen producing packed-bed reactors and the community transition along the operation time. *Renew. Energy* 97, 266–273. doi:10.1016/j.renene.2016.05.082
- Castelló, E., Perna, V., Wenzel, J., Borzacconi, L., Etchebehere, C., 2011. Microbial community composition and reactor performance during hydrogen production in a UASB reactor fed with raw cheese whey inoculated with compost. *Water Sci. Technol.* 64, 2265–2273. doi:10.2166/wst.2011.706
- Chang, S., Li, J., Liu, F., Yu, Z., 2012. Effect of different gas releasing methods on anaerobic fermentative hydrogen production in batch cultures. *Front. Environ. Sci. Eng.* 6, 901–906. doi:10.1007/s11783-012-0403-1
- Cisneros-Pérez, C., Carrillo-Reyes, J., Celis, L.B., Alatríste-Mondragón, F., Etchebehere, C., Razo-Flores, E., 2015. Inoculum pretreatment promotes differences in hydrogen production performance in EGSB reactors. *Int. J. Hydrogen Energy* 40, 6329–6339. doi:10.1016/j.ijhydene.2015.03.048
- Cisneros-Pérez, C., Etchebehere, C., Celis, L.B., Carrillo-Reyes, J., Alatríste-Mondragón, F., Razo-Flores, E., 2017. Effect of inoculum pretreatment on the microbial community structure and its performance during dark fermentation using anaerobic fluidized-bed reactors. *Int. J. Hydrogen Energy* 42, 9589–9599. doi:10.1016/j.ijhydene.2017.03.157
- Contreras-Dávila, C.A., Méndez-Acosta, H.O., Arellano-García, L., Alatríste-Mondragón, F., Razo-Flores, E., 2017. Continuous hydrogen production from enzymatic hydrolysate of *Agave tequilana* bagasse: Effect of the organic loading rate and reactor configuration. *Chem. Eng. J.* 313, 671–679. doi:10.1016/j.cej.2016.12.084
- Cord-Ruwisch, R., Mercz, T.I., Hoh, C.Y., Strong, G.E., 1997. Dissolved hydrogen concentration as an on-line control parameter for the automated operation and optimization of anaerobic digesters. *Biotechnol. Bioeng.* 56, 626–634. doi:10.1002/(SICI)1097-0290(19971220)56:6<626::AID-BIT5>3.0.CO;2-P
- Dash, S., Ng, C.Y., Maranas, C.D., 2016. Metabolic modeling of clostridia: Current developments and applications. *FEMS Microbiol. Lett.* 363, 1–10. doi:10.1093/femsle/fnw004
- Davila-Vazquez, G., Cota-Navarro, C.B., Rosales-Colunga, L.M., de León-Rodríguez, A., Razo-Flores, E., 2009. Continuous biohydrogen production using cheese whey: Improving the hydrogen production rate. *Int. J. Hydrogen Energy* 34, 4296–4304. doi:10.1016/j.ijhydene.2009.02.063
- Elbeshbishy, E., Dhar, B.R., Nakhla, G., Lee, H.-S., 2017. A critical review on inhibition of dark biohydrogen fermentation. *Renew. Sustain. Energy Rev.* 79, 656–668. doi:10.1016/j.rser.2017.05.075
- Etchebehere, C., Castelló, E., Wenzel, J., del Pilar Anzola-Rojas, M., Borzacconi, L., Buitrón, G., Cabrol, L.,

- Carminato, V.M., Carrillo-Reyes, J., Cisneros-Pérez, C., Fuentes, L., Moreno-Andrade, I., Razo-Flores, E., Filippi, G.R., Tapia-Venegas, E., Toledo-Alarcón, J., Zaiat, M., 2016. Microbial communities from 20 different hydrogen-producing reactors studied by 454 pyrosequencing. *Appl. Microbiol. Biotechnol.* 100, 3371–3384. doi:10.1007/s00253-016-7325-y
- Fan, K.S., Kan, N.R., Lay, J.J., 2006. Effect of hydraulic retention time on anaerobic hydrogenesis in CSTR. *Bioresour. Technol.* 97, 84–89. doi:10.1016/j.biortech.2005.02.014
- Gagen, E.J., Denman, S.E., Padmanabha, J., Zadbuke, S., Jassim, R. Al, Morrison, M., McSweeney, C.S., 2010. Functional gene analysis suggests different acetogen populations in the bovine rumen and tammar wallaby forestomach. *Appl. Environ. Microbiol.* 76, 7785–7795. doi:10.1128/AEM.01679-10
- Giovannini, G., Donoso-Bravo, A., Jeison, D., Chamy, R., Ruíz-Filippi, G., Vande Wouwer, A., 2016. A review of the role of hydrogen in past and current modelling approaches to anaerobic digestion processes. *Int. J. Hydrogen Energy* 41, 17713–17722. doi:10.1016/j.ijhydene.2016.07.012
- Goldberg, R.N., Alberty, R.A., 2010. Standard Transformed Gibbs Energies of Formation for Biochemical Reactants, in: Lundblad, R.L., Macdonald, F.M. (Eds.), *Handbook of Biochemistry and Molecular Biology*. CRC Press, pp. 551–553.
- Hung, C.-H., Chang, Y.-T., Chang, Y.-J., 2011. Roles of microorganisms other than *Clostridium* and *Enterobacter* in anaerobic fermentative biohydrogen production systems – A review. *Bioresour. Technol.* 102, 8437–8444. doi:10.1016/j.biortech.2011.02.084
- Jones, R.J., Massanet-Nicolau, J., Guwy, A., Premier, G.C., Dinsdale, R.M., Reilly, M., 2015. Removal and recovery of inhibitory volatile fatty acids from mixed acid fermentations by conventional electro dialysis. *Bioresour. Technol.* 189, 279–284. doi:10.1016/j.biortech.2015.04.001
- Jones, R.J., Massanet-Nicolau, J., Mulder, M.J.J., Premier, G., Dinsdale, R., Guwy, A., 2017. Increased biohydrogen yields, volatile fatty acid production and substrate utilisation rates via the electro dialysis of a continually fed sucrose fermenter. *Bioresour. Technol.* 229, 46–52. doi:10.1016/j.biortech.2017.01.015
- Kidanu, W.G., Trang, P.T., Yoon, H.H., 2017. Hydrogen and volatile fatty acids production from marine macroalgae by anaerobic fermentation. *Biotechnol. Bioprocess Eng.* 22, 612–619. doi:10.1007/s12257-017-0258-1
- Kim, D.H., Han, S.K., Kim, S.H., Shin, H.S., 2006. Effect of gas sparging on continuous fermentative hydrogen production. *Int. J. Hydrogen Energy* 31, 2158–2169. doi:10.1016/j.ijhydene.2006.02.012
- Kisielewska, M., Dębowski, M., Zieliński, M., 2015. Improvement of biohydrogen production using a reduced pressure fermentation. *Bioprocess Biosyst. Eng.* 38, 1925–1933. doi:10.1007/s00449-015-1434-3
- Kleerebezem, R., Van Loosdrecht, M.C.M., 2010. A Generalized Method for Thermodynamic State Analysis of Environmental Systems. *Crit. Rev. Environ. Sci. Technol.* 40, 1–54. doi:10.1080/10643380802000974
- Köpke, M., Held, C., Hujer, S., Liesegang, H., Wiezer, A., Wollherr, A., Ehrenreich, A., Liebl, W., Gottschalk, G., Dürre, P., 2010. *Clostridium ljungdahlii* represents a microbial production platform based on syngas. *Proc. Natl. Acad. Sci.* 107, 13087–13092. doi:10.1073/pnas.1004716107
- Leaphart, A.B., Lovell, C.R., 2001. Recovery and Analysis of Formyltetrahydrofolate Synthetase Gene Sequences from Natural Populations of Acetogenic Bacteria Recovery and Analysis of Formyltetrahydrofolate Synthetase Gene Sequences from Natural Populations of Acetogenic Bacteria. *Appl. Environ. Microbiol.* 67, 1392–1395. doi:10.1128/AEM.67.3.1392
- Lee, K.-S., Tseng, T.-S., Liu, Y.-W., Hsiao, Y.-D., 2012. Enhancing the performance of dark fermentative hydrogen production using a reduced pressure fermentation strategy. *Int. J. Hydrogen Energy* 37, 15556–15562. doi:10.1016/j.ijhydene.2012.04.039
- Luo, G., Karakashev, D., Xie, L., Zhou, Q., Angelidaki, I., 2011. Long-term effect of inoculum pretreatment on fermentative hydrogen production by repeated batch cultivations: Homoacetogenesis and methanogenesis as

- competitors to hydrogen production. *Biotechnol. Bioeng.* 108, 1816–1827. doi:10.1002/bit.23122
- Massanet-Nicolau, J., Jones, R.J., Guwy, A., Dinsdale, R., Premier, G., Mulder, M.J.J., 2016. Maximising biohydrogen yields via continuous electrochemical hydrogen removal and carbon dioxide scrubbing. *Bioresour. Technol.* 218, 512–517. doi:10.1016/j.biortech.2016.06.115
- Oswald, F., Stoll, I.K., Zwick, M., Herbig, S., Sauer, J., Boukis, N., Neumann, A., 2018. Formic Acid Formation by *Clostridium ljungdahlii* at Elevated Pressures of Carbon Dioxide and Hydrogen. *Front. Bioeng. Biotechnol.* 6. doi:10.3389/fbioe.2018.00006
- Othman, M., Ariff, A.B., Rios-Solis, L., Halim, M., 2017. Extractive fermentation of lactic acid in lactic acid bacteria cultivation: A review. *Front. Microbiol.* 8, 1–7. doi:10.3389/fmicb.2017.02285
- Poolman, B., Konings, W.N., 1988. Relation of growth of *Streptococcus lactis* and *Streptococcus cremoris* to amino acid transport. *J. Bacteriol.* 170, 700–707.
- Ratti, R.P., Delforno, T.P., Okada, D.Y., Varesche, M.B.A., 2015. Bacterial communities in thermophilic H₂-producing reactors investigated using 16S rRNA 454 pyrosequencing. *Microbiol. Res.* 173, 10–17. doi:10.1016/j.micres.2015.01.010
- Redwood, M.D., Orozco, R.L., Majewski, A.J., Macaskie, L.E., 2012. Electro-extractive fermentation for efficient biohydrogen production. *Bioresour. Technol.* 107, 166–174. doi:10.1016/j.biortech.2011.11.026
- Rittmann, B.E., McCarty, P.L., 2001. *Environmental Biotechnology: Principles and Applications*, McGraw-Hill Series in Water Resources and Environmental Engineering.
- Rogers, P.L., Bramall, L., McDonald, I.J., 1978. Kinetic analysis of batch and continuous culture of *Streptococcus cremoris* HP1. *Can J Microbiol* 24, 372–380.
- Ryan, P., Forbes, C., Colleran, E., 2008. Investigation of the diversity of homoacetogenic bacteria in mesophilic and thermophilic anaerobic sludges using the formyltetrahydrofolate synthetase gene. *Water Sci. Technol.* 57, 675–680. doi:10.2166/wst.2008.059
- Saady, N.M.C., 2013. Homoacetogenesis during hydrogen production by mixed cultures dark fermentation: Unresolved challenge. *Int. J. Hydrogen Energy* 38, 13172–13191. doi:10.1016/j.ijhydene.2013.07.122
- Schiel-Bengelsdorf, B., Dürre, P., 2012. Pathway engineering and synthetic biology using acetogens. *FEBS Lett.* 586, 2191–2198. doi:10.1016/j.febslet.2012.04.043
- Tan, Y., Liu, J., Chen, X., Zheng, H., Li, F., 2013. RNA-seq-based comparative transcriptome analysis of the syngas-utilizing bacterium *Clostridium ljungdahlii* DSM 13528 grown autotrophically and heterotrophically. *Mol. Biosyst.* 9, 2775–2784. doi:10.1039/c3mb70232d
- Tapia-Venegas, E., Cabrol, L., Brandhoff, B., Hamelin, J., Trably, E., Steyer, J., Ruiz-Filippi, G., 2015. Adaptation of acidogenic sludge to increasing glycerol concentrations for biohydrogen production. *Appl. Microbiol. Biotechnol.* 8295–8308. doi:10.1007/s00253-015-6832-6
- Thamacharoensuk, T., Kitahara, M., Ohkuma, M., Thongchul, N., Tanasupawat, S., 2015. *Sporolactobacillus shoreae* sp. nov. and *Sporolactobacillus spathodeae* sp. nov., two spore-forming lactic acid bacteria isolated from tree barks in Thailand. *Int. J. Syst. Evol. Microbiol.* 65, 1220–1226. doi:10.1099/ijs.0.000084
- Van Ginkel, S., Logan, B.E., 2005. Inhibition of biohydrogen production by undissociated acetic and butyric acids. *Environ. Sci. Technol.* 39, 9351–9356. doi:10.1021/es0510515
- Wan, J., Jing, Y., Zhang, S., Angelidaki, I., Luo, G., 2016. Mesophilic and thermophilic alkaline fermentation of waste activated sludge for hydrogen production: Focusing on homoacetogenesis. *Water Res.* 102, 524–532. doi:10.1016/j.watres.2016.07.002
- Xu, K., Liu, H., Du, G., Chen, J., 2009. Real-time PCR assays targeting formyltetrahydrofolate synthetase gene to enumerate acetogens in natural and engineered environments. *Anaerobe* 15, 204–13. doi:10.1016/j.anaerobe.2009.03.005

- Xu, S., Fu, B., Zhang, L., Liu, H., 2015. Bioconversion of H₂/CO₂ by acetogen enriched cultures for acetate and ethanol production: the impact of pH. *World J. Microbiol. Biotechnol.* 31, 941–950. doi:10.1007/s11274-015-1848-8
- Xue, C., Zhao, J., Chen, L., Yang, S.T., Bai, F., 2017. Recent advances and state-of-the-art strategies in strain and process engineering for biobutanol production by *Clostridium acetobutylicum*. *Biotechnol. Adv.* 35, 310–322. doi:10.1016/j.biotechadv.2017.01.007
- Zhao, B., Wang, L., Li, F., Hua, D., Ma, C., Ma, Y., Xu, P., 2010. Kinetics of d-lactic acid production by *Sporolactobacillus* sp. strain CASD using repeated batch fermentation. *Bioresour. Technol.* 101, 6499–6505. doi:10.1016/j.biortech.2010.03.069

Appendix

Methodology of the systematic review of dark fermentation (section 1.3.1)

A.1 Database construction

The literature review was performed through the Web of Science® principal database using the keyword combinations “biohydrogen + CSTR” and “dark fermentation + CSTR”. From the resulted articles only those actually containing experiments on dark fermentation, in continuous stirred tank reactors, with suspended biomass and soluble substrates were selected.

Afterward, an exhaustive review of the selected articles aimed to gather physicochemical parameters, operational conditions and response variables of all the different steady states reported within each article. A complete list of the collected variables is shown in Table A1.

Table A1. List of variables reviewed and considered for the statistical analysis.

Variables	Units
Reactor total volume	L
Reactor working volume	L
Inoculum type	-
Microorganisms identified in the inoculum	-
Type of Inoculum pretreatment	-
Temperature of heat pretreatment	°C
Time of heat pretreatment	h
Complexity of substrate	Simple or complex
Substrate	<i>e.g.</i> glucose, hydrolysate, cheese whey, etc.

Inlet substrate concentration	g carbohydrates/L, g COD/L, mmol substrate/L
OLR	g carbohydrates/L-d, g COD/L-d, mol substrate/L-d
pH	-
Temperature	°C
HRT	h
Head space	% (v/v)
Stirring velocity	rpm
Carbohydrate converted	%
Substrate converted	g carbohydrates/L, g COD/L, mmol substrate/L
Substrate conversion rate	g carbohydrates/L-d, g COD/L-d, mol substrate/L-d
Biomass concentration	g SSV/L, g COD/L
H ₂ in gas	%
CO ₂ in gas	%
H ₂ yield	mol H ₂ /mol hexose, mmol H ₂ /g COD
H ₂ production rate	L H ₂ /L-d, mol H ₂ /L-d, L H ₂ /g SSV-d
Metabolites production rate	g/L-d, g COD/L-d
VFA concentration	g/L, mol/L
Ethanol concentration	g/L, mol/L
Butanol concentration	g/L, mol/L
Acetate/Butyrate ratio	-

In cases where the information was presented in graphs, the figure was imported into an image specialized software (GIMP software), where the variables of interest were calculated based on the coordinates of the image platform. On the other hand, composed variables (*i.e.* those that can be expressed as function of other variables) that were not explicitly reported were computed using the available information when possible.

To conduct its preparation, depuration and analysis, the constructed database was finally loaded into the R environment (R Development Core Team, 2011).

A.2 Unifactorial and multifactorial statistical analysis

The constructed dataset was curated to remove low represented substrates, for example glycerol, VFA mixture, and mixtures of these with other model substrates (*e.g.* glucose + glycerol). Moreover, to conduct the parametric analysis, the normality of numeric variables was graphically

inspected; as most variables did not follow a normal distribution, they were transformed as defined in the Table A2.

Table A2. Variables transformed to fit a normal distribution.

Variables	Units	Transforming function $f(x)$
Inlet substrate concentration	g carbohydrates/L	$x^{(1/2)}$
OLR	g COD/L	$x^{(1/3)}$
	g COD/L-d	$x^{(1/3)}$
	mol substrate/L-d	$x^{(1/3)}$
HRT	h	$x^{(1/5)}$
Substrate converted	g COD/L	$x^{(1/2)}$
Substrate conversion rate	mol substrate/L-d	$x^{(1/6)}$
	g COD/L-d	$x^{(1/3)}$
Biomass concentration	g SSV/L	$x^{(1/4)}$
	g COD/L	$x^{(1/4)}$
H ₂ yield	mol H ₂ /mol hexose	$x^{(1/2)}$
H ₂ production rate	L H ₂ /L-d	$x^{(1/3)}$
	mol H ₂ /L-d	$x^{(1/3)}$
	L H ₂ /g SSV-d	$x^{(1/4)}$
Metabolites production rate	g/L-d	$x^{(1/3)}$
	g COD/L-d	$x^{(1/3)}$
Formate concentration	g/L	$x^{(1/3)}$
Acetate concentration	g/L	$x^{(1/3)}$
Propionate concentration	g/L	$x^{(1/4)}$
	g/L	$x^{(1/4)}$
Butyrate concentration	g/L	$x^{(1/3)}$
Lactate concentration	g/L	$x^{(1/3)}$
Ethanol concentration	g/L	$x^{(1/3)}$

The unifactorial and multifactorial analyses of variance (ANOVA) were performed with R base functions. In the case of multifactorial ANOVA, the model was done using the top-down strategy (Zuur et al., 2009). Moreover, given the unbalanced design of the gathered data, the type II sum of squares was used to compute the size effects parameters (Langsrud, 2003). The models were validated through visual inspection of Q-Q plot and residuals (data not shown). To deal with

continuous variables (*e.g.* substrate concentration, temperature, organic loading rate, etc.), these were grouped into new variables with 3-6 levels.

On the other hand, unifactorial and multifactorial linear regression models were constructed following the top-down strategy and type II sum of squares to keep only significant variables ($p < 0.05$). The normality and homoscedasticity were validated by visual inspection.

A.3 Multivariate analysis

Pearson's correlation analysis was conducted to investigate the degree of interaction between the multiple variables collected from literature. In this analysis, the normalized database was used. To visualize the correlation results, the *corrplot* package was used to construct a correlation matrix that shows significant correlations at a p values equal or lower than 0.1.

To further analysis the database structure, a PCA analysis was carried out using R software and *facto-extra* package. The PCA is a multivariate technique that computes synthetic variables (principal components), which are mutually independent, uncorrelated, mathematically represented as a linear combinations of the original variables, and that account for as much of the variance of the original data as possible. In this procedure, the normalized database was used as well.

A.4 References

Langsrud Ø (2003) ANOVA for unbalanced data: Use Type II instead of Type III sums of squares. *Stat Comput* 13:163–167. doi: 10.1023/A:1023260610025

R Development Core Team R (2011) R: A Language and Environment for Statistical Computing

Zuur AF, Ieno EN, Walker NJ, et al (2009) Mixed Effects Models and Extensions in Ecology with R. *Stat Biol Heal* 579 p. doi: 10.1007/978-0-387-87458-6

About the author

Rodolfo Palomo Briones (Torreón, Coahuila, 1989) started his Biochemical Engineering studies in 2006 at the Instituto Tecnológico de Morelia (Morelia, Michoacán). In 2010 he spent one year at the Laboratorio de Investigación en Procesos Avanzados de Tratamiento de Aguas (Querétaro, Querétaro), part of the Universidad Nacional Autónoma de México, under the direction of Dr. Germán Buitrón. During that year, he was involved in research on microbial fuel cells. In 2011, he obtained his bachelor's degree with the thesis "Effect of the external resistance on phenol degradation in microbial fuel cells". Afterward, he began his master studies at the Instituto Potosino de Investigación Científica y Tecnológica (IPICYT) under the direction of Dra. Sonia Lorena Arriaga García. During that time, he got involved in research about biofiltration coupled to heterologous proteins production. As part of that work, he carried out an academic stay of 3 months at Duke University (Durham, NC, USA) under the supervision of Dr. Marc Deshusses. In 2013, he obtained his master's degree with the thesis "Effect of operational parameters on methanol biofiltration coupled to Ech42 production". From September 2013 to December 2014, he was associate researcher in a project aiming to assess the wastewater reuse in gold mining activities under the supervision of Dr. Elías Razo Flores. In January 2015, he joined the biohydrogen research group, also under the direction of Dr. Razo, and started his doctoral studies on the topic "Strategies of control of microbial communities during dark fermentation". As part of the doctoral research, he did an academic stay, under the direction of Dr. Nicolas Bernet and Dr. Eric Trably, at the Laboratoire de Biotechnologie de l'Environnement (Narbonne, France), which is part of the Institut National de la Recherche Agronomique.

Scientific articles

Published or accepted

- **Palomo-Briones, R.** Trably, E., López-Lozano, N.E., Celis, L.B., Méndez-Acosta, H.O., Bernet, N., Razo-Flores, E. 2018. Hydrogen metabolic patterns driven by *Clostridium-Streptococcus* community shifts in a continuous stirred tank reactor. *Applied Microbiology and Biotechnology*, 102: 2465-2475
- **Palomo-Briones, R.**, López-Gutiérrez, I., Islas-Lugo, F., Galindo-Hernández, K.L., Munguía-Aguilar, D., Rincón-Pérez, J.A., Cortés-Carmona, M.A., Alatríste-Mondragón, F., Razo-Flores, E. 2018. Agave bagasse biorefinery: Processing and perspectives. *Clean Technologies and Environmental Policies*, 20 (7) 1423-1441

- **Palomo-Briones, R.**, Esquivel-González, S., Aizpuru, A., Gómez-Hernández, N., Casas-Flores, S., Barba de la Rosa, A. P., Arriaga, S. 2018. Microbial contamination in methanol biofilters inoculated with a pure strain of *Pichia Pastoris*: a potential limitation for waste revalorization. *Biotechnology Progress*, in press.
- **Palomo-Briones, R.**, Razo-Flores, E., Bernet, N., Trably, E. 2017. Dark-fermentative biohydrogen pathways and microbial networks in continuous stirred tank reactors: Novel insights on their control. *Applied Energy*, 198 77-87.
- **Palomo-Briones, R.**, Ovando-Franco, M., Razo-Flores, E., Celis, L.B., Rangel-Méndez, J.R., Vences-Álvarez, E., Cruz, R., Lázaro, I., Briones-Gallardo, R. 2016. An overview of reclaimed wastewater reuse in gold heap leaching. *Mineral Processing and Extractive Metallurgy Review*, 37 (4) 274-285.
- **Palomo-Briones, R.**, De la Rosa, P., Arriaga, S. 2015. Effect of operational parameters on methanol biofiltration coupled with Endochitinase 42 production. *Biochemical Engineering Journal*, 100, 9-15

To be submitted

- Palomo-Briones, R., Celis, L.B., Méndez-Acosta, H.O., Bernet, N., Trably, E., Razo-Flores, E. 2018. Enhancement of mass transfer conditions to increase the productivity and efficiency of dark fermentation. *Fuels*. To be submitted.
- Palomo-Briones et al. 2018. Systematic review of dark fermentation in continuous stirred-tank reactors. *Energy and Environmental Science*. To be submitted.

Popular science articles

- **Palomo-Briones, R.**, Ríos-del-Toro, E., Calderón-Soto, L.F., Bravo-Vidales, A.P., Gómez Muñoz, C., Ocegüera-Contreras, E. 2016. Compuestos contaminantes de la atmósfera: ¿cuáles son sus efectos? y, sobre todo, ¿cómo eliminarlos? *Ciencia*, enero-marzo 2016, volumen 67, número 1.
- Jacobo S. Abreu-Sherrer, Melissa, K. Ávila-Argaez, María de las Nieves Barranco-León, Miguel A. Beltrán-Santoyo, Carlos E. Flores-Chaparro, Laura B. Jiménez-Bermúdez, María Guadalupe Maldonado-Díaz, Dody Morales-Sánchez, Brenda L. Muñoz-Flores, **Rodolfo Palomo-Briones**, Raúl I. Rentería-Tamayo, Jorge C. Ríos-Hurtado, Rigoberto Santoyo-Cisneros, Eduardo Toral-Sánchez, Felipe Alatríste-Mondragón, Ernesto I. Badano. La ética y el desarrollo de la ciencia y tecnología en México. 2012. *Elementos* 88, 2012. pp 35-39.